CHARLES UNIVERSITY IN PRAGUE, FACULTY OF SCIENCE

Department of Analytical Chemistry

A CONTRIBUTION TO THE DETERMINATION OF NITRO, AMINO, AND HYDROXY DERIVATIVES OF NAPHTHALENE USING ELECTROCHEMICAL METHODS

A Thesis Submitted as the Basis for the Award

of the PhD Degree

Prague 2006 **Karolina Pecková**

I declare that all the results which are used and published in this Thesis have been obtained by my own experimental work and that all the ideas taken from work of others are properly referred to in the text and the literature survey.

Prague, 20. 7. 2006

Karolina Pecková

This dissertation is based on experiments carried-out in the period from 2001 till 2006 at the Department of Analytical Chemistry, Charles University, Prague. During this period, the research visits to Professor Josino C. Moreira from Laboratory of Electroanalysis of the National School of Public Health, Oswaldo Cruz Foundation (ENSP/FIOCRUZ), Rio de Janeiro, Brazil and Professor Greg M. Swain's research group at Michigan State University, East Lansing, MI, USA were completed. Further experiments were done at J. Heyrovský Institute of Physical Chemistry of the Academy of Sciences of the Czech Republic.

I would like to express acknowledgements to all who have supported my research efforts during this time. Let me thank especially to **Prof. RNDr. Jiří Barek, CSc.,** my supervisor at the Department of Analytical Chemistry, Prague for his kind leading my doctoral program and support in organizing research visits, and other members of the Department, particularly Doc. RNDr. Jiří Zima, CSc. and Prof. RNDr. František Opekar, CSc for their help on HPLC with amperometric detection. Further, I acknowledge Dr. Bogdan Yosypchuk from J. Heyrovský Institute of Physical Chemistry of the Academy of Sciences for providing the silver solid amalgam electrodes and the know-how of their treatment and Dr. Tomáš Navrátil for valuable discussions on elimination voltammetry with linear scan. I thank also to Professor Josino C. Moreira from Laboratory of Electroanalysis of the Oswaldo Cruz Foundation, Rio de Janeiro, Brazil and Professor Greg M. Swain's from Michigan State University, East Lansing, USA for kind supervising during my research visits and challenging experience not only on chemistry I could be part of in their home countries.
Last, but not at least I thank to my parents, sisters, colleagues in the lab and all my friends for the support and fun during my graduate studies.

The financial support of my work was provided by the following sources: University Development Fund 2793/2003, Grant Agency of the Czech Republic (projekt 203/03/0182), and Josef and Marie Hlávka´s Foundation.

Contents

List of symbols and abbreviations

1-AN	1-aminonaphthalene
1-NN	1-nitronaphthalene
1-NP	1-nitropyrene
1-OHN	1-hydroxynaphthalene
2-AN	2-aminonaphthalene
2-NN	2-nitronaphthalene
2-OHN	2-hydroxynaphthalene
α	confidence level
α	charge transfer coefficient
ε	molar absorbance coefficient
λ	wavelength
τ	drop time
A.U.	absorbance units
AdSV	adsorptive stripping voltammetry
APAHs	amino derivatives of polycyclic aromatic hydrocarbons
BR	Britton-Robinson
c	molar concentration
CAS	Chemical Abstract Services
C_{18}	octadecyl
CHLD	chemiluminescence detector
CPE	carbon paste electrode
CV	cyclic voltammetry
DC	direct current
DCTP	direct current tast polarography
DCV	direct current voltammetry
DME	dropping mercury electrode
DNA	deoxyribonucleic acid
DMF	dimethylformamide
DP	differential pulse
DPP	differential pulse polarography
DPV	differential pulse voltammetry
$E_{1/2}$	half wave potential
E_{acc}	accumulation potential

ECD	electron capture detector
EC-MS	electron capture - mass spectrometry
ED	electrochemical detector
E_{DP}	peak potential of degradation product
E_{det}	detection potential
eds.	editors
e.g.	exempli gratia (for example)
EI	electron impact
E_p	peak potential
EPA	Environmental Protection Agency
eq.	equiation
EVLS	elimination voltammetry with linear scan
FD	fluorescence detector
FID	flame ionization detector
GC	gas chromatography
GC-FID	gas chromatography with flame ionization detector
GC-NICI-MS	gas chromatography-negative-ion chemical ionization mass spectrometry
GC-MS	gas chromatography-mass spectrometry
h	height of the mercury electrode reservoir
HMDE	hanging mercury drop electrode
HPLC	high performance liquid chromatography
HPLC-ED	high performance liquid chromatography-electrochemical detection
i.d.	inner diameter
i.e.	id est (that is)
IARC	International Agency for Research on Cancer
I_{lim}	limiting current
I_p	peak current
k_{phot}	rate constant of photodegradation
L	liter (dm^{-3})
LLE	liquid-liquid extraction
LOD	limit of determination
m	flow rate of the dropping mercury electrode
m-AgSAE	mercury meniscus modified silver solid amalgam electrode
m-AuSAE	mercury meniscus modified gold solid amalgam electrode
m-CuSAE	mercury meniscus modified copper solid amalgam electrode
MeOH	methanol

MeSAE	metal solid amalgam electrode
MF-MeSAE	mercury film modified metal solid amalgam electrode
m-MeSAE	mercury meniscus modified metal solid amalgam electrode
MS	mass spectrometric detection
MS/MS	tandem mass spectrometry
N	naphthalene
n	number of exchanged electrons
NICI	negative-ion chemical ionization
NPAHs	nitro derivatives of polycyclic aromatic hydrocarbons
NPD	nitrogen-phosphorus detector
o.d.	outer diameter
OHPAHs	hydroxy derivatives of polycyclic aromatic hydrocarbons
PAHs	polycyclic aromatic hydrocarbons
p-MeSAE	polished metal solid amalgam electrode (without liquid mercury)
p.	page
Pt-μCD	amperometric detector with platinum microcylindrical electrode
Pt-TD	amperometric detector with platinum tubular electrode
R	correlation coefficient
RP	reversed phase
RSD	relative standard deviation
SPE	screen printed carbon electrode
SPE	solid phase extraction
t_{acc}	accumulation time
TBAI	tetrabutylammoniumiodide
TEA	thermal energy analyzer
TIC	total ionic current
TID	thermionic ionization detector
TLC	thin layer chromatography
UNESCO	United Nations Educational, Scientific and Cultural Organization
USA	United States of America
UV	ultraviolet part of the spectrum
v/v	volume/volume
VIS	visible part of the spectrum
vs.	versus
v_{sc}	scan rate
$w_{1/2}$	peak width at the half height

1

Introduction

This dissertation has been submitted as a contribution to the ever growing efforts of environmental analysis. It was elaborated under the framework of a long term research at UNESCO Laboratory of Environmental Electrochemistry in Prague to develop highly sensitive and selective methods for determination of polycyclic aromatic hydrocarbons (PAHs) and their nitro, amino, and hydroxy derivatives.

PAHs and their derivatives constitute a class of biologically active organic pollutants generated in a variety of chemical processes. PAHs are ubiquitous in the environment, their higher occurrence in urban and industrial areas is given by the fact that they are formed during incomplete combustion, thus they are present in automobile exhausts and industrial exhalations. They are released to atmosphere preferably associated with submicron-size particles. When released into the atmosphere, PAHs are exposed to a variety of gaseous compounds, including stable molecules and highly reactive intermediates as free radicals or electronically excited species, originated from absorption of radiation. These interactions result in an introduction of functional groups to the aromatic system of the parent molecule. The polar fractions of the aerosols were found to be highly complex, containing several hundred PAH derivatives, including compounds with hydroxy, nitro, ketone, quinone, aldehyde, and carboxylic acid substituents. These derivatives may have even higher mutagenicity compared to nonsubstituted PAHs, thus the analysis of atmospheric aerosols and other environmental samples is of great concern.

Naphthalene is the simplest and most volatile of all PAHs, worldwide present in environmental sources (air, soil, water) and in a variety of critical workplaces. Since 2000, naphthalene has posed a great problem for environmental and occupational medicine, because significant carcinogenic effects have been associated with naphthalene exposure in animal investigations. To evaluate the exposure of humans to naphthalene, the urinary concentrations of its metabolites – hydroxynaphthalenes in the general population and in subjects occupationally exposed to naphthalene are monitored. Nitronaphthalenes are the most abundant nitroderivatives of PAHs (NPAHs) in urban air, their health risk is causatively connected to the generation of active species binding to DNA, which are responsible for their mutagenicity. Aminonaphthalenes are possible metabolites of nitronaphthalenes and their toxicity is well known for more than hundred of years, because there were extensively used as intermediates in the production of azo dyes.

Owing to the extremely wide range of matrices, where PAHs and their derivatives can be present, the often small amounts of individual compounds and a myriad of interfering

substances present in, analytical methods are required which are not only extremely sensitive, but can also provide great selectivity.

Many chromatographic techniques have been brought to cope with the separation and quantitation of solutes in such complex samples. Although gas chromatography with selective detectors is widely used, it is rather limited to the low polarity and relatively high volatility compounds. Reversed phase high-performance liquid chromatography with a wide range of detection techniques becomes an option to be considered for its ability to resolve lower volatile, thermally unstable, polar compounds with high sensitivity of detection. It offers numerous combinations of custom-tailored stationary phases along with various organic modificators of the eluent for the separation of complex mixtures. Electroanalytical methods represent a useful alternative to more frequent chromatographic methods, they meet the stringent conditions on sensitivity, although the selectivity is often presented as a weak point in analysis of complex matrices. However, the selectivity can be increased when applying preliminary separation step or it is not required in case that electroanalytical methods are used to estimate the sum of analytes or as cheap screening methods monitoring the presence of derivatives of interest in a complex matrix. Moreover, the study of polarographic and voltammetric behaviour of biologically active organic compounds can provide a great amount of information about their electron-transfer reactions. This can be useful in elucidation of the mechanism of their interaction with living cells, because both electrochemical and biological reactions are essentially heterogenous processes occurring at the electrode-solution or enzyme-solution interface.

With respect to above mentioned facts, the aim of the Thesis was the development of sensitive electroanalytical methods for the determination of 1-nitronaphthalene, 2-nitronaphthalene, 1-aminonaphthalene, 2-aminonaphthalene, 1-hydroxynaphthalene, and 2-hydroxynaphthalene. The Thesis presented consists of several chapters each of which is dealing with a particular analytical issue in the electroanalytical determination of naphthalene derivatives. The applicability of different electroanalytical detection techniques was studied in order to obtain low limits of determination for studied derivatives. The main attention was paid to nitronaphthalenes, because these compounds are polarographicly reducible, thus a variety of electroanalytical methods at classical electrode materials as mercury and non-traditional materials as mercury amalgams can be compared for their determination. Moreover, they are widely extended in the environment in a number of matrices, thus the development of new methods for their sensitive determination is of great concern.

The introductory part of the Thesis is reviewing the origin, occurrence, biological impact and metabolic activity of nitro, amino, and hydroxy derivatives of PAHs, with main focus on the nitroderivatives of PAHs. Also the current state of the analytical methods being used for the analysis of studied compounds is summarized (Chapter 2). The following Chapters 3 and 4 are devoted to the study of electrochemical behaviour of 1-nitronaphthalene and 2-nitronaphthalene with the purpose to develop sensitive methods for their determination. Two electrode materials were tested: In Chapter 3, the electroanalytical behaviour of studied analytes using DC tast polarography and differential pulse polarographic at classical dropping mercury electrode is compared to the voltammetric methods (differential pulse voltammetry and adsorptive stripping voltammetry) at hanging mercury drop electrode. Chapter 4 presents the results on voltammetry using meniscus modified silver solid amalgam electrode and comparison of the electrochemical behavior of studied analytes using this electrode and mercury electrodes. The newly developed methods were used in Chapter 5 to analyze the model matrices – drinking and river water. Liquid-liquid extraction and solid-phase extraction of 1-nitronaphthalene and 2-nitronaphthalene were used for their preliminary separation and preconcentration. In Chapter 6, the developed electroanalytical methods at mercury electrodes were applied for the monitoring of the efficiency of safe destruction procedure of nitronaphthalenes as laboratory waste contaminants. An attempt to identify the products of their photolytical degradation was made. The research carried out in Chapter 7 turns to electrochemical detection after HPLC separation of selected analytes. Oxidizable naphthalene and nitronaphthalene metabolites – 1-aminonaphthalene and 2-aminonaphthalene, and 1-hydroxynaphthalene and 2-hydroxynaphthalene – were determined using a new type of laboratory-made miniaturized amperometric detector, based on a platinum microwire working electrode.

2

Polycyclic aromatic hydrocarbons and their nitro, amino, and hydroxy derivatives in environment

2.1 General characterization

The compounds studied in the thesis are mainly selected derivatives of naphthalene. Six of its monoderivatives were studied, namely 1- and 2- nitro, 1- and 2-amino, and 1- and 2-hydroxynaphthalene. These compounds belong to important environmental pollutants and may exhibit serious genotoxic and/or carcinogenic effects. In following chapters, their origin and occurrence in the environment, fate in organism, toxicological properties and analytical methods for their determination will be discussed. As special concern in the thesis is on mononitronaphthalenes, the typical representatives of nitrated polycyclic aromatic hydrocarbons (NPAHs), this class of compounds together with the precursors of all studied compounds, the polycyclic aromatic hydrocarbons (PAHs) is accentuated in following overview.

Some of physico-chemical and biological properties of studied analytes are summarized in Table 2.1. For all the compounds, CAS name and registry number, abbreviation used in this thesis, structural and chemical formula, appearance and monoisotopic molecular weight are listed below. It also includes dissociation constants [1], and specification of pure substances used in this project. Toxicological data are presented according to the International Agency for Research on Cancer (IARC) classification [2]: Group 1: The agent (mixture) is carcinogenic to humans. The exposure circumstance entails exposures that are carcinogenic to humans; Group 2A: The agent (mixture) is probably carcinogenic to humans. The exposure circumstance entails exposures that are probably carcinogenic to humans; Group 2B: The agent (mixture) is possibly carcinogenic to humans. The exposure circumstance entails exposures that are possibly carcinogenic to humans; Group 3: The agent (mixture, or exposure circumstance) is not classifiable as to carcinogenicity in humans; Group 4: The agent (mixture, or exposure circumstance) is probably not carcinogenic to humans.

Table 2.1 *Physico-chemical and biological properties of 1-nitronaphthalene, 2-nitronaphthalene, 1-aminonaphthalene, 2-aminonaphthalene, 1-hydroxynaphthalene, and 1-hydroxynaphthalene.*

1-NITRONAPHTHALENE Abbreviation: **1-NN**

CAS name: Naphthalene,1-nitro-

CAS registry number: 86-57-7

Chemical formula: $C_{10}H_7NO_2$

Relative molecular mass: 173.17

Appearance: Yellow crystals

IARC Group: 3

Structural Formula

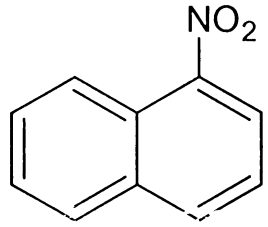

Producer: Fluka Purity: 99%

2-NITRONAPHTHALENE Abbreviation: **2-NN**

CAS name: Naphthalene,2-nitro-

CAS registry number: 581-89-5

Chemical formula: $C_{10}H_7NO_2$

Relative molecular mass: 173.17

Appearance: Colourless to yellow crystals

IARC Group: 3

Structural Formula

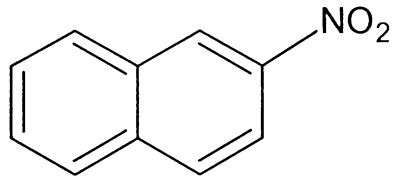

Producer: Fluka Purity: > 85%

1-AMINONAPHTHALENE Abbreviation: **1-AN**

CAS name: Naphthalene,1-amino-

CAS registry number: 134-32-7

Chemical formula: $C_{10}H_9N$

Relative molecular mass: 143.19

Appearance: White crystals

pKa: 3.92

IARC Group: 3

Structural Formula

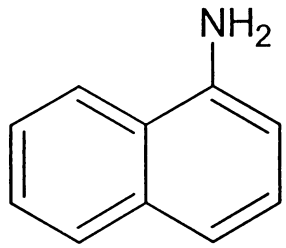

Producer: Fluka Purity: 99%

2-AMINONAPHTHALENE Abbreviation: **2-AN**

CAS name: Naphthalene,2-amino-

CAS registry number: 91-59-8

Chemical formula: $C_{10}H_9N$

Relative molecular mass: 143.19

Appearance: White to reddish crystals

pKa: 4.16

IARC Group: 1

Structural Formula

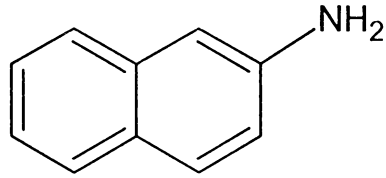

Producer: Aldrich Purity: 95%

1-HYDROXYNAPHTHALENE Abbreviation: **1-OHN**

CAS name: Naphthalene,1-hydroxy-

CAS registry number: 90-15-3

Chemical formula: $C_{10}H_8O$

Relative molecular mass: 144.18

Appearance: White, grey or tan crystals

pKa: 9.34

IARC Group: not classified

Structural Formula

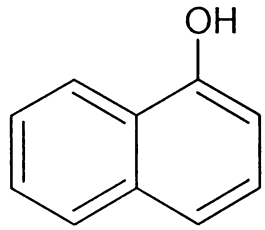

Producer: Aldrich Purity: 99%

2-HYDROXYNAPHTHALENE Abbreviation: **2-OHN**

CAS name: Naphthalene,1-hydroxy-

CAS registry number: 135-19-3

Chemical formula: $C_{10}H_8O$

Relative molecular mass: 144.18

Appearance: White or yellowish crystals

pKa: 9.51

IARC Group: not classified

Structural Formula

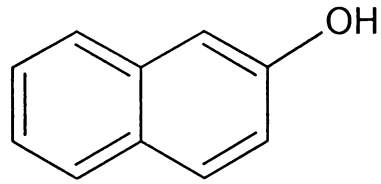

Producer: Aldrich Purity: 99%

2.2 Sources, formation, occurrence and biological effects of polycyclic aromatic hydrocarbons and their derivatives

2.2.1 Polycyclic aromatic hydrocarbons

PAHs represent an extensively studied group of chemical contaminants, because they are ubiquitous in the nature and have been shown to be positive in different genotoxicity tests as well carcinogenic in various animal species. These compounds can be formed by thermal decomposition of any organic material containing carbon and hydrogen resulting in at least two condensed ring system. The formation is based on two major mechanisms: (i) pyrolysis or incomplete combustion, (ii) carbonization process. The latter process leads to PAHs formation of non-anthropogenic origin in fossil fuels formed at low temperature over millions of years [3]. During incomplete combustion or pyrolysis, PAHs are supposed to be generated from small fragments via radical pathways. Once formed, they may undergo further pyrolytic reactions to form larger PAHs by intermolecular condensation or cyclization. The amount of PAHs formed depends on both the type of organic material and the temperature. In addition, PAHs are released from forest fires and volcanic eruptions [4]. Nevertheless, most of the PAHs are of anthropogenic origin generated mainly by incomplete combustion of petroleum derived products. These activities include i.e. processing of coal, crude oil and natural gas, including coal coking, coal conversion, petroleum refining and production of carbon blacks, creosote, coal tar and bitumen. Other human activities contributing to PAHs production are: (i) aluminum, iron and steel production in plants and foundries, (ii) heating in power plants and residences, open fires and cooking, (iii) combustion of refuse in incinerators, (iv) motor vehicle traffic, and (v) tobacco smoke [4,5,6]. Approximately 1000 tons of PAHs are released annually into the atmosphere through human activities. The concentrations of PAHs can be 10 000 times higher in industrial areas than in residential areas [7]. Their further distribution in environment is determined by physico-chemical properties. As PAHs are hydrophobic with low solubility in water, their affinity for the aquatic phase is lower than for the organic one. Therefore, they concentrate in organic fractions of aerosols, soil, sediments, and biota.

Naphthalene (N) is the simplest and most volatile from PAHs, therefore it prevails in gaseous phase of aerosols while other PAHs are present mainly in the particulate portion. In investigations of different gaseous and particulate extracts from air the following PAHs (in order of abundance) were detected: Naphthalene > fluorene > phenanthrene > fluoranthene > pyrene > benzo[a]pyrene [7,8,9]. The high occurrence of N is given by its presence in both

natural and anthropogenic sources. It is a natural constituent of coal tar and crude oil. Major anthropogenic sources of N are exhausts from motor vehicles and jets, residential heating with fossil fuels, gasoline burning and industrial plants. The worldwide industrial production of this substance is in the order of hundred thousand tons, EU producing about 200 000 tons [10] and USA about 215 000 tons annually [11]. It is mainly produced as a feedstock in the manufacture of phthalic anhydride for the synthesis of phthalate plasticizers and resins. Furthermore, it is used in the production of azo-dyes, 2-hydroxynaphthalene (an important intermediate in chemical industry) and naphthalene sulphonates, which are often used as plasticizers for concrete, dispersants and tanning agents in rubber and leather industry. Consumers can come across with naphthalene in products such as moth repellents, toilet-bowl deodorants and shaving brushes. A significant source of direct exposure is cigarette smoke [4].

The fate of PAHs in organisms is still subject of wide research. They enter the organism typically by ingestion, inhalation, or adsorption through the skin. The adverse effects of N in humans include nausea, vomiting, liver necrosis, convulsions, fever, anemia, and coma [7]. For many years, N had been considered as a non-carcinogen. Since 2000, when the US National Toxicology Program revealed clear evidence of its carcinogenic activity in rats, international agencies have reclassified N as a potential human carcinogen[12,13]. The IARC has concluded that there is **sufficient evidence** in experimental animals, but **inadequate evidence** in humans for the carcinogenicity of N, which was classified as **possibly carcinogenic to humans, group 2B** [13].

The substance itself does not seem to induce cancer in contrast to PAHs of higher molecular weight such as benzo[a]pyrene or dibenzo[a,l]pyrene. Their carcinogenicity is predominantly associated with the formation of diol-epoxides, which are largely resistant to the enzymatic hydrolysis, and so reach the DNA and form corresponding DNA adducts [10,14]. On the other hand, the N diol-epoxides are hydrolyzed to tetrahydroxynaphthalenes having no mutagenic properties. The main metabolic pathways of N in mammals are depicted at Fig. 2.1. From listed intermediates, the naphthoquinones (7, 10) were mentioned recently to be suspicious from cancer genesis. These electrophilic agents may lead to increased formation of reactive oxygen species inducing oxidative DNA damage or to increased covalent adducts formation with nucleophilic groups of the DNA bases. Both ways open possibilities to pathological modifications of healthy cells with subsequent carcinogenic processes [10]. Although studies concerning the mechanism of N cancer initiation are still on the hypothesis level, there is no hesitance of its carcinogenicity. Despite this fact, the exposure limits of N have not been lowered yet and are typically 50 mg m^{-3} for the workplaces atmosphere [10].

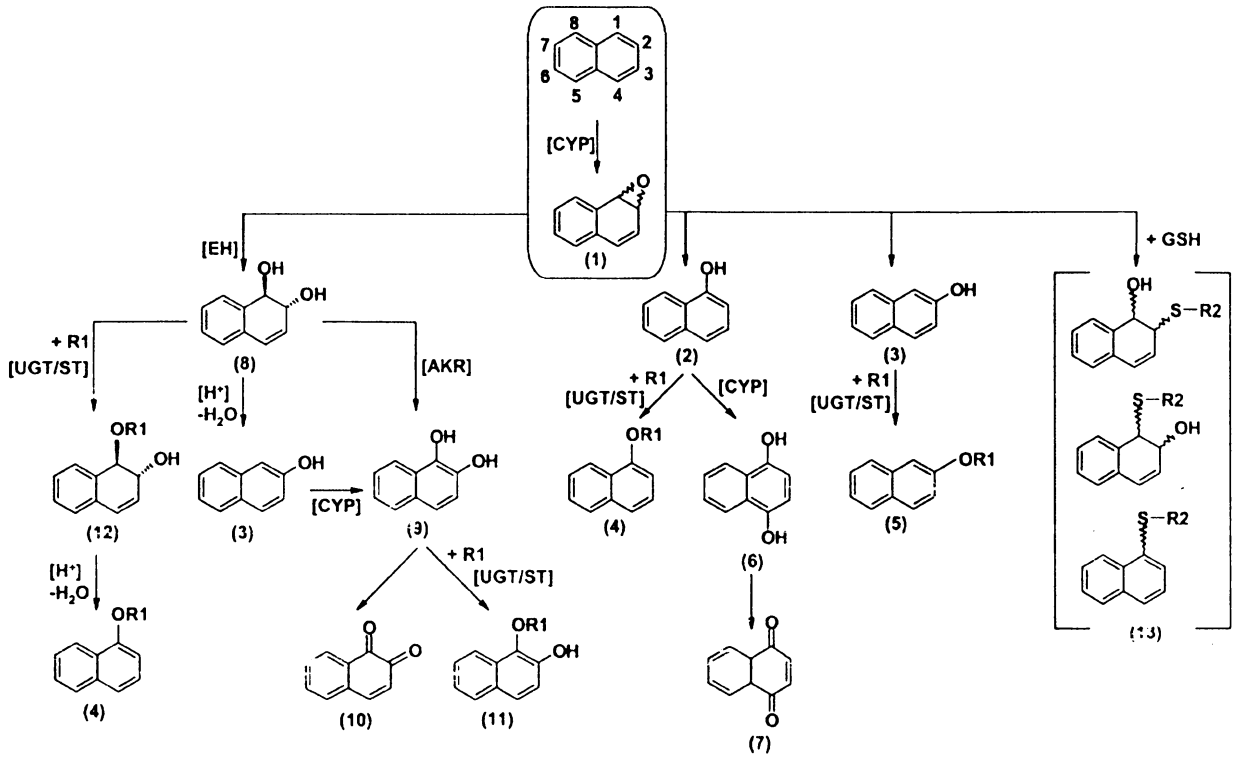

[Participating enzymes]: CYP – cytochrome P450-dependent mono-oxygenase enzymes; UGT/ST – UDP glucuronyltransferase/sulphotransferase; EH – epoxide hydrolase; AKR – aldo-keto reductase.
GSH – glutathione-SH; R1 – glucuronic acid/sulphate residue, R2 – N-acetyl-L-cysteine

Figure 2.1 ***Main metabolic pathways of naphthalene in mammals*** [10]***:***
Naphthalene is metabolized first to naphthalene 1,2-oxide (1). This reactive intermediate can subsequently undergo several reactions that lead to different hydroxylated polar metabolites, which are predominantly eliminated via the kidney. If the epoxides are not directly conjugated and excreted in the urine, they can undergo a spontaneous rearrangement to form 1-hydroxynaphthalene (2) and 2-hydroxynaphthalene (3). Both naphthols can be sulfated or glucuronidated and directly eliminated as conjugates (4) and (5). Additionally, 1-hydroxynaphthalene can be oxidized to form 1,4-dihydroxynaphthalene (6), which becomes further oxidized to form 1,4-naphthoquinone (7). Furthermore, the epoxide (1) can be hydrolysed by epoxide hydrolyse activity to form trans-1,2-dihydro-1,2-dihydroxynaphthalene (8). This dihydrodiol can be metabolized by three different pathways: (i) it becomes dehydrated to 2-naphthol (3), or (ii) it is oxidized to 1,2-naphthalenediol (9). This 1,2-naphthalenediol is the precursor either of 1,2-naphthoquinone (10) or of the corresponding glucuronide/sulphate conjugate (11). The third pathway (iii) for the dihydrodiol (8) is the glucuronic acid/sulphate conjugation (12) with potential subsequent dehydration (4). The formation of premercapturic and mercapturic acids, resulting from the glutathione conjugation, is another (13) pathway in the metabolism of naphthalene. Overall, 30 different naphthalene metabolites have been identified in the urine of mammals so far.

2.2.2 Nitro derivatives of polycyclic aromatic hydrocarbons

2.2.2.1 Sources and formation

Three main sources of NPAHs are believed to contribute significantly to the NPAHs occurrence in environment [15,16]: (i) the industrial production; (ii) NPAHs originating as direct or indirect products of incomplete combustion; (iii) NPAHs formed in the atmosphere from the gas-phase reactions of PAHs (generally adsorbed on particulate matter and themselves products of incomplete combustion) with four rings or less.

Ad (i): Only a few NPAHs including 1- and 2-NN are produced industrially. The treatment of naphthalene with mixed sulfuric/nitric acids at 60 °C yields 95% 1-NN and 5% 2-NN, together with traces of dinitronaphthalenes and dinaphthols [17]. From these products, 1-NN is used almost exclusively for catalytic reduction to 1-aminonaphthalene. Further uses, such as use as a deblooming agent for petroleum and oils and as a component in the formulation of explosives, are of historical interest only. 1,5- and 1,8-dinitronaphthalene formed at higher temperatures (80-100 °C) during the reaction are used as intermediates in the production of sensitizing agents for ammonium nitrate explosives or colorant intermediates for naphthoperinones synthesis [17]. Nevertheless, the industrial production of NPAHs is negligible in comparison with the total volume of chemicals produced worldwide and may contribute more significantly only to local pollution.

Ad (ii): During combustion processes, NPAHs are formed by the reactions of PAHs with nitrating species that are provided by the conversion of nitrogen and oxygen at high temperatures [18]. According to their volatility and polarity, NPAHs are distributed between the particle and vapor phase of combustion gases. Usually, 1-nitropyrene, 2-nitrofluorene, and 3-nitrofluoranthene are the dominating substances in the particulate phase and 1-nitropyrene is therefore used as a marker of NPAHs formation by combustions processes.

Ad (iii): The gas-phase formation of NPAHs from their parent PAHs with four rings or less in the atmosphere is thought to produce the majority of ambient NPAHs [19]. It was first independently proposed by Pitts et al. [20] and Jäger [21] in 1978. Pitts used his results seven years later to explain the unexpected presence of 2-nitrofluoranthene and 2-nitropyrene in particulate organic matter sampled in the Los Angeles basin in California [22]. These two NPAHs have not been identified in any combustion products, but later were found in different locations of USA [23,24], Europe [25,26,27] as well as in forest and remote areas of America and Asia [28]. Further studies showing differences in daytime/nighttime [24,29,30] and seasonal [31,32]

concentrations of certain NPAHs provided further support for the gas-phase formation of NPAHs. As result, three mechanisms for formation of NPAHs in the atmosphere from PAHs were proposed:

- Daytime gas-phase reaction: Hydroxyl radical addition to the PAH followed by reaction with nitrogen dioxide and loss of a water molecule (formation of 2-nitrofluoranthene, 2-nitropyrene, and 3-nitrofluorene);
- Nighttime gas-phase reaction: Nitrate radical addition to the PAH followed by reaction with nitrogen dioxide and loss of nitric acid (formation of high yields of 2-nitrofluoranthene, nitronaphthalenes and methylnitronaphthalenes);
- Heterogeneous gas-particle interaction of parent PAHs adsorbed onto particles with nitrating agents (would be expected to produce electrophilic nitration products). This has been shown to occur in the laboratory under conditions of very high concentrations of nitrogen dioxide. Recent ambient measurements suggest that some 9-nitroanthracene may be formed by heterogeneous reactions during transport [21].

In Fig. 2.2, the main proposed pathway for formation of nitronaphthalenes, the nighttime reaction of naphthalene (1) with nitrate radical NO_3 is depicted. It occurs by the initial addition of the nitrate radical to the aromatic ring to form a nitratocyclohexadienyl-type radical (2), which then decomposes back to reactants, reacts with nitrogen dioxide forming nitronaphthalenes (3), or decomposes forming naphthols (4) and nitronaphthols (5) (ref. [33]). In ambient atmosphere, the radical is formed by the reaction of nitrogen dioxide with ozone (Eq. 2.1). The concentration of the NO_3 radical is low during daylight hours because of its rapid photolysis (photolysis lifetime at solar noon of approximately 5 s) (Eq. 2.2) and the rapid reactions of nitrate with nitric oxide (Eq. 2.3) and nitric oxide with ozone (Eq. 2.4) [34]. During nighttime hours the average NO_3 concentrations in the lower troposphere over continental areas have been estimated as 510^8 molecules/cm^3 (~20 ppt) [19].

$$NO_2 + O_3 \leftrightarrow NO_3 + O_2 \quad (2.1)$$

$$NO_3 \leftrightarrow NO_2 + O \quad (2.2)$$

$$NO_3 + NO \rightarrow 2NO_2 \quad (2.3)$$

$$NO + O_3 \rightarrow NO_2 + O_2 \quad (2.4)$$

The reaction yields of 1-NN and 2-NN were estimated to be 3-24.4% for each compound when simulating in laboratory nighttime reactions in N_2O_5 - NO_3 - NO_2 - air mixtures [19,33]. Nevertheless, it was proved the smaller amounts of both compounds are formed also during the daytime reaction with hydroxyl radical [19].

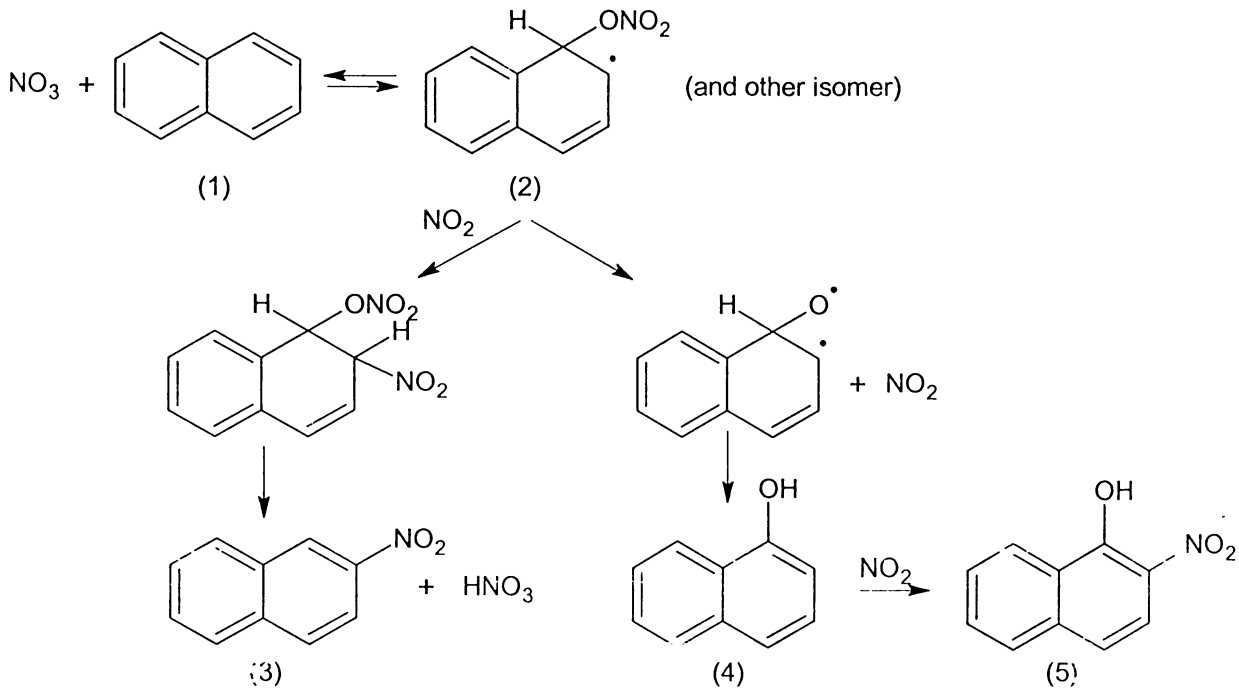

Figure 2.2 *Proposed pathway for formation of nitronaphthalenes in N_2O_5 - NO_3 - NO_2 - air mixtures* [33].

To identify the source of pollution, the NPAHs profile, or the relative quantities of certain "marker" PAHs, is a pointer to the source of formation of the NPAH. The most abundant nitro isomers of pyrene, fluorene and fluoranthene observed in diesel exhaust are 3-nitrofluoranthene, 2-nitrofluorene, and 1-nitropyrene, whereas the isomers formed from the hydroxyl radical reactions of these PAHs in atmosphere are 2-nitrofluoranthene, 3-nitrofluorene, and 2-nitropyrene. Other less important pathways of NPAHs production are endogenous formation of NPAHs in the body due to reaction of PAHs ingested in food or inhaled in ambient air with nitrogen dioxide from, for example, cigarette smoke [35,36].

2.2.2.2 Occurrence and concentration levels of NPAHs in the environment

As mentioned above, one of the main primary sources of NPAHs include combustion gases. Thus, NPAHs have been observed in vehicle exhaust (particularly diesel), industrial emissions and emissions from domestic residential heating/cooking and wood burning together with hundreds of other organic compounds. The concentration of NPAHs differs substantially from sample to sample, e.g. concentrations of 7-165 $\mu g\, g^{-1}$ of the marker 1-nitropyrene have been reported in diesel particulate phase [37]. 1-NN and 2-NN as the most volatile NPAHs are typically found exclusively in the vapor phase of combustion gases.

The highest levels of NPAHs in the environment have been reported in urban air as a result of traffic and domestic heating. The secondary source of NPAHs in ambient air is the gas phase formation from parent PAHs discussed in previous chapter. Nitronaphthalenes have been reported many times to be the most abundant NPAHs in traffic impacted and industrial areas, mostly in the gas-phase of air, 2-nitrofluoranthene, 9-nitrophenanthrene and 9-nitroanthracene being usually the most abundant NPAHs observed in ambient particulate organic matter extracts. However, in the ambient air samples where vapor-phase as well as particulate phase NPAHs have been measured, the more volatile nitronaphthalenes and methylnitronaphthalenes prevailed [23,38]. Interestingly, nitronaphthalenes have been identified as the most present NPAHs also in Antarctica (1-200 fg m^{-3} range) [39]. The concentration levels of 1- and 2-NN in ambient air found in heavy polluted areas are listed in Table 2.2. In urban and suburban sites the concentrations of NPAHs depend, for example, on the climatic conditions (the concentrations of most NPAHs are several times higher in summer and autumn than in winter and spring), the dayphase, the number and regulation of traffic vehicles and the type of heating used. In cities, the levels of most abundant NPAHs mentioned above can reach values about 4 ng m^{-3}, however, in urban areas of developed countries they are usually lower, below 1 ng m^{-3}.

Other typical sources of NPAHs include photocopier toners, carbon black, foodstuffs and soil sediments [40,41], in Table 2.3 concentrations of nitronaphthalenes in selected matrices are given. In food, the highest concentrations have been found in spices and smoked food, but also in vegetables and fruits, probably due to atmospheric pollution. Surveys of NPAHs levels in beverages by Schlemitz and Pfannhauser showed that substantial concentrations of NPAHs were present in tea and coffee [42,43]. They have investigated six NPAHs including 1-NN and 2-NN and found very high concentrations of NPAHs (128 μg kg^{-1}) and PAHs (7536 μg kg^{-1}) in Mate tea, which is roasted with combustion fumes to gain its unique aroma. Other teas had NPAHs concentrations of around 20 μg kg^{-1} with 1- and 2-NN concentration < 1 μg kg^{-1}. Although NPAHs are usually not very soluble in water, the authors found that up to 25% of the NPAH concentration could be measured in the tea water. It is possible that other components of the tea act as co-solvents and increase the solubility of NPAHs in the tea water. The presence of NPAHs and PAHs in tea probably originates from several sources, including technological processes used during the preparation of tea, such as roasting and drying, and atmospheric pollution.

The other often mentioned source of NPAHs – cigarette smoke – is still questionable, although parent PAHs have been detected in tobacco smoke [44], there are no reports of NPAHs

in cigarette smoke condensate. 1-NN, 1-nitropyrene and others were not detected at a detection level of <10 ng/cigarette [45] or <50 pg [46]. Nevertheless, mutagenic effect can be induced by the presence of even a single molecule, therefore sources of direct exposure, such as cigarette smoke are counted as highly hazardous.

Table 2.2 *The concentrations of 1-NN and 2-NN in gas particulate (P) and vapor (V) phase of ambient air in selected heavily polluted areas (adapted from ref. [16]).*

Location; type of sample	Phase	Concentration [ng m^{-3}]			Ref.
		1-NN	2-NN	Total NPAHs	
Glendora, California, USA; daytime (nighttime) composite sample	V+P	2.7 (5.7)	2.6 (3.1)	5.8 (11.1)	47
Concord, California, USA; daytime composite sample	V+P	0.1	0.17	0.59	47
Redlands, California, USA; nighttime sample	V	4.7	2.3	13	48
Fresno, California, USA; daytime composite sample, December-January	V+P	0.39	0.55	1.4	29
Sapporo, Japan	P	0.9	0.55	2.22	49
Houston, Texas, USA; annual average	V+P	0.35	0.07	0.6	38
Florence, Italy; 48 hours average, January–February	P	0.21	0.23	1.5	50

Table 2.3 *The occurrence and concentration levels of 1-NN and 2-NN in human environment (adapted from ref. [16]).*

Matrix	Concentration [μg kg^{-1}]		Ref.
	1-NN	2-NN	
river water, Japan	$1.3 \cdot 10^{-3}$	$11.7 \cdot 10^{-3}$	51
incinerator ash	$(1.59\text{-}2.86) \cdot 10^{3}$	$(1.06\text{-}3.46) \cdot 10^{3}$	52
lettuce, parsley	–	<0.2	43
spices (paprika / marjoram / caraway)	–	7.8 / 3.6 / 3.1	43
smoked cheese	0.6	–	53
smoked meat / grilled meat	–	10.2 / 0.1	43
smoked fish / grilled fish	0.2 / 0.3	–	53
smoked sausage / grilled sausage	–	8.2 / <0.2	43
Earl Grey tea	0.90	1.38	42
mate tea: roasted / green	0.47 / nd	4.09 / 1.52	42
Formosa Sencha (green tea)	nd	1.05	42
peppermint tea	0.46	0.85	42
fruit tea (instant)	0.82	0.22	42
coffee (ground beans)	4.0	30.1	53

– no data available; nd - not detected

2.2.2.3 Metabolism, mutagenicity and carcinogenicity of NPAHs

NPAHs constitute a group of chemicals with a wide spectrum of genotoxic, mutagenic and/or carcinogenic properties. The toxic effects are extensively studied since 1977, when it was discovered that organic extracts of collected particles from several places exhibit direct mutagenicity when tested in the Ames *Salmonella typhimurium* bacterial assay [54]. Non-substitued PAHs, also abundant in such samples, are mutagenic only after metabolic activation. The knowledge of metabolism of NPAHs is indispensable when elucidating mutagenic and carcinogenic effects of NPAHs. Due to the large amount of compounds, the metabolism *in vivo* of only a few substances, including 1-nitropyrene and 2-nitrofluorene, has been studied in detail. However, from the results on studied compounds, it seems that there are at least five metabolic activation pathways through which mutations can be induced by NPAHs in bacterial and mammalian systems and/or through which DNA binding occurs. These are (see Figure 2.3) [55,56,57]:

1) nitroreduction;

2) nitroreduction followed by esterification (in particular acetylation)

3) ring oxidation;

4) ring oxidation and nitroreduction;

5) ring oxidation and nitroreduction followed by esterification.

In bacteria, nitroreduction seems to be the major metabolic pathway whereas the fungus *Cunninghamella elegans* is an example of where NPAHs are metabolized by ring oxidation [58]. The studies of mammalian metabolism proved that enzymes involved in metabolic pathways – in particular those of cytochrome P450 – may be different in metabolism of a specific NPAH [59] and may vary from species to species and in different target organs [60,61]. The nitroreduction of NPAHs *in vivo* probably occurs mainly by bacteria in the intestinal tract. Both bacterial and mammalian enzymatic systems are capable of reductively metabolizing NPAHs under anaerobic and aerobic conditions, as depicted in Fig. 2.4. The nitroreduction of a NPAH (I) may involve one- and/or two-electron transfers and results in the formation of the corresponding nitrosoPAH (III), further reduction to the *N*-hydroxyaminoPAH (IV) and final reduction to the aminoPAH (V), which are excreted in the urine after acetylation. The reaction proceeds via one nitro radical (II) and two non radical intermediates (III and IV). In mammalian cells, nitroreduction is catalyzed by a variety of enzymes, including NADPH cytochrome P450 reductase [62]. In oxidative metabolism on the aromatic ring, the first step is transformation to phase I primary metabolites, such as epoxides, phenols and dihydrodiols, and then to secondary metabolites, such as diol epoxides, tetrahydrotetrols and phenol

epoxides. In mammalian systems, the phase I metabolites are then conjugated with glutathione, sulfate or glucuronic acid to form phase II metabolites, which are more polar and water soluble than the parent hydrocarbons. On reaching the intestine, the conjugated metabolites can be deconjugated by the intestinal microflora and absorbed, entering the enterohepatic recirculation. Further nitroreduction and *N*-acetylation can occur, resulting in the excretion in urine and faeces.

The toxic effects of NPAHs are attributed to the formation of free reactive nitroaromatic anion radicals and with conjugation reactions of metabolism intermediates with the cellular macromolecules such as proteins and DNA. The key place for the mutagenic activation is the nitrogroup after reduction to hydroxylamine, which is instable and readily forms electrophilic nitrenium ion ($-N^+$), which binds to DNA [55,63]. This reaction can occur also after deacetylation (to arylhydroxyamines) or *O*-acetylation (e.g., 1,8- and 1,6-dinitropyrene). Some NPAHs (e.g., 6-nitrobenzo[*a*]pyrene) may be mutagenic only after activation by oxidation to reactive epoxides or dihydrodiol epoxides, nevertheless this activation is less common. The main DNA adducts detected with NPAHs *in vivo* and *in vitro* are *N*-(deoxyguanosin-8-yl) (C8-substituted deoxyguanosine [dG]) derivatives. The DNA adducts resulting from the nitroreduction of NPAHs are better characterized than those arising from oxidative metabolism, although the latter may be of more importance in mammalian metabolism. There is recent evidence for oxidative metabolism, e.g., in the genotoxicity of 2-NN in human lymphoblastoid cell lines [64].

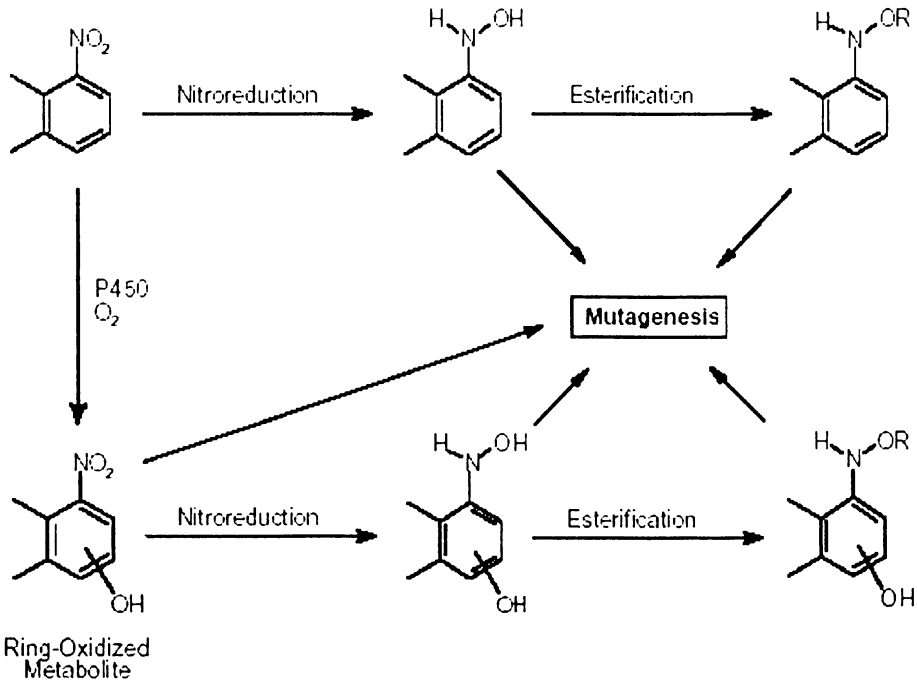

Figure 2.3 *Metabolic activation pathways of NPAHs leading to mutation* [55].

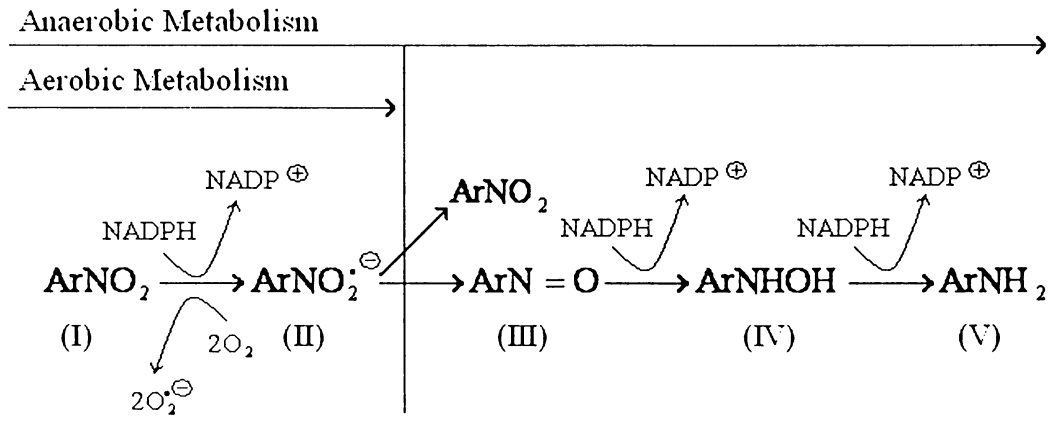

Figure 2.4 *Aerobic and anaerobic metabolism of NPAHs.*

The toxicological effects of NPAHs are subjects of ongoing studies. Some NPAHs are known carcinogens (e.g. 1-nitropyrene, 6-nitrochrysene, 2-nitrofluorene), and almost all NPAHs are proved mutagens *in vitro*. Mutagenicity screening studies are of big importance because about half of all carcinogenic chemicals tested in animals are mutagens that damage DNA in microbial short-term tests [65]. Elucidation of the relationships between the structural and electronic features of NPAHs (i.e. the first half-wave reduction potential, the orientation and number of the nitro group, the molecular dimensions, degree of aromaticity, hydrophobicity and the number of electrons involved in the first step of the nitroreduction) and their biological activities, including mutagenicity, may prove useful in predicting the human health risks posed by these compounds. For example, the mutagenic potency of dinitroderivatives in *Salmonella typhimurium* was revealed to be higher for several NPAHs including dinitronaphthalenes than that of mononitroderivatives and increasing tendency towards higher mutagenic potency with increasing number of rings (two to four), not followed for NPAHs with five rings, was revealed [66]. These two trends are in concordance with high mutagenicity of dinitropyrene derivatives. The orientation of the nitro group is another important structural factor in determining the mutagenic activity of NPAHs - it is suggested that NPAHs with their nitro group oriented perpendicular or nearly perpendicular to the plane of the aromatic rings generally exhibit weak or no mutagenicity [67,68,69], probably because of the inability of the aromatic system to fit into the active site of the bacterial nitroreductases due to steric interactions [67]. From the electrochemical point of view, interesting are studies showing positive correlation between reduction potential and direct mutagenicity of structurally similar NPAHs [69]. For nitrated naphthalenes including 1-NN and 2-NN a good

correlation was reported between the cytosolic nitroreductase activities from rat liver and single electron reduction potential measured by cyclic voltammetry [70].

1-NN and 2-NN have been examinated on genotoxicity *in vitro* on bacteria, fungi, plants and mammalian or human cells and *in vivo* studies on *Drosophila megalomanster* and rodents. 1-NN induced no sex-linked recessive lethal mutations, but did induce somatic mutation/recombinations in *Drosophila*. *In vitro* results on bacteria and mammalian cells further indicated DNA damage and gene mutations. Studies on 2-NN revealed inconclusive results on genotoxicity *in vivo* on *Drosophila megalomanster* and rodents. On the other hand, i*n vitro* results on gene mutation in bacteria and human cells revealed clearly positive results. However, there are little data from studies on experimental animals and no data available from studies in humans on the carcinogenicity of 1- and 2-NN. Therefore, the IARC overall evaluation for both compounds is that they are **not classifiable as to their carcinogenicity to humans, group 3** (ref. [2]).

2.2.3 Amino derivatives of polycyclic aromatic hydrocarbons

Amino derivatives of polycylic aromatic hydrocarbons (APAHs) are together with PAHs and NPAHs well known chemical mutagens and/or carcinogens. In comparison to the latter mentioned classes of compounds, APAHs are mainly of anthropogenic origin, because they are very useful chemicals from an industrial point of view. They have been extensively used in manufacturing of dyes, as additives to polymer and rubber compounds, or as intermediates in the manufacturing of other industrial chemicals, e.g. pesticides, medicines, and surfactants [71,72,73]. Thus, they are rarely intended to be present in the final product, but can be found as residuals from incomplete reactions, as by-products, or as degradation products either from intermediate chemicals or final products [71,73,74]. Therefore, they can be found in a variety of workplaces and also in the industrial effluents. APAHs including aminonaphthalenes have been further identified in crude oil and oil distillation products, as well as in cigarette smoke and river water [72,73]. Further, APAHs are metabolites of their parent NPAHs and can be formed in small amounts in radical atmospheric reactions. The most important issue is their toxicological effect.

Many APAHs are toxic compounds and/or suspected human carcinogens [71,75,76]. The combination of a potentially high exposure and high toxicity explains why the use of these chemicals is monitored and regulated [77,78,79,80]. A correlation between aromatic amine exposure and human cancer was first reported already in 1895, as bladder cancer was observed among

workers in dye industry [81]. 2-AN was probably one of causative agents in this case, because other studies conducted independently in the 1950s and 1960s showed that occupational exposure to 2-AN, either alone or as an impurity in other compounds, is causally associated with the occurrence of bladder cancer in humans [82]. The latent period between exposure and development of bladder cancer is lengthy [83], but for longer exposure than 5 years the cancer developes in more than 95 % of cases [84]. The carcinogenicity of 2-AN was confirmed also by oral administration in many animal species (hamsters, dogs and nonhuman primates). Mutagenic effect was confirmed in yeast, plants and bacteria [85]. These results substantiated the classification of 2-AN as **carcinogenic to humans (IARC, Group 1)**. On the other hand, the carcinogenicity of 1-AN is equivocal – an excess occurrence of bladder cancer was observed in workers who had been exposed to commercial 1-AN for five or more years who had not also been engaged in the production of 2-AN. However, commercial 1-AN made at that time may have contained 4-10% of 2-AN [82]. No carcinogenic effects of 1-AN were observed following oral administration to mice, hamsters and dogs [82]. No data are available on the genetic and related effects of 1-AN in humans, nevertheless it is mutagenic to bacteria [85]. Novadays, the overall evaluation of IARC categorizes 1-AN **as not classifiable as to its carcinogenicity to humans (Group 3)**.

The different biological effects of both compounds are probably caused by different metabolic pathway in the organism. Metabolic activation of the carcinogenic aromatic amines proceeds by pathways involving either an initial hydroxylation of the amine group (N-hydroxylation) followed by further enzyme-mediated reactions or ring-hydroxylation in *ortho* position to the amine. N-hydroxylation is the primary stage in the conversion of aromatic amines to their ultimate carcinogenic forms. Many of these activated aromatic amines or their more stable conjugates are transported to the bladder. The acidic conditions of the urine facilitate the formation of reactive electrophile, nitrenium ion $Ar\text{-}N^{+}\text{-}R$ (Ar aryl group, R alkyl, aryl or hydrogen atom) that interacts with the tissue. 2-AN is N-hydroxylated to the reactive product N-hydroxy-2-naphthylamine, that is transported to the bladder as the N-glucuronide, which is unstable at low pH values [41]. This product reacts with variety of macromolecules under mildly acidic conditions. Nucleoside adducts 1-(N-deoxyguanosinyl)-2-naphthylamine, 2-(N-deoxyguanosinyl)-2-naphthylamine and purine ring-opened derivative 1,5-(2,6-diamino-4-oxo)pyrimidinyl-N-deoxyriboside-3-(2-naphthylurea) have been identified *in vitro* after enzymatic hydrolysis of DNA. On the other hand, 1-AN appears to be non-carcinogenic, most likely because the ring hydroxylation occurs at the expense of N-hydroxylation. If, however, N-hydroxy-1-naphthylamine is synthesized, it acts as

N-hydroxy-2-naphthylamine. Even though 2-aminonaphthalene used to be very important in the manufacture of the so-called tar or aniline dyes, it is no longer produced because of its adverse effects to humans and can still be found only as a by product of technical processes [86].

2.2.4 Hydroxy derivatives of polycyclic aromatic hydrocarbons

Hydroxy derivatives of PAHs (OHPAHs) are of big importance mainly in monitoring of human exposure to PAHs, because following inhalative, oral or dermal resorption PAHs are converted to epoxy and hydroxy derivatives by various enzymes, as described in chapter 2.2.1. Thus, measuring of PAHs metabolites in urine represent a direct approach to assess working and living conditions. 1-hydroxypyrene, the only urinary metabolite of pyrene, is preferentially used as a biomarker for PAH exposure at workplaces, because pyrene is present in most of PAHs mixtures [87,88,89,90]. Apart from 1-hydroxypyrene, the determination of various phenanthrene metabolites [89,91] as well as selected isomeric hydroxybenzo[*a*]pyrenes [90,92] in urine has been described. 1-OHN and 2-OHN as major metabolites of naphthalene [10] were used for the assessment of human occupational and environmental exposure to PAHs, at naphthalene producing plant [93], plant processing naphthalene oil [94], iron foundries [95,96], creosote impregnation facilities [97], and for workers employed in road bituminization [98]. In an extended study conducted in Germany on 277 volunteers, the highest 1-OHN and 2-OHN levels were found in urine of converter bricklayers (120.1 μg L^{-1}), coal-tar distillation workers (56.0 μg L^{-1}), and coking plant workers (29.5 μg L^{-1}). A good correlation was found between naphthalene in air and urinary naphthols concentrations. Biological monitoring revealed concentrations of the sum of both metabolites in smokers to be increased by a factor 1.6-6.4 compared to that in non-smokers at the same workplaces [99]. Elevated levels of naphthols for cigarette smokers were reported also in other studies [96, 100, 101]. Further, naphthols are degradation products [102] and also metabolites [103] of several widely used pesticides such as carbaryl (1-naphthyl-methylcarbamate), a broad-spectrum industrial insecticide registered for use in USA, Canada and many european countries [104]. 1-OHN is the major degradation product of this pesticide. Moreover, both 1-OHN and 2-OHN have been used as a raw materials for many purposes in the pharmaceutical industry [105]. Therefore, determination of 1-OHN in the presence of 2-OHN is also important in these applications. The toxicological data for 1- and 2-OHN are inconsistent. Both are not classified by the IARC.

2.3 Analytical methods for determination of PAHs and their derivatives

Chemical properties of PAHs and their nitro, amino, and hydroxy derivatives offer a variety of determination modes. The UV-spectrophotometric detection is universal for all mentioned classes of compounds after HPLC separation, similarly the flame ionisation detector (FID) can be employed in connection with gas chromatography (GC). Nevertheless, other methods may provide higher sensitivity and selectivity for determination in complex matrices and are often preferred. The determination requires usually an extraction and purification step depending on the matrix. In following chapter the common methods for the determination of PAHs and their nitro, amino, and hydroxy and derivatives are summarized. The electrochemical methods have been used less frequently so far, some examples concerning the use of HPLC with electrochemical detection (HPLC-ED) methods are specified in Table 2.4, enclosed at the end of this chapter.

2.3.1 Polycyclic aromatic hydrocarbons

The ubiquity of PAHs in the environment requires ambient monitoring especially of air, water and soils by certified national institutions using validated methods. PAHs are extracted from samples with a Soxhlet apparatus or ultrasonically (from filters loaded with particulate matter, vehicle exhausts, sediments), by liquid-liquid partition or solid phase extraction (water samples), after sample dissolution (fats, vegetable, mineral oil) or alkaline digestion with a selective solvent (meat products). Extracted samples are usually further purified by column chromatography, particularly on alumina, silica gel, or Sephadex LH-20, but also by thin-layer chromatography. Identification and quantitation of PAHs is routinely performed by GC-MS and GC-FID or by HPLC with ultraviolet, fluorescence and more recently mass spectrometric detection, generally in series. In gas chromatography, fused silica capillary columns are used, with polysiloxanes as stationary phases; silica-C_{18} columns are commonly used in HPLC [4]. As the efficiency of separation that can be achieved with HPLC columns is much lower than that with capillary gas chromatography, HPLC is generally less suitable for analysis of samples containing complex PAH mixtures. The advantages of HPLC derive from the possible choise of column packing materials, enabling separation of various isomers that cannot be separated efficiently on the usual capillary GC columns and the capabilities of the detectors with which it is used. Beside the selective and sensitive

fluorescence detection, the electrochemical activity of higher PAHs also allows determination by amperometric methods using normal-sized electrodes or microelectrodes as working electrodes [106,107]. Amperometric detection should be universally applicable, since all PAHs can be determined by electrooxidation giving radical cations [108] and can be used for the determination of non-fluorescent PAHs. The merits of amperometric detection, such as sensitivity, limits of detection and linear range are comparable or slightly better than those of UV detectors [106,109]. The applicability of HPLC-ED was demonstrated e.g. on the analysis of selected PAHs listed in the German drinking water standard in water samples [106]. The analytical methods for PAHs determination are regularly reviewed [4,110,111].

2.3.2 Nitro derivatives of polycyclic aromatic hydrocarbons

The determination of NAPHs in environmental samples is of particular interest because of their possible mutagenic and carcinogenic effects. Not only their quantitation, but also isomer-specific identification is often requested, as the biological activity depends on the position of the nitro substituent. The problems in the analysis are presented by a variety of environmental matrices, where NPAHs occur. As they are very complex, the samples often contain thousands of compounds, including parent PAHs and other closely related derivatives (in particular oxygenated PAHs such as aldehydes, ketones and carboxylic acids), which tend to coelute with NPAHs under a variety of liquid and gas chromatographic conditions and are present at concentrations 1 or 2 orders of magnitude higher than those of the nitro substituted compounds [112,113]. A direct analysis of NPAHs is therefore often not possible and the analytical methods must include an extensive sample cleanup and preliminary extraction and prefractionation step.

Some methods for NPAHs determination are more of historical importance, e.g. thin layer chromatography (TLC), which is rather simple and inexpensive technique. The detection and characterization of seven NPAHs by fluorescence quenching after TLC was described already by Jäger in 1978 [21] – NPAHs were reduced with potassium borohydride solution to the corresponding APAHs, which are intensely fluorescent. Limit of detection for 1-NN was 500 ng. UV illumination before and after application of potassium borohydride solution was used also by TLC at plates coated with a silica gel layer for determination of PAHs and their amino and nitro derivatives; dichloromethane pure, and in mixture with *n*-hexane and methanol was used as mobile phases [114]. TLC has been used for a preliminary separation of NPAH as well [21].

The more frequently used methods for NPAHs determination were subject of several reviews [41,115,116,117] and include [16]:

- gas chromatography combined with a FID [118,119,120,121], the thermionic (TID) or nitrogen-phosphorus selective [122,123] detector (NPD), electron capture detector (ECD) [120], or chemiluminiscence-based thermal energy analyzer (TEA) [124,125,126]. The last one is very selective, because only compounds containing NO_2 and NO functional groups can be detected, therefore the detector has been employed for analysis of complex mixtures with detection limits as low as 8 and 7 pg for 1-NN and 2-NN, respectively [124]. The ECD gives strong signal to other electronegative species such as oxygenated PAHs, but is usually more sensitive. Detection limit of 1 pg was reported for 1-NN [120]. GC-NPD analysis has been shown to be a valuable screening technique for NPAHs in complex samples such as diesel praticulate following a prefractionation using another instrumental technique [122]. The universal FID is more frequently used for measuring of retention characteristics of NPAHs [118,119], its use in practical analysis is very confined due to low sensitivity and selectivity [120,121].
- HPLC combined with fluorescence [127,128,129](FD), chemiluminiscence (CHLD) [130,131,132], or electrochemical [129,133,134,135] detector. The FD works only after reduction of NPAHs to APAHs, because NPAHs produce very low yield of fluorescence after irradiation by the UV light, as a result of the strong electron withdrawing effect of a nitro group. Several methods were developed to reduce NPAHs to APAHs, e.g. by using on-line zinc [129,131] or Pt/Rh reduction [128,132,136]. In the above methods, an extra-column was required for packing the zinc powder or Pt/Rh-coated alumina. The detection limits for CHLD can be about two orders lower than those with fluorescence [132,136]. For 1-nitropyrene, limit of determination (LOD) of $4 \cdot 10^{-10}$ mol L^{-1} using CHLD was achieved, for dinitroderivatives of pyrene it was even one order of magnitude lower [136]. Another alternative is the use of the electrochemical method for NPAHs reduction prior fluorescence or chemiluminiscence detection [127]. Moreover, electrochemical detection in itself has been applied as a simple, sensitive, and reproducible method for the reducible NPAHs [135]. Some examples of HPLC-ED determinations are characterized in Table 2.4.
- gas chromatography-mass spectrometry (GC-MS) in electron impact (EI) [120,124,137,138], positive ion chemical ionization [139,140141,142] or negative ion chemical ionization (NICI) electron capture (EC) [120,137,141] mode. GC-MS provides information on the actual structure of molecules and therefore can allow identification of compounds when no standard is available. GC-NICI-MS is a very powerful technique for analysis of air and diesel

particulates [140,141]. The detection limit can be as low as 0.3 pg for 1-NN per injection [139]. The LODs achieved by EI ionisation are usually higher [137], i.e. Sekyra [138] has analyzed NPAHs in air particulate matter with LOD 5 pg for both 1-NN and 2-NN.

- EC-MS, which also provides adequate sensitivity and selectivity for the analysis of NPAHs in most matrices [113]; however, there is still difficulty due to interference from oxyPAHs [143].
- tandem mass spectrometry (MS/MS) [142]. Combining this technique with GC-EC gives four „separation" stages: a chromatographic separation, a selective ionization method and two mass spectrometric analyses [144].

More recent developments in this field include (i) selective detection of several NPAHs by using time-of-flight MS [145,146]; (ii) a method using supercritical fluid extraction and on-line multidimensional chromatographic methods (normal-phase high-performance liquid chromatography coupled to a high-resolution GC) and ion trap detector MS [27,147]; and (iii) particle beam liquid chromatography-MS with NICI mode [148]. Using this method, the detection limits for several NPAHs were at the picogram level. However, the most volatile 1-NN and 2-NN were not detectable even at microgram levels, which was explained by their loss in the momentum separator. Alternative separation methods, e.g. micellar electrokinetic chromatography, succeeded in separation of mononitro-naphthalenes and biphenyls, however, no application to real matrix was presented [149].

It follows from this overview that the analysis of NPAHs in real samples requires a complex approach and can be hindered by a lack of adequate instrumental sensitivity or selectivity and limited availability of native and isotope-labelled standards. The full identification and quantification of sample composition requires often a combination of several analytical techniques. The electrochemical methods of detection, which will be discussed in next chapter, offer the possibility of inexpensive and fast screening of environmental matrices as alternative to the time consuming and expensive separation approaches. Moreover, the studies on electrochemistry of NPAHs are unevitable when developing new electrochemical detectors, which enable relatively selective and sensitive detection of NPAHs after their chromatographic separation. This detection is based on the electrochemical reaction of analytes at the electrode surface, which requires electrically conductive, and oxygen free mobile phase and samples. Oxygen reduction current causes an increase in the background current and also limits the useful working electrode potential window. To avoid the presence of oxygen, connecting tubing in the HPLC system impermeable to oxygen has to be used and mobile phase must be degassed. Typical detectors

are of the thin-layer [133,150,151] or wall-jet [152] type using three electrode system with working, reference and auxiliary electrode. Largely, a glassy carbon [133,152] or a gold/mercury [150,151] working electrodes have been used. Most electrochemical detectors were operating in the constant reductive amperometric mode. Attempts to use the detector in the differential-pulse mode were not very successful [150]. Some examples for HPLC-ED determination of nitronaphthalenes are listed in Table 2.4.

2.3.3 Amino derivatives of polycyclic aromatic hydrocarbons

Aromatic amines are another class of environmental pollutants, introduced in chapter 2.2.3. The analytical methods for their identification in environment depend on the matrix similarly to PAHs. Low cost and simple direct spectrometric and electrochemical methods could by used for analysis of more simple matrices, e.g. urine, where APAHs are present as biological markers, in assessing human exposure to their parent NPAHs [117]. The spectrometric methods for the determination of APAH are performed directly or after derivatization [153,154], which is based on the formation of azodyes. The electrochemical methods take the advantage of anodic oxidation of the amino group, therefore voltammetric methods as DC and differential pulse voltammetry on suitable solid or carbon paste electrodes have been applied to determination of APAHs [155,156]. The electrochemical behaviour of 1-AN, 2-AN, and 2-aminobiphenyl has been studied at carbon paste electrode (CPE), screen printed carbon electrode (SPE), and on both electrodes modified with α-, β- and γ-cyclodextrin. The values of LODs were approximately one order of magnitude lower for the modified SPE than those for modified CPE and reached the levels as low as 10^{-9} mol dm^{-3} (ref. [157]). Rotating glassy carbon electrode was also used for the determination of 4-aminobiphenyl in acetic acid (0.1 mol L^{-1})/methanol media with detection limit of $5 \cdot 10^{-7}$ mol L^{-1} when using differential pulse voltammetry[158]. Spectrophotometric and voltammetric determination of trace amounts of 2-AN in waste waters was published by Stará et al. [159]. They used a graphite electrode modified by corund in $NaClO_4$/methanol media.

The selectivity of both named techniques is low, therefore, the attention has to be paid to the sample preparation before analysis. For complex matrices, it is inevitable to use one of the separation techniques. Mostly chromatographic techniques have been used, i.e. TLC, GC and HPLC. Novadays, TLC is not often used for the determination of APAHs due to limited selectivity, somewhat improvement can be achieved by application of two-dimensional

technique. 1-AN and 2-AN were successfully separated by TLC at aluminium oxide [160], silicagel [161], and silicagel impregnated with cadmium sulphate [162].

Gas chromatography has been often used for the analysis of APAH in complex matrices for its high separation efficiency, short analysis time and sensitivity of selected detectors. However, GC analysis of free amines generally has some inherent problems related to the difficulty in handling low-molecular mass amines because of their high water solubility and the tendency to be adsorbed and decompose on the column. A common method of overcoming these problems is the conversion of APAHs to relatively non-polar derivatives, such as acyl, silyl, dinitrophenyl, permethyl, Shiff base, carbamate, sulfonamide and phosphoamide compounds [163]. Furthermore, introducing of halogen and phosphorus containing groups in molecules enables the use of electron capture detector (ECD) and flame photometric detector (FPD). For derivatized and non-derivatized APAHs, a wide variety of other detectors, such as flame thermiionic (FTD), and non-flame thermiionic specific detector (TSD), alkali flame ionisation (AFID), and chemiluminiscence (CHLD) detector can be used [166]. Besides these techniques, MS detection [164,165] has been often employed to provide structure information for unequivocal APAHs identification.

HPLC is considered as more suitable in comparison to GC, as direct determination of APAHs is possible. The separations have been employed almost entirely in RP mode on C_{18} phase with several types of detectors, i.e. spectrophotometric[166,167,168], amperometric [169,170,171], fluorescence [172,173], and chemiluminescence [173]. The lowest detection limits are usually achieved using chemiluminiscence and fluorescence detectors and can reach the values about 10^{-9} mol L^{-1} (ref. [171,173]), the LODs achievable with amperometric detection are about one order of magnitude higher [172]. Different sample matrices were analyzed including urine [171,172], river [168] and seawater [169], rat skin [167] and waste gas [166], crude oil and derived products [173], and food [174]. Selected HPLC-ED methods for determination of 1- and 2-AN with their detection limits and electrode chracterization are listed in Table 2.4. Extended reviews on GC and HPLC analysis of APAHs are given in ref. [163]. As an alternative to these methods, conventional capillary electrophoresis with UV and electrochemical detection has been recently applied to the analysis of aromatic amines [175]. Microchip CE devices with amperometric detection at boron-doped diamond microelectrodes was recently emloyed for the detection of aromatic amines in spiked river water [176].

2.3.4 Hydroxy derivatives of polycyclic aromatic hydrocarbons

The development of analytical methods for determination of OHPAHs is focused on their presence in biological matrices, particularly urine, where they occur as metabolites of parent PAHs. HPLC with fluorescence detection is the most commonly employed technique due to its sensitivity and selectivity and 1-hydroxypyrene as biomarker of PAHs exposure is usually included as one of the analytes of interest in the studies [177,178,179]. Spectrophotometric, amperometric [177], and mass spectrometric detectors [180] were used only in a few cases. Interest has existed also in the application of gas chromatography with electron capture [181], flame ionization [94], and mass spectrometric detector [97]. Some of the most extensive GC-MS work has been performed by Grimmer and co-workers [97]. Overviews of investigations of PAH metabolites using HPLC and GC-MS can be found in summaries by Jongeneelen[182]. Other biological matrices containing OHPAHs are rarely investigated, e.g. capillary zone electrophoresis with laser induced fluorescence detection was used for analysis of hydroxypyrene derivatives in hepatopancreas samples from the terrestrial isopods and flatfish bile samples from individuals exposed to polluted sediments or crude oil [183]. Several methods were developed for the analysis of aerosol samples, e.g. Galceran and Moyano detected OHPAHs at pg m^{-3} level when using HPLC-ED setup with flow-through large-surface porous graphite electrode [184]. The HPLC-ED methods, where 1-OHN was determined, is specified in Table 2.4.

Analytes	Matrix	Extraction Technique	Detection system characterization	LOD [mol L^{-1}]	Ref.
acenaphthylene, fluoranthene, benzo[a]pyrene, and other 4 PAHs	ground, rain, river surface, and drinking water	SPE on C_{18} - phase	1) UVD (λ = 300 nm) 2) amperometric detection at GC WE, wall jet, E_{det} = +1.35 V vs. Ag/AgCl	1) UVD: $1.8 \cdot 10^{-7}$ - $3.1 \cdot 10^{-6}$ 2) ED:$3.4 \cdot 10^{-8}$ - $4.6 \cdot 10^{-7}$ After extraction: ED: ~ 10^{-11}	106
1-AN, aniline, methyl aniline, diphenylamine	sea water	In-line extraction on "pre-concentration" column (C_8 - phase)	1) coulometric detection, dual porous GC WE (Coulochem Model 5010) 2) amperometric detection, thin layer cell with GC WE	1) CD: $1.5 \cdot 10^{-8}$ 2) AD: $1.5 \cdot 10^{-9}$ Both after preconcentration step	169
2-AN	waste gases	absorption of the gas in diluted HCl	1) diode array UV 2) amperometric detection at GC WE, E_{det} = +0,7V vs. Ag/AgCl	1) $3.5 \cdot 10^{-7}$ 2) $7 \cdot 10^{-8}$	166
2-AN and other 9 aromatic nitrogen compounds	rodent skin tissue	sonication in MeCN	amperometric detection, thin layer cell with GC WE	~ $5 \cdot 10^{-8}$ - $4 \cdot 10^{-7}$	167
1-OHN	pesticide Carbaryl	direct injection after alkaline hydrolysis	amperometric detection, boron-doped diamond thin-film electrode, E_{det} = +0.9 V vs. Ag/AgCl	~ $5 \cdot 10^{-9}$	185
2-NN, 1-NP and others	air and diesel particulate matter	1) Soxhlet extraction with CH_2Cl_2 2) ultrasonic extraction by 40% CH_2Cl_2 in hexane	1) amperometric detection, thin layer cell with gold/mercury WE, E_{det} = –0.5 V vs. Ag/AgCl (3 mol L^{-1} KCl) 2) FD after Zn "on-line" reduction	1) $1.2 \cdot 10^{-8}$ 2) $2 \cdot 10^{-9}$	129
2-NN, 1-NP + other 7 oxy- and NPAHs	atmospheric aerosol	ultrasonic extraction by CH_2Cl_2	amperometric detection at GC WE, wall jet, E_{det} = –0.65 V vs. Ag/AgCl	2-NN: $8.7 \cdot 10^{-8}$ 1-NP: $3.3 \cdot 10^{-7}$	152
1-NN, 1-NP and other NPAHs	diesel soot	ultrasonic extraction by CH_2Cl_2	amperometric detection, thin layer cell with GC WE; E_{det} = –0.6 V vs. Ag/AgCl	1-NN: $5.8 \cdot 10^{-7}$ 1-NP: $4 \cdot 10^{-7}$	133

GC – glassy carbon; WE – working electrode; SPE – solid phase extraction; ED – electrochemical detection; UVD – spectrophotometric UV detection; CD – coulometric detection; AD – amperometric detection; MeCN – acetonitril; 1-NP – 1-nitropyrene; E_{det} – detection potential

Table 2.4 *Selected analytical methods for the HPLC-ED determination of PAHs and their nitro, amino, and hydroxy derivatives.*

2.4 References

1. Weast R.C. (Ed.): *CRC Handbook of Chemistry and Physics, 67th Edition*, D160-162. CRC Press, Boca Raton, USA 1987.
2. URL: *http://www.iarc.fr/*, accessed 10. 11. 2005.
3. Bjørseth A., Becher G., in: *PAH in Work Atmospheres: Occurrence and Determination.* CRC Press, Boca Raton, USA 1986.
4. World Health Organisation: *Selected Non-heterocyclic Polycyclic Aromatic Hydrocarbons*, IPCS Environmental Health Criteria 202. WHO, Geneva 1998.
5. IARC: *Polynuclear Aromatic Compounds, Part 3, Industrial Exposures in Aluminium Production, Coal Gasification, Coke Production, and Iron and Steel Founding, IARC Monographs on the Evaluation of Carcinogenic Risk of the Chemical to Man.* Vol. 34, IARC Press, Lyon 1984.
6. IARC: *Polynuclear Aromatic Compounds, Part 4, Bitumens, Coal-tars and Derived Products, Shale-oils and Soots, IARC Monographs on the Evaluation of Carcinogenic Risk of the Chemical to Man.* Vol. 35, IARC Press, Lyon 1985.
7. Rodriguez A. D., Marttelo R. O., Graf U., Villalobos-Petroni R., Gomey-Arroyo S.: *Mutat. Res.* 341, 235-247 (1995).
8. Henderson T. R., Li A. P., Royer R. E., Clark C. R.: *Environ. Mutagen.* 3, 211-220 (1981).
9. Arey J., Zielinska B., Atkinson R., Winter A. M.: *Mutat. Res.* 281, 67-76 (1992).
10. Preuss R., Angerer J., Drexler H.: *Int. Arch. Occup. Environ. Health* 76, 556-576 (2003).
11. URL: *http://ntp.niehs.nih.gov/ntp/roc/eleventh/profiles/s116znph.pdf*, accessed 13.10.2005.
12. US Environmental Protection Agency (US EPA): URL: *http://www.epa.gov/ttn/atw/hlthef/naphthal.html#ref7*, accessed 25.11.2005.
13. IARC: *Some traditional herbal medicines, some mycotoxins, naphthalene and styrene, IARC Monographs on the Evaluation of Carcinogenic Risk of the Chemical to Man.* Vol. 82, IARC Press, Lyon 2002.
14. Szeliga J., Dipple A.: *Chem. Res. Toxicol.* 11, 1-11 (1998).
15. White C. M.: *Nitrated Polycyclic Aromatic Hydrocarbons*, p. 376. Huethig, Heidelberg 1985.
16. World Health Organization: *Selected Nitro- and Nitro-Oxy-Polycyclic Aromatic Hydrocarbons*, IPCS Environmental Health Criteria 229. WHO, Geneva 2003.
17. Booth G., in: *Ullmann's encyclopedia of industrial chemistry* (eds. Elvers. B., Hawkins S., Schulz G.), p. 411-455. VCH, Weinheim 1991.
18. Scheepers P. T. J., Bos R. P.: *Int. Arch. Occup. Environ. Health* 64, 149-161 (1992).
19. Atkinson R. Arey J.: *Environ. Health Perspect.* 102, 117-126 (1994).
20. Pitts J. N. Jr., van Cauwenberghe K. A., Grosjean D., Schmid J. P., Fitz D. R., Belser W. L. J., Knudson G. B., Hynds P. M.: *Science* 202, 515-519 (1978).

21. Jäger J.: *J. Chromatogr.* 152, 575-578 (1978).
22. Pitts J. N. Jr., Sweetman J. A, Zielinska B., Winer A. M., Atkinson R.: *Atmos. Environ.* 19, 1601-1608 (1985).
23. Arey J., Zielinska B., Atkinson R., Winer A. M.: *Atmos. Environ.* 21, 1437-1444 (1987).
24. Zielinska B., Arey J., Atkinson R., Winer A. M.: *Atmos. Environ.* 23, 223-229 (1989).
25. Ramdahl T., Zielinska B., Arey J., Atkinson R., Winer A. M., Pitts J. N. Jr.: *Nature* 321, 425-427 (1986).
26. Ciccioli P., Cecinato A, Brancaleoni E., Draisci R., Liberti A.: *Aerosol. Sci. Technol.* 10, 296-310 (1989).
27. Feilberg A., Poulsen M. B., Nielsen T., Skow H.: *Atmos. Environ.* 35, 353-366 (2001).
28. Ciccioli P., Cecinato A., Brancalconi E., Frattoni M., Zacchei P., Miguel A. H., Vasconcellos P. C.: *J. Geophys. Res.* 101, 19567-19581 (1996).
29. Hunt G. T. Maisel B. E.: *Organ. Comp.* 24, 55-61 (1995).
30. Vasconcellos P. C., Artaxo P. E., Ciccioli P., Cecinato A., Brancalconi E., Frattoni M.: *Quim. Nova* 21, 385-393 (1998).
31. Bayona J. M., Casellas M., Fernández P., Solanas A. M., Albaigés J.: *Chemosphere* 29, 441-450 (1994).
32. Marino F., Cecinato A., Siskos P. A.: *Chemosphere* 40, 533-537 (2000).
33. Sasaki J., Aschmann S. M., Kwok E. S. C., Atkinson R., Arey J.: *Environ. Sci. Technol.* 31, 3173-3179 (1997).
34. Atkinson R., Baulch D. L., Cox R. A., Hampson R. F. Jr., Kerr J. A., Troe J.: *J. Phys. Chem. Ref. Data* 21, 1125-1568 (1992).
35. Kanoh T., Fukuda M., Hayami E., Kinouchi I., Nishifuji K., Ohnishi Y.: *Mutat. Res.* 245, 1-4 (1990).
36. Miyanishi K., Kinouchi T., Kataoka K., Kanoh T., Ohnishi Y.: *Carcinogenesis* 17, 1483-1490 (1996).
37. Levsen K.: *Fresenius Z. Anal. Chem.* 331, 467-478 (1988).
38. Wilson N. K., McCurdy T. R., Chuang J. C.: *Atmos. Environ.* 29, 2575-2584 (1995).
39. Vincenti M., Maurino V., Minero C., Pelizzetti E.: *Int. J. Environ. Anal. Chem.* 79, 257-272 (2001).
40. Jacob J., Karcher W., Belliardo J. J., Dumler R., Boenke A.: *Fresenius J. Anal. Chem.* 340, 755 - 767 (1991).
41. Cvačka J., Barek J., Fogg A. G., Moreira J. C., Zima J.: *Analyst* 123, 9R-18R (1998).
42. Schlemitz S., Pfannhauser W.: *Z. Lebensm.-Unters. Forsch.* 205, 305-310 (1997).
43. Schlemitz S., Pfannhauser W.: *Z. Lebensm.-Unters. Forsch.* 203, 61-64 (1996).
44. IARC: *Tobacco smoking. IARC Monographs on the Evaluation of the Carcinogenic Risk of Chemicals to Humans,* p. 139. Vol. 38, IARC Press, Lyon 1986.
45. El-Bayoumy K., O'Donnel M., Hecht S. S., Hoffmann D.: *Carcinogenesis* 6, 505-507 (1985).
46. Williams R., Sparacino C., Petersen B., Bumgarner J., Jungers H., Lewtas J.: *Int. J.*

Environ. Anal. Chem. 26, 27-49 (1989).
47. Atkinson R., Arey J., Winer A. M., Zielinska B., Dinoff T. M., Harger W. P., McElroy P. A.: *A survey of ambient concentrations of selected polycyclic aromatic hydrocarbons (PAH) at various locations in California* (Report A5-185-32), p. 181. Riverside, University of California, Statewide Air Pollution Research Center 1988.
48. Gupta P., Harger W. P., Arey J.: *Atmos. Environ.* 30, 3157-3166 (1996).
49. Tokiwa H., Sera N., Kai M., Horikawa K., Ohnishi Y., in: *Genetic toxicology of complex mixtures* (eds. Waters M. D., Daniel F. B., Lewtas J., Moore M. M., Nesnow S.), p. 165-172. Plenum Press, New York 1990.
50. Berlincioni M., Croce G., Ferri F., Iacovella N., La Rocca C., Lolini M., Megli A., Pupp M., Rizzi L., Baldassarri TL., di Domenico A.: *Fresenius Environ. Bull.* 4, 169-174 (1995)
51. Takahashi Y., Nakagawa J., Hosokawa N., Asano M., Morita M.: *Kankyo Kagaku* 5, 207-214 (1995). *CA* 123:349623
52. Librando V., Liberatori A., Fazzino S. D.: *Polycycl. Arom. Comp.* 3, 587-594 (1993).
53. Schlemitz S., Pfannhauser W.: *Food Addit. Contam.* 13, 969-977 (1996).
54. Finlayson-Pitts B. J., Pitts J. N. Jr.: *Science* 276, 1045-1052 (1997).
55. Fu P. P.: *Drug Metab. Rev.* 22, 209-268 (1990).
56. Fu P. P., Herreno-Saenz D.: *Environ. Carcinogen. Ecotoxicol. Rev.* 17, 1-43 (1999).
57. Purohit V., Basu A. K.: *Chem. Res. Toxicol.* 13, 673-692 (2000).
58. Cerniglia C. E., Somerville C. C., in: *Biodegradation of nitroaromatic compounds* (ed. Spain J. C.), p. 99-115. Plenum Press, New York 1995.
59. Chae Y. H., Yun C-H., Guengerich F. P., Kadlubar F. F., El-Bayoumy K.: *Cancer. Res.* 53, 2028-2034 (1993).
60. Howard P. C., Aoyama T., Bauer S. L., Gelboin H. V., Gonzalez F. J.: *Carcinogenesis* 11, 1539-1542 (1990).
61. Guengerich F. P., Parikh A., Turesky R. J., Josephy P. D.: *Mutat. Res.* 428, 115-124 (1999).
62. Djuric Z., Potter D. W., Heflich R. H., Beland F. A.: *Chem-Biol. Interact.* 59, 309-324 (1986).
63. Stiborová M.: *Chem. Listy* 96, 784-791 (2002).
64. Sasaki J. C., Arey J., Eastmond D. A., Parks K. K., Phousongphouang P. T., Grosovsky A. J.: *Mutat. Res.* 445, 113-125 (1999).
65. Ames B. N.: *Environ. Mol. Mutagen.* 14, 66-77 (1989).
66. Tokiwa H., Nakagawa R., Ohnishi Y.: *Mutat. Res.* 91, 321-325 (1981).
67. Fu P. P., Chou M. W., Miller D. W., White G. L., Heflich R. H., Beland F. A.: *Mutat. Res.* 143, 173-181 (1985).
68. Fu P. P., Chou M. W., Beland F. A., in: *Polycyclic aromatic hydrocarbon carcinogenesis: Structure-activity relationships* (eds. Yang S. K., Silverman B. D.), p. 37-65. CRC Press, Boca Raton, Florida 1988.

69. Jung I. I., Shaikh A. U., Heflich R. H., Fu P. P.: *Environ. Mol. Mutagen.* 17, 169-180 (1991).
70. Iwata N., Fukuhara K., Suzuki K., Miyata N., Takahashi A.: *Chem.-Biol. Ineract.* 85, 187-197 (1992).
71. Oh S. W., Kang M. N., Cho C. W., Lee M.W.: *Dyes Pigments* 33, 119-135 (1997).
72. Pradyok P.: *A Comprehensive Guide to the Hazardous Properties of Chemical Substances*. John Wiley & Sons Inc., New York 1999.
73. Hutzinger O.: *The Handbook of Environmental Chemistry*. Springer-Verlag, Heidelberg 1984.
74. Wirts M., Salthammer T.: *Environ. Sci. Technol.* 36, 1827-1832 (2002).
75. Benigni R., Passerini L.: *Mutat. Res. - Rev. Mutat. Res.* 511, 191-206 (2002).
76. IARC: *IARC Monographs on the Evaluations of Carcinogenicity to Humans*. Vols. 4, 16, 27, Suppl. 7, IARC Press, Lyon 1972-2005.
77. Ahlström L.-H., Raab J., Mathiasson L.: *Anal Chim. Acta* 552, 79-80 (2005).
78. EU-Commission, Synoptic document – draft of provisional list of monomers and additives used in the manufacture of plastics and coatings intended to come into contact with foodstuffs updated to 25 January 2003, Scientific Committee for Food, Brussels, Belgium 2003.
79. EU-Commission, Directive 2002/72/EC of 6 August 2002 relating to plastic materials and articles intended to come into contact with foodstuffs, *Off. J. Eur. Commun.*, L 220, p. 18 (2002).
80. Directive, 2002/61/EC of 19 July 2002 amending for the nineteenth time Council Directive 76/769/EEC relating to restrictions on the marketing and use of certain dangerous substances and preparations (azocolourants), *Off. J. Eur. Commun.*, L 243, p. 15 (2002).
81. Searle Ch. E.: *Chemical Carcinogens,* second edition. ACS Monograph 182, American Chemical Society, Washington, D.C. 1984.
82. IARC: IARC Monographs on the Evaluations of Carcinogenicity to Humans. Vol. 4, 87-111, IARC Press, Lyon 1974.
83. Fishbein L., in: *The Handbook of Environmental Chemistry: Anthropogenic compounds*, Vol. 3, Part C, p. 1-40. Springer-Verlag, Berlin 1984.
84. Alberts B., Johnson A., Lewis J., Raff M., Roberts K., Walter P.: *Molecular Biology of The Cell,* fourth edition, p. 1318. Garland Science, New York 2002.
85. IARC: *Genetic and Related Effects: An Updating of Selected IARC Monographs from Volumes 1 to 42 Monographs*, Suppl. 6, p. 406-414. IARC Press, Lyon 1987.
86. Angerer J., Lewalter J., Neumann H. G., Schaller K. H.: *Analysis of Hazardous Substances in Biological Materials*, Vol. 1, p. 17-30, 1983.
87. Grimmer G., Jacob J., Dettbarn G., Naujack K.-W.: *Int. Arch.Occup. Environ. Health* 69, 231-239 (1997).
88. Jongeneelen F. J., Anzion R. B. M., Henderson P. T.: *J. Chromatogr.* 413, 227-232 (1987).

89. Kuusimaki L., Peltonen Y., Mutanen P., Peltonen K., Savela K.: *Int. Arch. Occup. Environ. Health* 77, 23-30 (2004).
90. Gendre C., Lafontaine M., Morele Y., Payan J. P., Simon P.: *Polycycl. Arom. Comp.* 22, 761-769 (2002).
91. Grimmer G., Dettbarn G., Jacob J.: *Int. Arch. Occup. Environ. Health* 65, 189-199 (1993).
92. Yang Y., Sjövall J., Rafter J., Gustafsson J.-A.: *Carcinogenesis* 15, 681-687 (1994).
93. Andreoli R., Manini P., Bergamaschi E., Mutti A., Franchini I., Niessen W. M. A.: *J. Chromatogr. A* 847, 9-17 (1999).
94. Bieniek G.: *Occup. Environ. Med.* 51, 357-359 (1994).
95. Hansen A. M., Onland O., Poulsen O. M., Sherson D., Sigsgaard T., Christensen J. M., Overgaard E.: *Int. Arch. Occup. Environ. Health* 65, 385-394 (1994).
96. Hansen A. M., Poulsen O. M., Sigsgaard T., Christensen J. M.: *Anal. Chim. Acta* 291, 341-347 (1994).
97. Heikkila P. R., Luotamo M., Riihimaki V.: *Scand. J. Work Environ. Health* 23, 199-205 (1997). *CA* 127:209565.
98. Knopp D., Schedl M., Achatz S., Kettrup A., Niessen R.: *Anal. Chim. Acta* 399, 115-126 (1999).
99. Preuss R., Drexler H., Bottcher M., Wilhelm M., Bruning T., Angerer J.: *Int. Arch. Occup. Environ. Health* 78, 355-362 (2005).
100. Chen C. F., Hung I. F., Chen R. K., *Polycycl. Arom. Comp.* 17, 171-177 (1999).
101. Yang M., Koga M., Katoh T., Kawamoto T.: *Arch. Environ. Contam. Toxicol.* 36, 99-108 (1999).
102. Pietrogrande M. C., Blo G., Bighi C.: *J. Chromatogr. A* 349, 63-66 (1985).
103. Hill R. H. Jr., Head S. L., Baker S., Gregg M., Shealy D. B., Bailey S. L., Williams C. C., Sampson E. J., Needham L. L.: *Environ. Res.* 71, 99-108 (1995).
104. URL: *http://www.pesticideinfo.org/Detail_ChemReg.jsp?Rec_Id=PC32816*, accessed 9.11. 2005.
105. Vincze A., Huszar M. L.: *J. Liq. Chromatogr.* 12, 2887-2892 (1989).
106. Nirmaier H. P., Fischer E., Meyer A., Henze G.: *J. Chromatogr. A* 730, 169-175 (1996).
107. Khaledi M. G., Dorsey J. G.: *Anal. Chim. Acta* 161, 201-209 (1984).
108. Coetzee J. F., Katzi G. H., Spurgeon J. C.: *Anal. Chem.* 48, 2170-2173 (1976).
109. Nirmaier H. P., Fischer E., Henze G.: *Electroanalysis* 10, 187-190 (1998).
110. Wise S. A., Sander L. C., May W. E.: *J. Chromatogr.* 642, 329-349 (1993).
111. Moriwaki H.: *Curr. Org. Chem.* 9, 849-857 (2005).
112. Schuetzle D.: *Environ. Health Perspect.* 47, 65-80 (1983).
113. Vincenti M., Minero C., Pelizzetti E., Fontana M., De Maria R.: *J. Am. Soc. Mass. Spectrom.* 7, 1255-1265 (1996).
114. Tyrpien K., Janoszka B., Bodzek D.: *J. Chromatogr. A* 774, 111-120 (1997).
115. Barek J., Cvačka J., Moreira J. C., Zima J.: *Chem. Listy* 90, 805-817 (1996).

116. Netto A. D. P., Moreira J. C., Dias A. E. X. O., Arbilla G., Ferreira L. F. V., Oliveira A. S., Barek J.: *Quimica Nova* 23, 765-773 (2000).
117. Moreira J. C., Barek J.: *Quimica Nova* 18, 362-367 (1995).
118. White C. M., Robbat Jr. A., Hoes R. M.: *Chromatographia* 17, 605-612 (1983).
119. Korhonen I. O. O., Lind M. A.: *J. Chromatogr.* 322, 71-81 (1985).
120. Oehme M., Manø S., Stray H.: *J. High Resolut. Chromatogr. & Chromatogr. Commun.* 5, 417-423 (1982).
121. Ramdahl T., Kveseth K., Becher G.: *J. High Resolut. Chromatogr. & Chromatogr. Commun.* 5, 19-26 (1982).
122. Paputa-Peck M. C., Marano R. S., Schuetzle D., Riley T. L., Hampton C. V., Prater T. J., Skewes L. M., Jensen T. E., Ruehle P. H , Bosch L. C., Duncan W. P.: *Anal. Chem.* 55, 1946-1954 (1983).
123. Warzecha L.: *J. High. Resol. Chromatogr.* 19, 639-642 (1996).
124. Yu W. C., Fine D. H., Chiu K. S., Biemann K.: *Anal. Chem.* 56, 1158-1162 (1984).
125. Robbat A. Jr., Corso N. P., Doherty P., Wolf M. H.: *Anal. Chem.* 58, 2078-2084 (1986).
126. Tomkins B. A., Brazell R. S., Roth M. E., Ostrum V. H., *Anal. Chem.* 56, 781-786 (1984).
127. Kuo C. T., Chen H. W., Lin S. T.: *Anal. Chim. Acta* 485, 219-228 (2003).
128. Tejada S. B., Zweidinger R. B., Sigsby J. E. Jr.: *Anal. Chem.* 58, 1827-1834 (1986).
129. MacCrehan W. A., May W. E, Yang S. D., Benner S. D.: *Anal. Chem.* 60, 194-199 (1988).
130. Li H., Westerholm R.: *J. Chromatogr. A* 664, 177-182 (1994).
131. Sigvardson K. W., Birks J. W.: *J. Chromatogr.* 316, 507-518 (1984).
132. Hayakawa K., Murahashi T., Butoh M., Miyazaki M.: *Environ. Sci. Technol.* 29, 928-932 (1995).
133. Jin Z., Rappaport S. M.: *Anal. Chem.* 55, 1778-1781 (1983).
134. Galceran M. T., Moyano E.: *Talanta* 40, 615-621 (1993).
135. Kuo C. T., Chen H. W.: *J. Chromatogr. A* 897, 393-397 (2000).
136. Hayakawa K., Noji K., Tang N., Toriba A., Kizu R., Sakai S., Matsumoto Y.: *Anal. Chim. Acta* 445, 205-212 (2001).
137. Siegmund B., Weiss R., Pfannhauser W.: *Anal. Bioanal. Chem.* 375, 175-181 (2003).
138. Sekyra M., Leníček J., Bednárková K., Beneš I.: *Chem. Listy* 94, 924-930 (2000).
139. Korfmacher W. A., Rushing L. G.: *J. High Resolut. Chromatogr. & Chromatogr. Commun.* 9, 293-295 (1986).
140. Campbell R. M., Lee M. L.: *Anal. Chem.* 56, 1026-1030 (1984).
141. Ramdahl T., Urdal K.: *Anal. Chem.* 54, 2256-2260 (1982).
142. Schuetzle D., Riley T. L., Prater T. J., Harvey T. M., Hunt D. F.: *Anal. Chem.* 54, 265-271 (1982).

143. Lewtas J., Nishioka M. G., in: *Nitroarenes: Occurrence, metabolism, and biological impact* (eds. Howard P. C., Hecht S. S., Beland F. A.), p. 61-72. Plenum Press, New York 1990.
144. Schilhabel J., Levsen K.: *Fresenius Z. Anal. Chem.* 333, 800-805 (1989).
145. Bezabeh D., Allen T., McCauley E., Kelly P., Jones A.: *J. Am. Soc. Mass. Spectrom.* 8, 630-636 (1997).
146. Tasker A. D., Robson L., Hankin S. M., Ledingham K. W. D., Singhal R. P., Fang X., Mc Canny T., Kosmidis C., Tzallas P., Langley A. J., Tadat P. F., Divall E. J.: *Laser Part. Beams* 19, 205-208 (2001).
147. Scheepers P. T. J., Velders D. D., Martens M. H. J., Noordhoek J., Bos J.: *J. Chromatogr. A* 677, 107-121 (1994).
148. Bonfanti L., Careri M., Mangia A., Manini P., Maspero M.: *J. Chromatogr. A* 728, 359-369 (1996).
149. Jia L., Yan J., Gao J., Chen X., Hu G., Wang Y., Xu M., Wang X.: *Microchem. J* 59, 364-371 (1997).
150. Rosenkranz H. S.: *Mutat. Res.* 101, 1-10 (1982).
151. MacCrehan W. A., May W. A.: *Anal. Chem.* 56, 625-628 (1984).
152. Galceran M. T., Moyano E.: *Talanta* 40, 615-621 (1993).
153. Younis T .I., Bashir W. A.: *Talanta* 42, 1121-1126 (1995).
154. Kargosha K., Ahmadi S. H., Ghassempour A., Arshadi M. R.: *Analyst* 124, 367-371 (1999).
155. Barek J., Cvačka J., Muck A., Quaiserová V., Zima J.: *Fresenius J. Anal. Chem.* 369, 556-562 (2001).
156. Barek J., Cvačka J., Muck A., Quaiserová V., Zima J.: *Electroanalysis* 13, 799-803 (2001).
157. Ferancova A., Korgova E., Labuda J., Zima J., Barek J.: *Electroanalysis* 14, 1668-1673 (2002).
158. Barek J., Berka A., Müller M., Zima J.: *Collect. Czech. Chem. Commun.* 50, 2853-2862 (1985).
159. Stará V., Kopanica M., Jeník J.: *Chem. Prum.* 40, 543 (1990).
160. Bieniek G.: *Chem. Anal.* 33, 807-810 (1988).
161. Haas R., Schreiber I., Losekam M., Koss G.: *Fresenius J. Anal. Chem.* 335, 980-981 (1989).
162. Yasuda K.: *J. Chromatogr.* 60, 144-179 (1971).
163. Kataoka H., Yamamoto S., Narimatsu S., in: *Handbook of analytical separations, Vol. 3 – Environmental Analysis* (ed. Kleiböhmer W.), p. 3. Elsevier Science 2001.
164. Grimmer G., Dettbarn G., Seidel A., Jacob J.: *Sci. Total Environ.* 247, 81-90 (2000).
165. Longo M., Cavallaro A.: *J. Chromatogr. A* 753, 91-100 (1996).
166. Lehotay J., Halmo F., Oktavec D., Lacuška M: *Chem. Listy* 93, 138-141 (1999).
167. Felice L. J., Schirmer R. E., Springer D. L. Veverka C. V.: *J. Chromatogr. A* 354, 442-448 (1986).

168. Galeano-Diaz T., Acedo M. I., Munoz de la Pena A., Sanchez-Pena M., Salinas F.: *Analyst* 119, 1151-1155 (1994).
169. Varney M. S., Preston M. R.: *J. Chromatogr. A* 348, 265-274 (1985).
170. Cvačka J., Opekar F., Barek J., Zima J.: *Electroanalysis* 12, 39-43 (2000).
171. Mocko V.: *PhD Thesis*. Charles University, Prague 2004.
172. Hansen A. M., Poulsen O. M., Christensen J. M., Hansen S. H.: *J. Chromatogr. B* 578, 85-90 (1992).
173. Sigvardson K. W., Kennish J. M., Birks J. W.: *Anal. Chem.* 56, 1096-1102 (1984).
174. Worobey B. L., Shields J. B.: *J. Assoc. Off. Anal. Chem.* 70, 1021-1024 (1987).
175. Huang X., You T., Li T., Yang X., Wang E.: *Electroanalysis 11*, 969-972 (1999).
176. Shin D. C., Tryk D. A., Fujishima A., Muck A., Chen G., Wang J.: *Electrophoresis* 25, 3017-3023 (2004).
177. Barek J., Bencko V., Cvačka J., Mejstřík V., Slámová A., Švagrová I., Zima J.: *Chem. Listy* 91, 871-876 (1997).
178. Angerer J., Mannschreck C., Gündel J.: *Int. Arch. Occup. Environ. Health* 70, 365-377 (1997).
179. Knopp D., Schedl M., Achatz S., Kettrup A., Niessen R.: *Anal. Chim. Acta* 399, 115-126 (1999).
180. Andreoli R., Manini P., Bergamaschi E., Mutti A., Franchini I., Niessen W. M. A.: *J. Chromatogr. A* 847, 9-17 (1999).
181. Heikkila P. R., Luotamo M., Riihimaki V.: *Scand. J. Work. Env. Hea.* 23, 199-205 (1997).
182. Jongeneelen F. J.: *Sci. Total Environ.* 199, 141-149 (1997).
183. Smith C. J., Walcott C. J., Huang W. L., Maggio V., Grainger J., Patterson J.: *J. Chromatogr. B* 778, 157-164 (2002).
184. Galceran M. T., Moyano E.: *J. Chromatogr. A* 715, 41-48 (1995).
185. Rao T. N., Loo B. H., Sarada B. V., Terashima C., Fujishima A.: *Anal. Chem.* 74, 1578-1583 (2002).

3

Polarography and voltammetry of 1- and 2-nitronaphthalene at mercury electrodes

3.1 Introduction

Because of the presence of reducible nitro moiety, trace amounts of NPAH can be determined using polarographic and voltammetric techniques. The long history of investigations on the electrochemistry of nitro-group containing compounds was started by Shikata in 1925 [1] with nitrobenzene as the first organic compounds studied by polarography. After that, the polarographic behavior of numerous dinitroderivatives of benzene has been investigated [2], but very little has been done with nitro compounds in the naphthalene series. The first publication dealing with polarography of 1-NN appeared in the late forties [3] and other papers concerning its reduction in acidic medium were published shortly after [4,5]. Later the polarographic reduction of nitronaphthalenes and their substituted derivatives in buffers containing 50 % - 80 % of ethanol was investigated [6,7,8]. These and other studies are listed in a historical overview in Table 3.1. The purpose of the studies span from analytical determinations over toxicological applications to studies of reduction mechanism. These studies confirmed that mononitronaphthalenes are reduced similarly to most nitroaromatics ($ArNO_2$) in a diffusion-controlled four-electron irreversible wave to the hydroxylamino derivative (ArNHOH) (Eq. 3.1). In acidic medium the protonated form of this hydroxylamine is further reduced in a two-electron process to the aminoderivative ($ArNH_2$) (Eq. 3.2).

$$ArNO_2 + 4e^- + 4H^+ \rightarrow ArNHOH + H_2O \qquad (3.1)$$

$$ArNHOH + 2e^- + 2H^+ \rightarrow ArNH_2 + H_2O \qquad (3.2)$$

The apparent four electron reduction of aromatic nitrocompound to the hydroxylamine, summarized in Eq. (3.1), takes place via the dihydroxylamine $ArN(OH)_2$, which dehydrates to yield the nitrosocompound (ArNO) (Eq. 3.3). The further reduction of ArNO, which occurs at potentials more positive than that of $ArNO_2$, thus appears as one step of the whole reduction process.

$$ArNO_2 \xleftarrow{2e^-,2H^+} ArN(OH)_2 \xrightarrow{-H_2O} ArNO \xleftarrow{2e^-,2H^+} ArNHOH \qquad (3.3)$$

The detailed mechanism of these processes was studied with nitrobenzene and its derivatives bearing an electron attracting substituent (e.g. 4-nitrobenzophenon, which has stable $ArN(OH)_2$ derivative) [9,10] and nitrosobenzene [11]. It was demonstrated by Laviron et al. that the reaction sequence (order of addition of electrons (e^-) and protons (H^+)) is independent of the potential [12], however is strongly dependent on the pH. These authors proposed a general reaction scheme for the reduction of nitroaromatics, composed of two 9-member square

schemes (see Fig. 3.1A), linked by the dehydration of the intermediate $ArN(OH)_2$. Each member of the scheme represents the possible intermediate during reduction, the reductions are written horizontally from the left to the right and the protonations downwards. The real pathway for a particular nitrocompound depends on pH of the supporting electrolyte, as the pK_a values characterizing the protonations (downwards reactions) are somewhat different for each derivative. However, the trends of the succession when passing from acidic to basic media can be generalized and are highlighted in the Fig. 3.1B. In the common pH range (0-14), the first step of the reduction is the electron uptake forming the nitroradical ($ArNO_2^{\cdot -}$) (Eq. 3.4):

$$ArNO_2 + e^- \leftrightarrow ArNO_2^{\cdot -} \qquad (3.4)$$

This hypothesis is novadays generally accepted, although in the past it was suggested that in acidic media the protonation of nitro group precedes the first electron uptake [13]. The formation of the nitroradical is well documented in alkaline medium, in the presence of surfactants, and in aprotic media [14]. Its increased stability in these cases can be interpreted as due to an inhibition of the rate of subsequent protonation of the $ArNO_2^{\cdot -}$, which is the rate determining step of the reduction. As most of NPAHs have limited solubility in aqueous media, their electrochemical behaviour is frequently studied in mixed media of appropriate organic solvent mixible with water, which may also effect the reduction mechanism.

In following chapters, modern electroanalytical techniques such as DC tast polarography (DCTP) and differential pulse polarography (DPP) at a classical dropping mercury electrode (DME), or differential pulse voltammetry (DPV) and adsorptive stripping voltammetry (AdSV) at a hanging mercury drop electrode (HMDE) for the determination of trace amounts 1-NN and 2-NN in mixed aqueous-methanol media will be compared in terms of optimum conditions for the determination, sensitivity and limits of determination. The mechanism of reduction and characters of cathodic currents will be investigated by DC polarography and cyclic voltammetry (CV). The theory of mentioned polarographic and voltammetric techniques is well described in monographs [15,16,17,18].

Analyte	pH of base electrolyte / $E_{1/2}$ **[V]** vs. reference electrode	**Base electrolyte composition; reference electrode**	**Purpose of the study**	Reference **/year**
1-NN	Acidic **–0.26**	0.1 mol L^{-1} HCl – 50% MeOH; calomel electrode (1 mol L^{-1})	Detection of 1-NN in the presence of 1-AN	3 **/1948**
Presumably **1-NN**	Non-aqueous media/ **–0.92**	Benzene-EtOH-LiCl	Detection of impurities (dinitronaphthalenes) in 1-NN	19 **/1951**
1-NN	**–0.12**	Concentrated H_2SO_4 (98.65 %); reference electrode not mentioned	Study of mechanism	4 **/1951**
1-NN	**–0.57**	Acetic acid with 1 mol L^{-1} ammonium acetate; mercury pool anode	Effect of the substituent on $E_{1/2}$	5 **/1952**
1-NN **2-NN**	pH 2.9 **–0.25** **–0.23**	pH 4.97 **–0.39** **–0.39**; pH 7.55 **–0.56** **–0.52**; pH 10.3 **–0.75** **–0.71**; Presumably aqueous buffer (not specified); SCE	Effect of the aromatic nucleus on $E_{1/2}$	20 **/1955**
1-NN	Acidic **–0.50; –1.0**	0.2 mol L^{-1} sodium acetate in 50% MeOH; reference electrode not mentioned	Detection of naphthalene in air after nitration	21 **/1956**
1-NN **2-NN**	pH 2.1 **–0.3; –0.65** **–0.3; –0.72**	pH 6.4 **–0.51** **–0.49**; pH 9.4 **–0.73** **–0.70**; pH 11.0 **–0.83** **–0.82**; 80% EtOH + aqueous buffer (not specified), SCE	Study of mechanism	6 **/1960**
1-NN **2-NN**	pH 0 **–0.05** –[a]	pH 2 **–0.20** **–0.23**; Glycine buffer - 55% EtOH; SCE	Effect of the aromatic nucleus on $E_{1/2}$ and its correlation with infrared spectra and kinetics of reduction	7 **/1961**
1-NN **2-NN**	Acidic **–0.110** **–0.115**	Neutral **–0.51** **–0.52**; Acidic medium: H_2SO_4: EtOH (1:1); Neutral medium: ammonium acetate: EtOH (1:1)	Study of mechanism	8 **/1972**
1-NN **2-NN**	pH 4.5 **–0.855** **–0.850**	4:1 DMSO – 0.1 mol L^{-1} acetate buffer; SCE	Relationship between $E_{1/2}$ and mutagenicity of nitroarenes	22/ **1984**

[a] Data not given

Abbreviations: $E_{1/2}$ – half wave potential; MeOH – methanol; EtOH – ethanol; SCE – saturated calomel electrode; DMSO – dimethylsulfoxide

Table 3.1 *The overview of studies dealing with DC polarography of 1- and 2- nitronaphthalene at a classical dropping mercury electrode.*

A

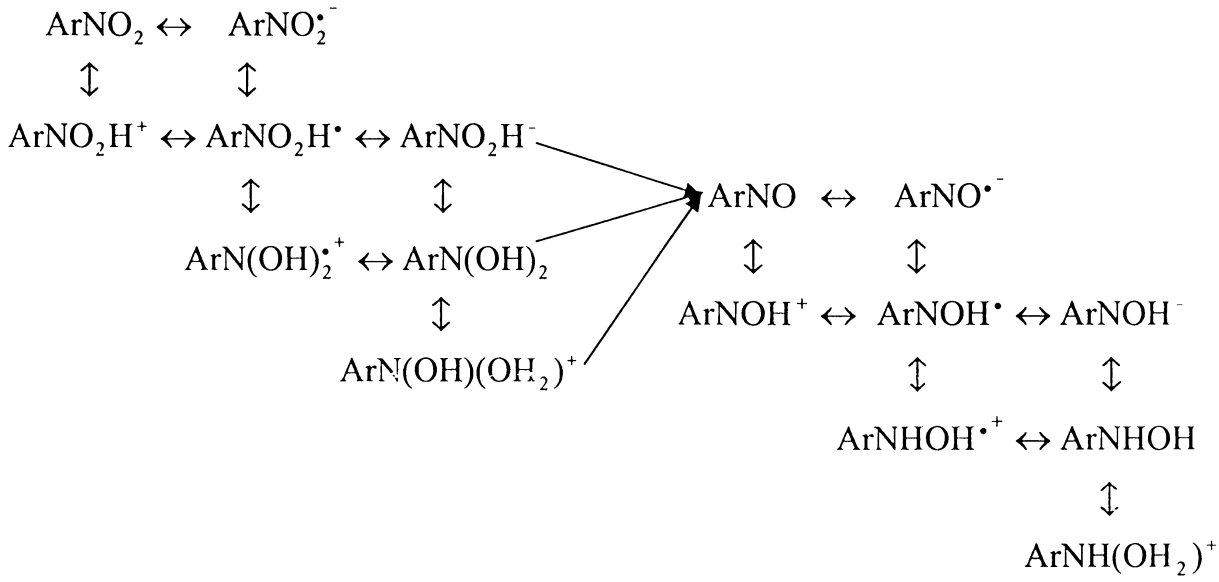

B

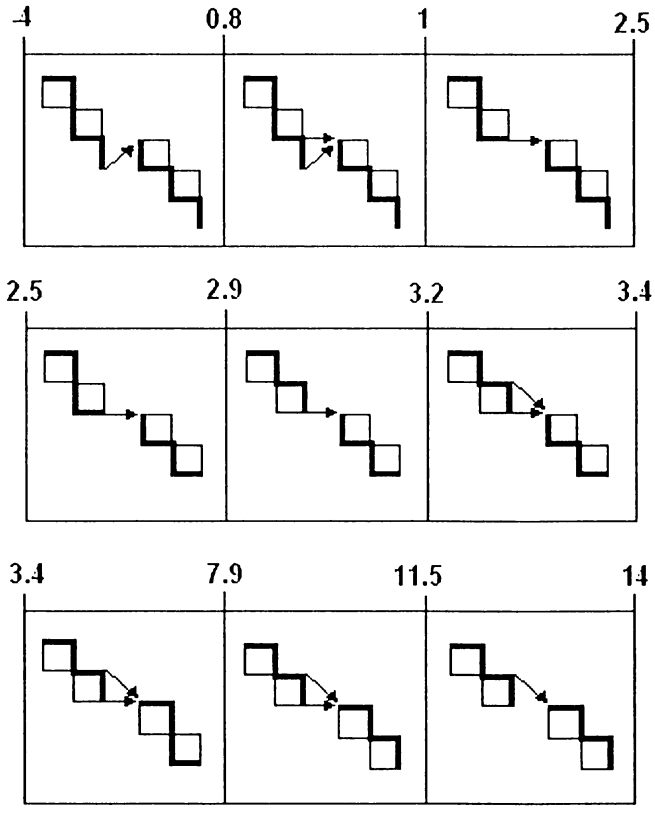

Figure 3.1 *A – The general reaction scheme for the reduction of an aromatic nitrocompound ($ArNO_2$) to the corresponding phenylhydroxylamine (ArNHOH).*

B – Schematic representation of the reaction path on Fig. 3.1A in pH regions indicated on the graph (adapted from ref. [12]).

3.2 Experimental

3.2.1 Reagents

The stock solutions of 1- and 2-NN ($c = 1 \cdot 10^{-3}$ mol L^{-1}) were prepared by dissolving 0.0173 g of the substance in 100 mL of methanol or dimethylformamide (DMF). The purity of the substances was controlled by HPLC [23]. More diluted solutions were prepared by exact dilution of the stock solution with methanol or DMF. All the solutions were stored refrigerated in the dark. Methanol, DMF, sodium hydroxide and lithium hydroxide were of analytical grade purity (Lachema, Czech Republic). Britton-Robinson buffers (BR buffers) were prepared in a usual way, i.e. by mixing a solution of 0.04 mol L^{-1} in phosphoric acid, 0.04 mol L^{-1} in acetic acid and 0.04 mol L^{-1} in boric acid with the appropriate amount of 0.2 mol L^{-1} sodium hydroxide solution [24]. Chemicals for the preparation of the Britton-Robinson buffers were obtained from Lachema. De-ionised water was produced by Milli-Q_{plus} system (Millipore, USA).

3.2.2 Apparatus

Measurements were carried out using a computer driven EcoTriboPolarograph with PolarPro software, version 4.0 (both EcoTrend, Prague, Czech Republic) in combination with a classical DME or HMDE, type UMμE (EcoTrend), a platinum wire auxiliary electrode and silver/silver chloride (1 mol L^{-1} KCl) reference electrode, to which all the potential values are referred. The parameters of the classical DME used in DC tast and DP polarography were as follows: At a mercury reservoir height of h = 81 cm, the flow rate was m = 0.48 mg s^{-1} and the drop time was τ = 5.8 s (at an applied voltage of 0 V in 0.1 mol L^{-1} KCl). The mercury flow rate was measured by dipping the tip of the capillary to a previously weighed beaker with a small amount of mercury for 300 s at constant height of the reservoir. Work with the DME was carried out at a polarization rate of 4 mV s^{-1} and controlled drop time of 1 s. For DPV and AdSV at HMDE, the maximum drop size attainable obtained by opening the valve for 100 ms, with a surface of 0.864 mm^2, and polarization rate of 20 mV s^{-1} were used. The modulation amplitude in pulse methods (DPP at DME, DPV and AdSV at HMDE) of –50 mV with pulse duration of 80 ms was used. Spectra were measured in quartz cuvettes (Hellma, Germany, optical path lengths 0.1 cm) vs. methanol in spectrophotometer Pye Unicam SP-400 UV/VIS (Cambridge, UK), the spectra in electronic format (Fig. 3.2) were obtained using diode array spectrophotometer HP 8453 (Hewlett Packard, Netherlands). The solution

pH was measured using Conductivity & pH meter Jenway 4330 (Jenway, England). pH values refer to those of the buffer, pH^f values refer to those of the resulting pH of the mixtures of the buffer with the organic component.

3.2.3 Procedures

The general procedure to obtain polarograms or voltammograms was as follows: A required amount of the stock solution of the test substance in methanol was placed in a 10 mL volumetric flask, an appropriate volume of methanol was added and the system was diluted to volume with a Britton-Robinson buffer of the required pH. Oxygen was removed from the measured solutions by bubbling with nitrogen for five minutes. A prebubbler containing a water-methanol mixture in the same ratio as in the polarographed solution was placed prior to the polarographic vessel. The calibration curves were measured in triplicate, the height of the peaks used for evaluation was measured from the straight line connecting the minima before and after the peak, if not stated otherwise. The statistical parameters of calibration dependences (i.e. slope, intercept, limit of determination) were calculated according to Oppenhelmer [25], Schwartz [26], and Ebel [27] using statistic software ADSTAT version 2.0 (Trilobyte, Czech Republic). This software uses confidence bands ($\alpha = 0.05$) for calculation of the limit of determination (LOD). It corresponds to the lowest signal for what relative standard deviation is equal 0.1 (ref. [28]). The ADSTAT software was also used to test the significance of the intercepts of linear calibration dependences. As these were basically non significant, the intercept values are not listed in tables summarizing parameters of calibration dependences (Table 3.3, 3.4, and 3.5). Exemptions are mentioned in the text.

3.2.4 Stability of stock solutions of 1- and 2-nitronaphthalene

The stability of the stock solutions of 1-NN and 2-NN ($c = 1 \cdot 10^{-3}$ mol L^{-1}) in methanol was monitored for 6 months, corresponding spectra are depicted in Fig. 3.2. The absorbance of the stock solution was measured at λ = 326 nm (1-NN) and λ = 303 nm (2-NN), where the absorption maxima appeared. The results of these measurements are summarized in Table 3.2. The calculated value of molar absorbance coefficient (ε) at this wavelength is $3.96 \cdot 10^3$ dm^3 mol^{-1} cm^{-1} and $8.01 \cdot 10^3$ dm^3 mol^{-1} cm^{-1} for 1-NN and 2-NN, respectively.

It follows from Table 3.2 that the stock solutions of 1-NN and 2-NN in methanol are stable for at least six months, because no observable decrease of concentration was observed.

Table 3.2 *Spectrophotometric stability studies of stock solutions of 1- and 2-NN ($c = 1 \cdot 10^{-3}$ mol L^{-1}) in methanol. The relative concentration c in % compared to the concentration of a fresh prepared solution is given.*

Days	0	1	3	5	10	26	87	215
c (1-NN) [%]	100	99.6	99.6	99.7	99.5	99.4	99.2	99.4
c (2-NN) [%]	100	99.8	99.8	99.6	99.5	99.2	99.3	99.2

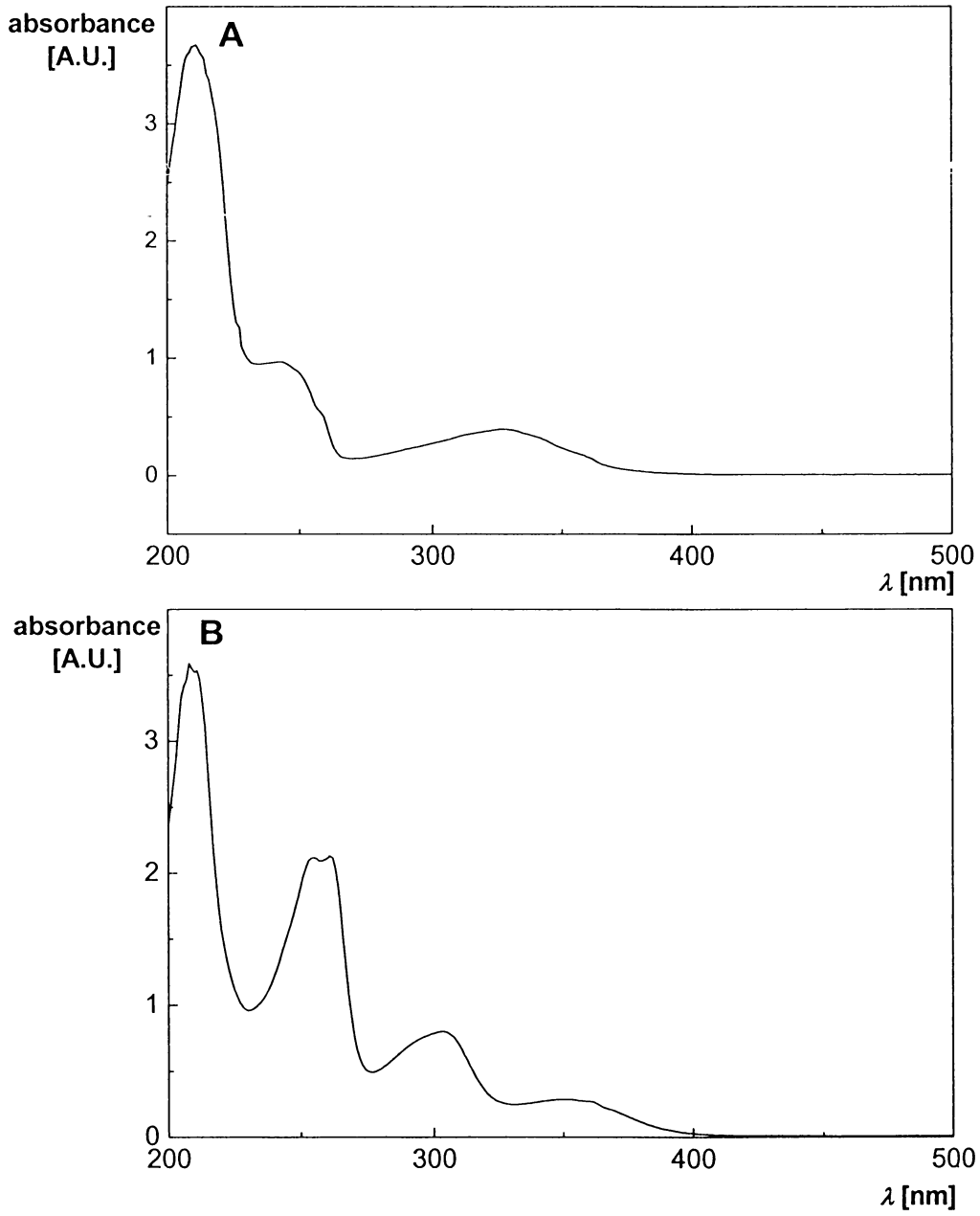

Figure 3.2 *UV spectrum of 1-NN (A) and 2-NN (B) in methanol ($c = 1 \cdot 10^{-3}$ mol L^{-1} of each analyte). Measured in 0.1 cm quartz cuvettes vs. methanol.*

3.3 Results and discussion

3.3.1 Polarographic determination of 1- and 2-nitronaphthalene at a dropping mercury electrode – DC tast polarography and differential pulse polarography

The influence of pH on DC tast polarograms of 1- and 2-NN was investigated in a mixed BR buffer - methanol (1:1) medium, obtained polarograms are depicted in Fig. 3.3. It can be seen that under these conditions the DC tast polarogram exhibits one, well developed irreversible wave in the whole investigated pH range. The dependence of the half wave potential ($E_{1/2}$) on the pH^f of the base electrolyte (Fig. 3.4) suggests equal number of exchanged electrons and protons in the range of pH^f 2.7-10.3. This wave corresponds to the reduction of 1- or 2-nitronaphthalene to corresponding hydroxylaminonaphthalene, according to Eq. (3.1). The half-wave potential of this first wave shifts to more negative values with increasing pH^f. This shift can be described in the range of pH^f 2.7-10.3 by following relationships:

1-NN: $E_{1/2}$ [V] = –0.069 pH^f + 0.010 (R = –0.9981) (3.5)

2-NN: $E_{1/2}$ [V] = –0.062 pH^f – 0.042 (R = –0.9976) (3.6)

In the range of pH^f 11.2-12.2, the $E_{1/2}$ values for both compounds do not change significantly.

At pH^f 2.7-5.9, a second, much lower, poorly developed irreversible wave can be seen, obviously corresponding to the further irreversible reduction of the hydroxylaminonaphthalene to 1- or 2-aminonaphthalene, according to Eq. (3.2). The half wave potential of this wave is also pH^f dependent for studied analytes:

1-NN: $E_{1/2}$ [V] = –0.142 pH^f – 0.023 (R = –0.9931) (3.7)

2-NN: $E_{1/2}$ [V] = –0.167 pH^f + 0.037 (R = –0.9865) (3.8)

The height of this wave is not easy to evaluate and therefore it is not suited for analytical purposes.

The height of the first wave is more or less constant for 1-NN in the whole pH range measured, nevertheless, the best developed and steepest waves were obtained in a mixed medium of BR buffer (pH 12.0) - methanol (1:1) (resulting pH^f of the mixture 12.2). Because the buffer capacity around this pH is already limited and the prevailing component of the buffer is NaOH, only 0.01 mol L^{-1} NaOH was used for measuring calibration dependences. The height of the wave is a linear function of 1-NN concentration within the concentration

range of $0.8 \cdot 10^{-7}$ -$1 \cdot 10^{-4}$ mol L^{-1} (see Table 3.3). In Fig. 3.5, the polarograms obtained in the lowest concentration range attainable are depicted.

For 2-NN, slight differences in wave-heights are observable, the highest limiting currents were obtained in a mixed medium of BR buffer (pH 8.0) - methanol (1:1) (resulting pH^f of the mixture 8.8), where calibration dependence was measured. The calibration curve is linear within the concentration range of $2 \cdot 10^{-6}$ -$1 \cdot 10^{-4}$ mol L^{-1}, the LOD is $2 \cdot 10^{-6}$ mol L^{-1}. Further, 0.01 mol L^{-1} NaOH - methanol (1:1, pH^f 12.2) as for 1-NN was also tested as supporting electrolyte, nevertheless the slope of calibration dependence was lower and the LOD ($4 \cdot 10^{-6}$ mol L^{-1}) higher than for mixed BR buffer - methanol (pH^f 8.8) medium.

The electrochemical behaviour of 1-NN and 2-NN using DPP at DME was studied analogically under the same conditions as above. It reflects the behaviour in DC tast polarography, thus both compounds give in the pH^f range of 2.7-12.2 one, well developed peak, which shifts towards more negative potentials with increasing pH^f. At pH^f 2.7-3.9 a second, much lower and poorly developed peak appears. Obtained polarograms are depicted in Fig. 3.6. The best developed and most easily evaluable peaks were obtained again in a mixed Britton-Robinson buffer - methanol (1:1) medium, pH^f 12.2 (1-NN) and pH^f 8.8 (2-NN). The parameters of calibration curves are summarized for both polarographic techniques in Table 3.3.

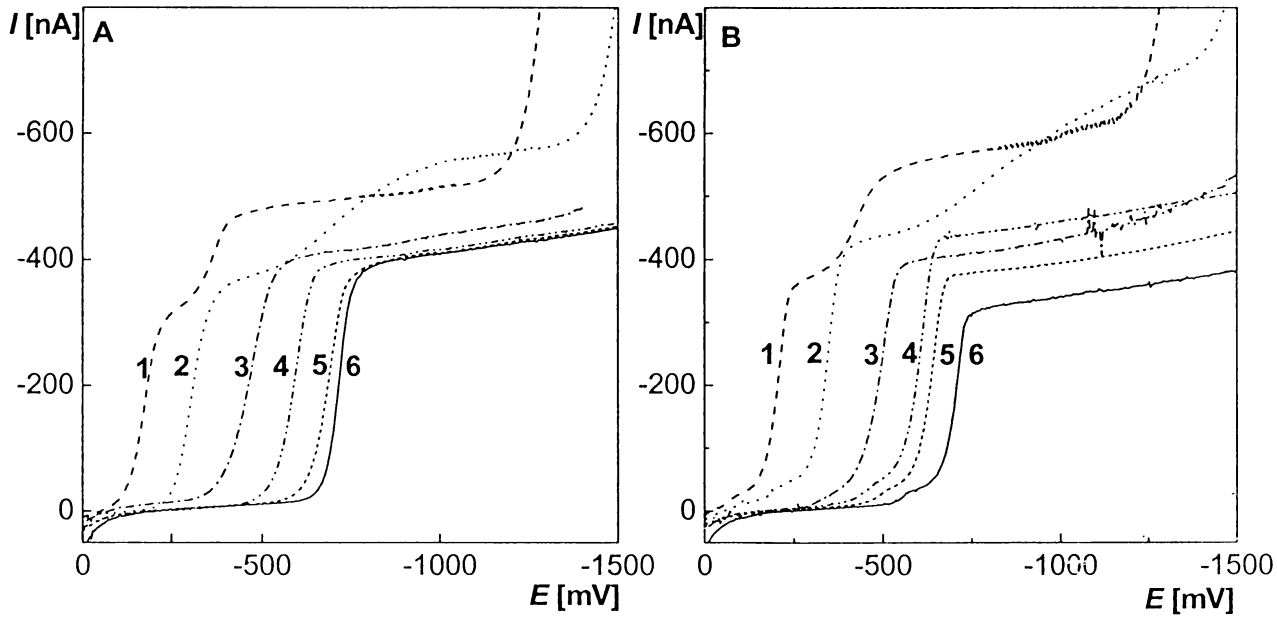

Figure 3.3 *Selected DC tast polarograms of 1-NN and 2-NN (c = $1 \cdot 10^{-4}$ mol L^{-1}) in BR buffer - methanol (1:1) mixture, resulting pH^f: 2.7 (1), 4.9 (2), 7.0 (3), 8.8 (4), 10.3 (5), and 12.2 (6).*

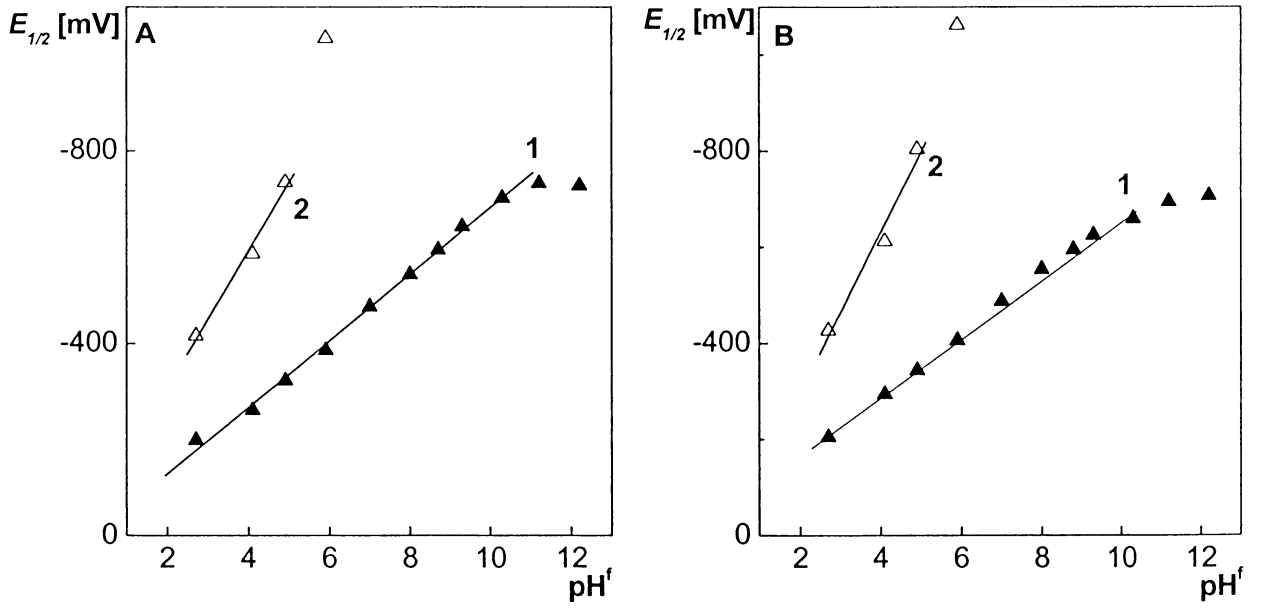

Figure 3.4 *The dependence of the half-wave potential $E_{1/2}$ of 1-NN and 2-NN (c = $1 \cdot 10^{-4}$ mol L^{-1}) on pH^f measured by DC tast polarography at DME. Base electrolyte: BR buffer - methanol (1:1) mixture.*

1 – the first wave; 2 – the second wave

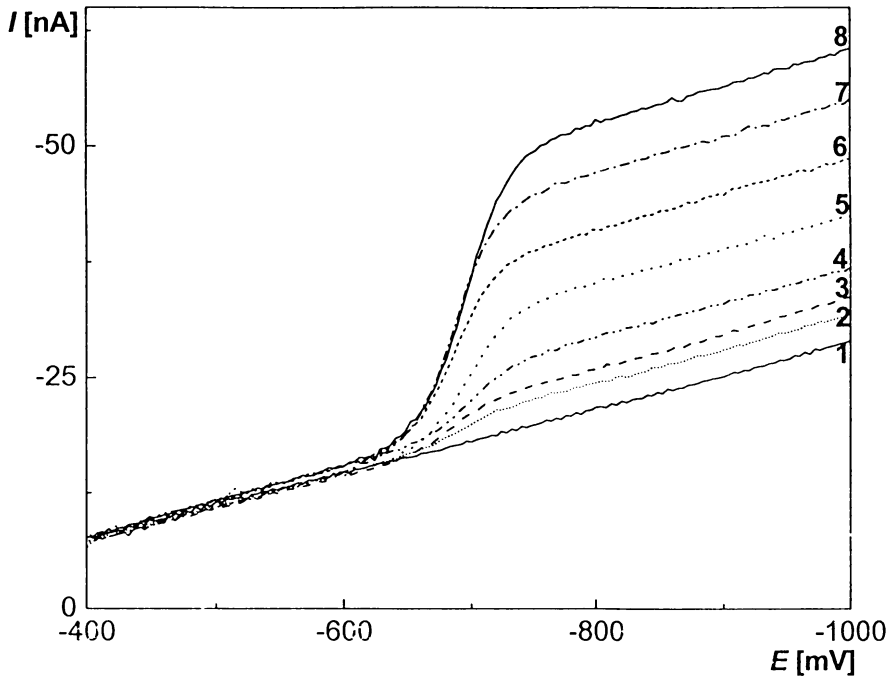

Figure 3.5 *DC tast polarograms of 1-NN in 0.01 mol L^{-1} NaOH - methanol mixture (1:1, pH^f 12.2), c (1-NN) = 0 mol L^{-1} (1), $8 \cdot 10^{-7}$ mol L^{-1} (2), $1 \cdot 10^{-6}$ mol L^{-1} (3), $2 \cdot 10^{-6}$ mol L^{-1} (4), $4 \cdot 10^{-6}$ mol L^{-1} (5), $6 \cdot 10^{-6}$ mol L^{-1} (6), $8 \cdot 10^{-6}$ mol L^{-1} (7), $10 \cdot 10^{-6}$ mol L^{-1} (8).*

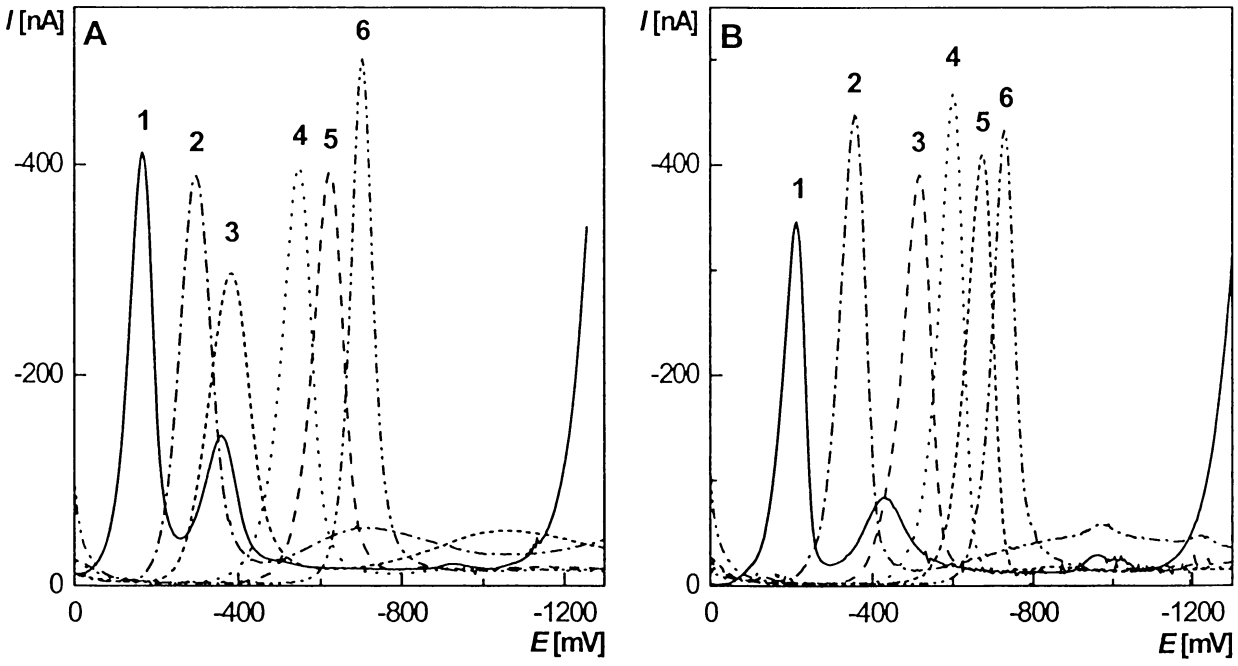

Figure 3.6 *Selected DP polarograms of 1-NN and 2-NN (c = $1 \cdot 10^{-4}$ mol L^{-1}) in a BR buffer - methanol (1:1) mixture, resulting pH^f: 2.7 (1), 4.9 (2), 7.0 (3), 8.8 (4), 10.3 (5), and 12.2 (6).*

Table 3.3 *Parameters of the calibration straight lines for the polarographic determination of 1-NN and 2-NN. Base electrolyte: 1-NN: 0.01 mol L^{-1} NaOH - methanol (1:1, pH[f] 12.0) mixture; 2-NN: BR buffer - methanol (1:1, pH[f] 8.8) mixture.*

Analyte	pH [a]	pH[f]	Concentration [mol L^{-1}]	Slope [mA mol^{-1} L]	Correlation coefficient	LOD [mol L^{-1}]
DC tast polarography						
1-NN	12.0	12.2	$(2\text{-}10)\cdot10^{-5}$	3.245 ± 0.187	0.9950	--
	12.0	12.2	$(0.8\text{-}10)\cdot10^{-6}$	2.970 ± 0.076	0.9987	$1\cdot10^{-6}$
2-NN	8.0	8.7	$(2\text{-}10)\cdot10^{-5}$	3.97 ± 0.325	0.9901	--
	8.0	8.7	$(2\text{-}10)\cdot10^{-6}$	3.69 ± 0.195	0.9958	$2\cdot10^{-6}$
DP polarography						
1-NN	12.0	12.2	$(2\text{-}10)\cdot10^{-5}$	4.863 ± 0.146	0.9987	--
	12.0	12.2	$(2\text{-}10)\cdot10^{-6}$	5.121 ± 0.178	0.9982	--
	12.0	12.2	$(2\text{-}10)\cdot10^{-7}$	5.217 ± 0.115	0.9993	$1\cdot10^{-7}$
2-NN	8.0	8.8	$(2\text{-}10)\cdot10^{-5}$	4.951 ± 0.192	0.9980	--
	8.0	8.8	$(2\text{-}10)\cdot10^{-6}$	4.794 ± 0.246	0.9967	--
	8.0	8.8	$(2\text{-}10)\cdot10^{-7}$	4.280 ± 0.201	0.9923	$2\cdot10^{-7}$

[a] pH of the Britton - Robinson buffer or 0.01 mol·L^{-1} sodium hydroxide

3.3.2 Voltammetric determination of 1- and 2-nitronaphthalene at a hanging mercury drop electrode – differential pulse voltammetry and adsorptive stripping voltammetry

Also for DPV at HMDE, the influence of pH^f on recorded voltammograms was investigated in mixtures of BR buffer pH 2.0-12.0 with methanol (1:1). As in previous cases, the substances give one or two (at pH^f 2.7-5.9) peaks. The dependence of the peak potential of the first peak (E_{p1}) on the pH^f in the range of 2.7-11.2 can be described by following equations:

1-NN: E_{p1} [V] = –0.065 pH^f + 0,022 (R = –0.9984) (3.9)

2-NN: E_{p1} [V] = –0.063 pH^f + 0.011 (R = –0.9967) (3.10)

The highest peaks were obtained in a mixed medium BR buffer (pH 12.0) - methanol (1:1) (resulting pH^f of the mixture 12.2) for both compounds (Fig. 3.7). In order to decrease the content of possible impurities in the supporting electrolyte, for the measurement of calibration curves, the buffer was replaced by 0.01 mol L^{-1} NaOH. Calibration curves were at first measured in a medium containing 50 % of methanol, after that the content of methanol was decreased to 10 %. The limit of determination in the medium containing lower concentration of methanol is about ten fold lower than for the medium with a higher content of methanol (see Tab. 3.4), due to presumably better adsorption of studied analytes at the electrode surface in the medium containing lower content of methanol. The calibration curves deviate from the linear course at concentrations higher than $5 \cdot 10^{-5}$ mol L^{-1}. This is presumably due to adsorption and following fouling of the electrode surface by reduction products. The DP voltammograms obtained for the lowest attainable concentration range of 1-NN are depicted in Fig. 3.8. A small peak in the base electrolyte curve, which coincides with the peak of 1-NN, is observable at the potential of –630 mV. This impurity is contained in the NaOH used, because its peak height decreases when diluting the base electrolyte with deionized water. Therefore, the calibration straight line was evaluated as shown in Fig. 3.9. Due to the presence of the impurity, the calibration curve for this concentration range does not come through the coordinate origin (Fig. 3.9, curve 1), which results in a statistically significant intercept. After the subtraction of the impurity peak height from peak heights of 1-NN, corrected values were obtained, giving practically zero, statistically non significant intercept (Fig. 3.9, curve 2).

To lower the detection limits obtained by DP voltammetry, the accumulation of 1-NN and 2-NN on the electrode surface was carried out. Supporting electrolyte without methanol

was used for the accumulation, due to presumptive better adsorption of studied analytes at the electrode surface. With 0.01 mol L^{-1} NaOH, the electrolyte base line was complicated by peaks of accumulated impurities observable also after its ten fold dilution. Therefore, 0.001 mol L^{-1} LiOH was used as supporting electrolyte for further measurements. At first, influence of the accumulation potential (E_{acc}) and time (t_{acc}) on the peak heights was investigated (Fig. 3.10) for the concentration of $1 \cdot 10^{-8}$ mol L^{-1}. For both compounds, the best developed and repeatable peaks were obtained at E_{acc} = –400 mV. 300 s and 120 s were chosen as optimum accumulation times for 1-NN and 2-NN, respectively. The difference in t_{acc} may be subscribed to differences in the structure of both compounds, further discussed in chapter 4.3.3. Calibration curve measured under optimized conditions (E_{acc} = –400 mV and t_{acc} = 300 s for 1-NN; E_{acc} = –400 mV and t_{acc} = 120 s for 2-NN) are linear in the concentration range of $2 \cdot 10^{-9}$-$1 \cdot 10^{-8}$ mol L^{-1} (Tab. 3.5), voltammograms corresponding to this lowest attainable concentration range are depicted in Fig. 3.11.

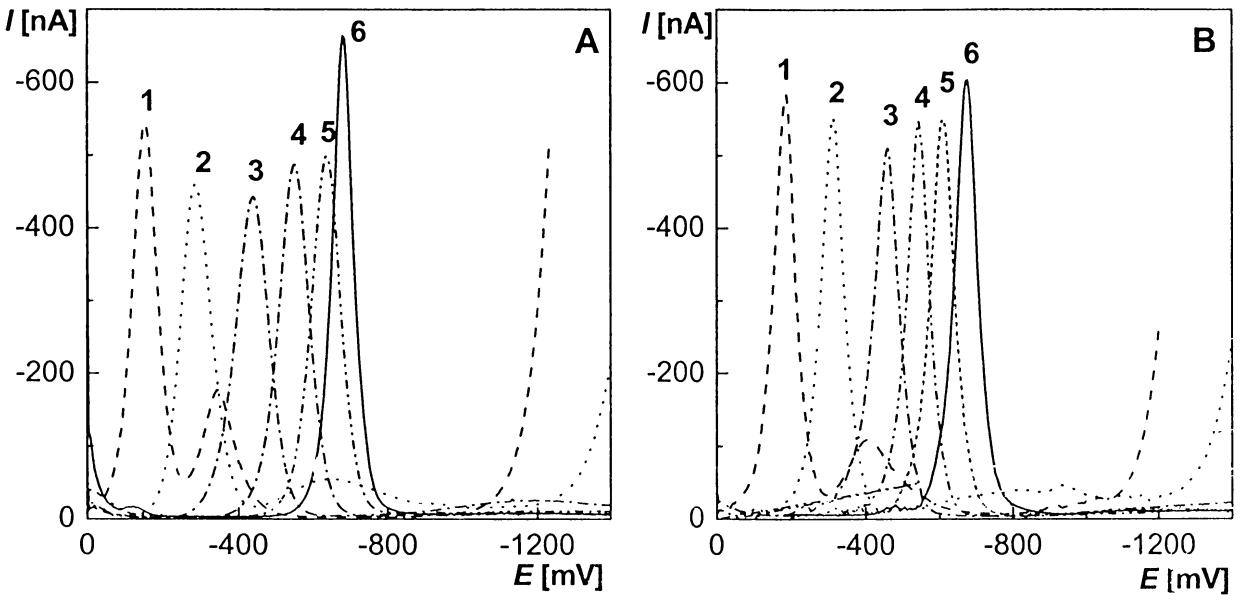

Figure 3.7 *Selected DP voltammograms of 1-NN and 2-NN ($c = 1 \cdot 10^{-4}$ mol L^{-1}) in a Britton-Robinson buffer - methanol (1:1) mixture, resulting pH[f]: 2.7 (1), 4.9 (2), 7.0 (3), 8.8 (4), 10.3 (5), and 12.2 (6).*

Table 3.4 *Parameters of the calibration straight lines for the DP voltammetric determination of 1-NN and 2-NN in a mixed 0.01 mol L^{-1} NaOH - methanol (9:1 and 1:1 medium.*

Analyte	pH [a]	pH[f]	Concentration [mol L^{-1}]	Slope [mA mol^{-1} L]	Correlation coefficient	LOD [mol L^{-1}]
1-NN	12.0	12.2 [b]	$(2\text{-}10)\cdot10^{-7}$	14.91 ± 1.15	0.9915	$2\cdot10^{-7}$
	12.0	12.0 [c]	$(2\text{-}10)\cdot10^{-6}$	42.58 ± 1.01	0.9991	--
	12.0	12.0 [c]	$(2\text{-}10)\cdot10^{-7}$	38.49 ± 0.62	0.9989	--
	12.0	12.0 [c]	$(2\text{-}10)\cdot10^{-8}$	38.74 ± 2.17	0.9952	$3\cdot10^{-8}$
2-NN	12.0	12.2 [b]	$(2\text{-}10)\cdot10^{-7}$	16.20 ± 1.25	0.9938	$3\cdot10^{-7}$
	12.0	12.0 [c]	$(2\text{-}10)\cdot10^{-6}$	39.15 ± 1.56	0.9982	--
	12.0	12.0 [c]	$(2\text{-}10)\cdot10^{-7}$	40.19 ± 0.75	0.9999	--
	12.0	12.0 [c]	$(2\text{-}10)\cdot10^{-8}$	41.87 ± 1.05	0.9963	$1\cdot10^{-8}$

[a] pH of the sodium hydroxide; [b] mixed 0.01 mol L^{-1} NaOH - methanol (1:1) medium; [c] mixed 0.01 mol L^{-1} NaOH - methanol (9:1) medium

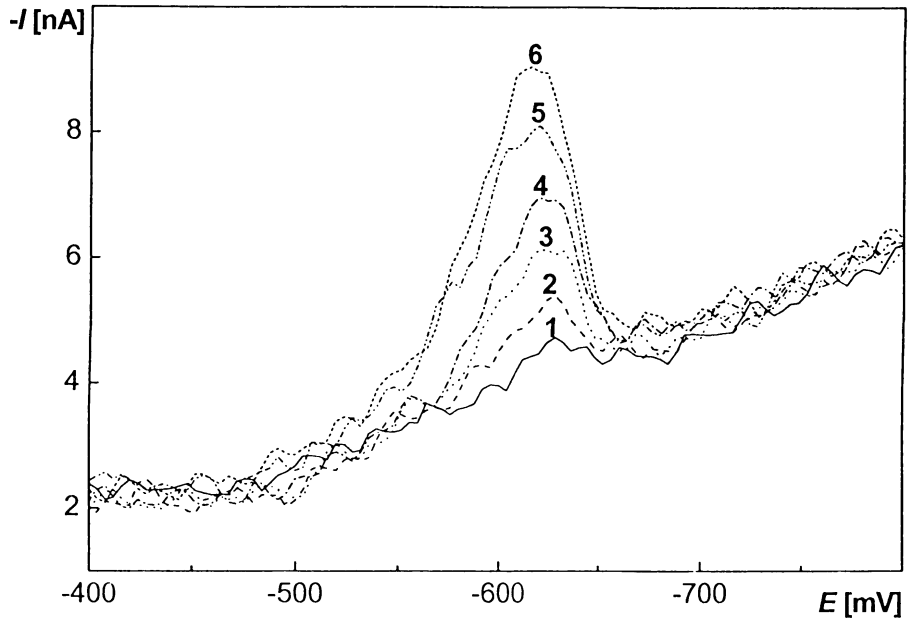

Figure 3.8 *DP voltammograms of 1-NN in 0.01 mol L^{-1} NaOH - methanol mixture (9:1, pH 12.0), c (1-NN) = 0 mol L^{-1} (1), $2 \cdot 10^{-8}$ mol L^{-1} (2), $4 \cdot 10^{-8}$ mol L^{-1} (3), $6 \cdot 10^{-8}$ mol L^{-1} (4), $8 \cdot 10^{-8}$ mol L^{-1} (5), $10 \cdot 10^{-8}$ mol L^{-1} (6).*

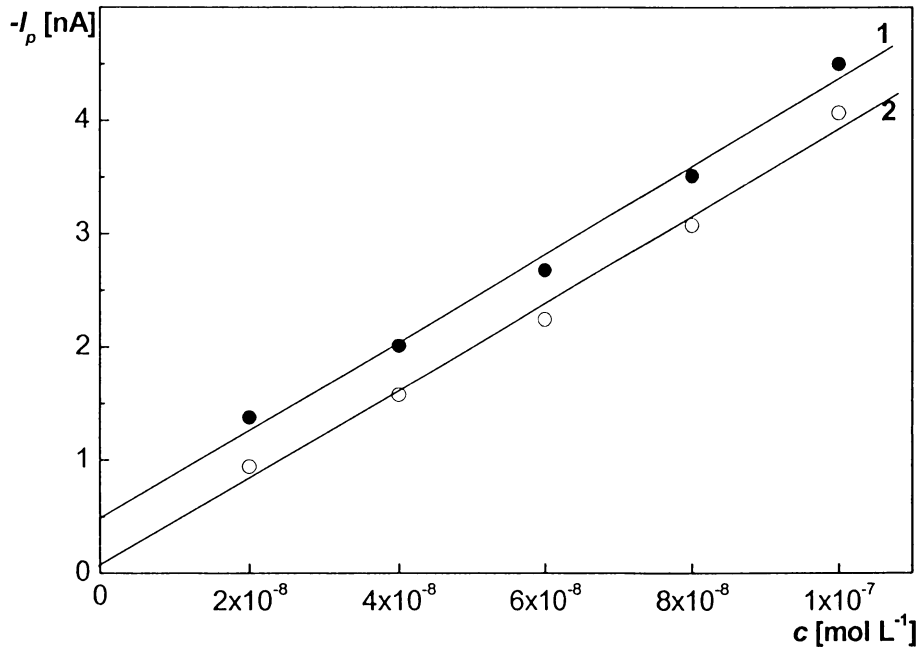

Figure 3.9 *The dependence of the peak height I_p of 1-NN on its concentration in the range of $2 \cdot 10^{-8}$-$1 \cdot 10^{-7}$ mol L^{-1}. Measured by DPV at HMDE in 0.01 mol L^{-1} NaOH - methanol mixture (9:1, pH 12.0).*

The dependence without (1) and after (2) the subtraction of the peak height of the coincideting peak in the base electrolyte.

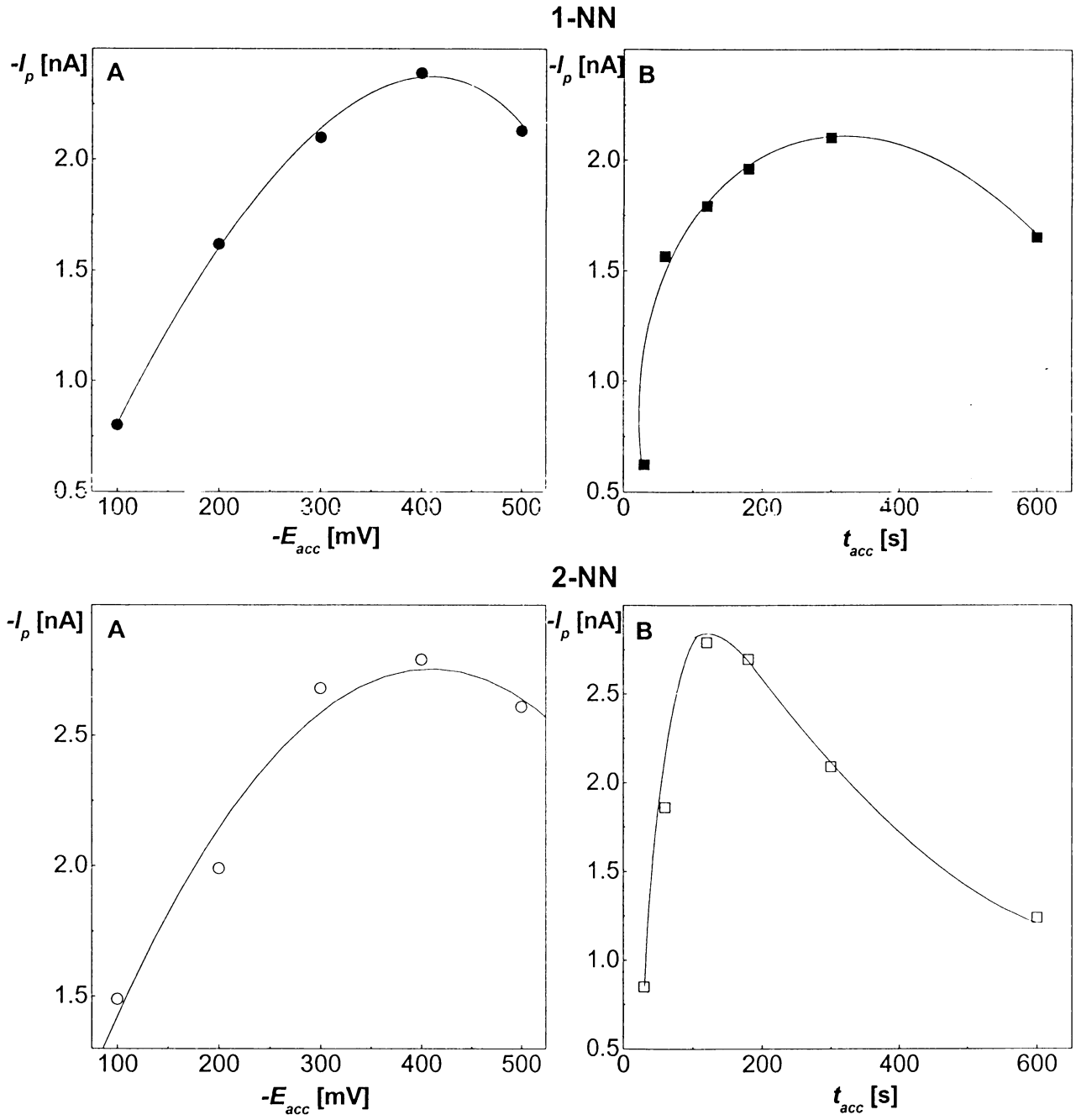

Figure 3.10 *Dependence of the height of the AdSV peak (I_p) of 1-NN (full symbols) and 2-NN (hollow symbols) on potential of accumulation E_{acc} (A) and the time of accumulation t_{acc} (B) in 0.001 mol L^{-1} LiOH.*

Conditions: 1-NN ($c = 1 \cdot 10^{-8}$ mol L^{-1}) – Fig. (A) t_{acc} = 300 s; Fig. (B) E_{acc} = –400 mV

2-NN ($c = 1 \cdot 10^{-8}$ mol L^{-1}) – Fig. (A) t_{acc} = 120 s; Fig. (B) E_{acc} = –400 mV

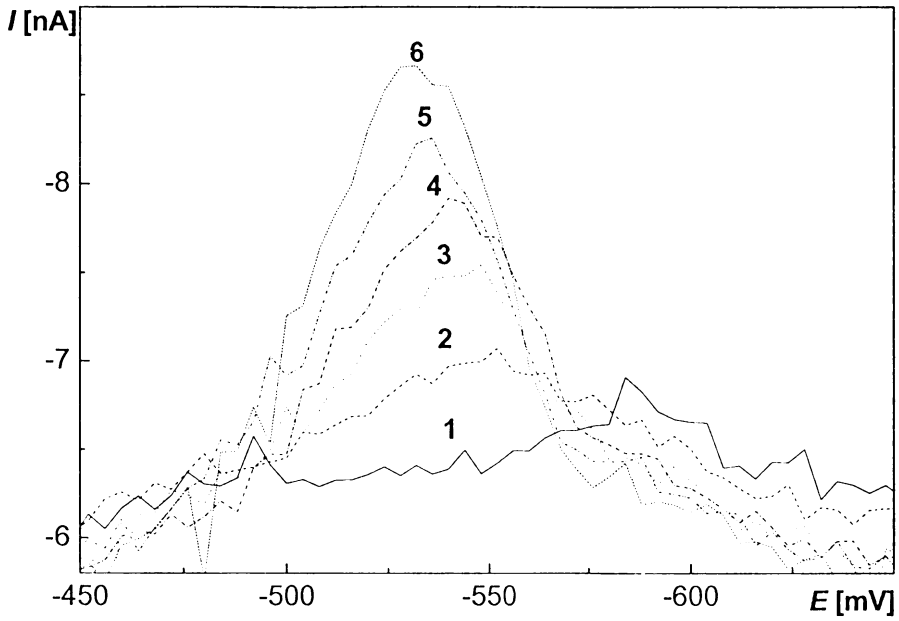

Figure 3.11 *Adsorptive stripping voltammograms of 2-NN in 0.001 mol L^{-1} LiOH, t_{acc} = 120 s, E_{acc} = –400 mV, c (2-NN) = 0 mol L^{-1} (1), $2 \cdot 10^{-9}$ mol L^{-1} (2), $4 \cdot 10^{-9}$ mol L^{-1} (3), $6 \cdot 10^{-9}$ mol L^{-1} (4), $8 \cdot 10^{-9}$ mol L^{-1} (5), $1 \cdot 10^{-8}$ mol L^{-1} (6).*

Table 3.5 *Parameters of the calibration straight lines for the AdS voltammetric determination of 1-NN and 2-NN.*

1-NN: AdSV at HMDE in 0.001 mol L^{-1} LiOH, t_{acc} = 300 s, E_{acc} = –400 mV

2-NN: AdSV at HMDE in 0.001 mol L^{-1} LiOH, t_{acc} = 120 s, E_{acc} = –400 mV

Analyte	pH	Concentration [mol L^{-1}]	Slope [mA mol^{-1} L]	Correlation coefficient	LOD [mol L^{-1}]
1-NN	10.6	$(2\text{-}10) \cdot 10^{-9}$	197.1 ± 8.3	0.9925	$2 \cdot 10^{-9}$
2-NN	10.6	$(2\text{-}10) \cdot 10^{-9}$	247.6 ± 6.2	0.9991	$2 \cdot 10^{-9}$

3.3.3 Cyclic voltammetry

Cyclic voltammetry is in the forefront of the study of the electron transfer and its consequences. The cyclic voltammetric response curve provides information about electron transfer kinetics and thermodynamics as well as the consequences of electron transfer. Hence, cyclic voltammetry experiments in mixed methanol – aqueous media, ratio 1:1 and 9:1, and nonaqueous media of dimethylformamide (DMF) with 0.1 mol L^{-1} tetrabutylammoniumiodide (TBAI) were carried out to investigate the mechanism of reduction. Britton-Robinson buffer was used as aqueous phase and various scan rates (20, 40, 80, 100, 160, 320, 640, 1280, 2560, and 5120 mV s^{-1}) were applied.

The peaks and trends at the recorded CVs were similar for the media containing aqueous phase - methanol in the ratio 9:1 and 1:1, for the latter the CVs of 1-NN and 2-NN (c=1·10^{-4} mol L^{-1}) at HMDE in methanol - Britton-Robinson buffer, pH 2.0, 7.0, and 12.0 (1:1, pH[f] 2.7, 8.0, and 12.2, respectively) are depicted in Fig. 3.12. The first, the second, and the twelfth cycle recorded at the scan rates of 100 mV s^{-1} are presented. The CVs were recorded from positive to negative potentials, the scan was reversed at the end of the potential window. The first cycle features the cathodic peak p^{c1} in all studied media, corresponding to the reduction of the nitro compound to the hydroxylamino derivative according to Eq. (3.1). In acidic media, this peak is accompanied by the second peak p^{c2} of consecutive reduction of the hydroxylamine to the amino derivative (Eq. 3.2). Neither of the peaks corresponds to a reversible process, as seen from the reversed scan. The anodic peak p^{a3} at the potential of 400-450 mV less positive than p^{c1} in this reversed scan corresponds to the two electron reversible oxidation of the hydroxylamine (ArNHOH) to a nitroso (ArNO) derivative; the reverse reaction produces cathodic p^{c3} in the second cycle:

$$\mathrm{ArNHOH} \leftrightarrow \mathrm{ArNO} + 2e^- + 2\mathrm{H}^+ \qquad (3.11)$$

There is a decrease of p^{c1}, probably because of fouling of the electrode surface by reaction products, and slight increase of p^{a3} and p^{c3} current in neutral and alkali media observable upon repetitive cycling. These peaks are only insinuated in acidic media when cycling behind p^{c2} (reduction to $ArNH_2$), but are obvious when reversing the scan immediately after p^{c1}, as the produced ArNHOH can be readily oxidized (Fig. 3.12A).

In alkaline medium (Fig. 3.12C), the peak p^{c1} appears in the first cathodic scan, however, this peak splits to two peaks p^{c1a} and p^{c1b} from the second scan. This peak-splitting, usually observable already in the first cycle, was reported for many analogical aromatic nitro compounds, e.g., nitrobenzene and its derivatives in 80% dioxane [29] and aprotic solvents like

acetonitrile and DMF at classical DME [30] or for mixed DMF - alkaline aqueous media at HMDE [13]. The same phenomenon was observed also in aqueous solutions containing organic surfactants [31,32,33,34,35]. Nitronaphthalenes were investigated in DMF containing 0.2 mol L^{-1} $NaNO_3$ [36,37] or tetraethylammonium perchlorate [38] as supporting electrolyte at mercury electrodes producing the same two peaks. The reduction pathway for all this cases was attributed to the following mechanism in two separate steps:

$$ArNO_2 + e^- \leftrightarrow ArNO_2^{\bullet -} \qquad (3.4)$$

$$ArNO_2^{\bullet -} + 3e^- + 4H^+ \leftrightarrow ArNHOH + H_2O \qquad (3.12)$$

The first step includes a fast reversible uptake of one electron forming a radical anion (Eq. 3.4), the second step is a slow three electron irreversible reduction summarized in Eq. (3.12). The rate determining step in Eq. (3.12) is the uptake of the second electron, forming a nitrosoanion, either directly or preceded by a protonization of the radical anion. Therefore, the sequence of the electron and proton uptakes in both steps depends strongly on the supporting electrolyte as well as on the structure of the nitrocompound. The stability of the nitro radical anion produced in Eq. (3.4) is obviously increased in media with lack of free protons necessary for the completion of Eq. (3.12), as is the case of aprotic solvents or strongly alkaline aqueous media. It was documented for mononitronaphthalene radical anions after their electrochemical generation in DMF [36,37,39] or for benzene nitro radical anions in alkaline aqueous solutions by ESR measurements [40] and electrochemical methods [31]. The splitting of p^{c1a} and p^{c1b} observed in Fig. 3.12C is the proof of a certain inhibition of the electrode kinetic due to the presence of reaction products from the first cycle around the HMDE surface. However, the consecutive reaction steps noted in Eq. (3.4) and (3.12) are not fully isolated, because when cycling only behind the p^{c1a} ($ArNO_2^{\bullet -}$), the p^{c3}/p^{a3} (ArNO/ArNHOH) pair is still present although its peak heights decrease (Figure 3.12C).

The full isolation of p^{c1a} and p^{c1b} can be observed in the cathodic scan in Fig. 3.13, obtained in DMF with 0.1 mol L^{-1} TBAI as supporting electrolyte. The expected stability of the nitroradical in this nonaqeous media was confirmed by the existence of the anodic peak p^{a1a}, corresponding to the oxidation of the nitroradical to the nitro derivative, according to Eq. (3.4). When the cathodic sweep was reversed after the p^{c1a} has been traversed, the ArNO/ArNHOH (p^{c3}/p^{a3}) couple can not be identified at the CVs, as the reduction to the ArNHOH is not completed (highlighted full line in Fig. 3.13). The potential difference in this case $\Delta(Ep^{c1a} - Ep^{c1b})$ is ~85 mV for both studied analytes, indicating rather quasi-reversibility of studied redox systems.

The last interesting feature at CVs in methanol containing media is the presence of the reversible p^{c4}/p^{a4} couple. The height of these peaks is increasing under repetitive cycling, however they are produced only when performing the scan in the potential range including p^{c3}/p^{a3} to p^{c1} reactions. When starting the cycling at more negative potentials than the ArNO/ArNHOH (p^{c3}/p^{a3}) pair can be recognized, neither of p^{c4} and p^{a4} peaks is observable, as clearly demonstrated in neutral media at Figure 3.12B. Moreover, these peaks were not obtained under any conditions in the nonaqueous media. These results indicate that the existence p^{c4}/p^{a4} pair is causatively connected to the nitrogroup reduction finished to ArNHOH, the completion of ArNO/ArNHOH redox reactions and the methanol - aqueous media. As the p^{c4}/p^{a4} couple appears also when the cycle is reversed after the p^{c1a} ($ArNO_2^{\cdot-}$) genesis and p^{a4} appears as first of p^{c4}/p^{a4} in the second anodic scan, thus some nitroradical iniciated reaction may be responsible for the formation of oxidizable product showing p^{a4}/p^{c4} pair of peaks. Similar peaks were also observed for dinitronaphthalenes in the same media [41], however, their exact identification would require a more extended mechanistic study.

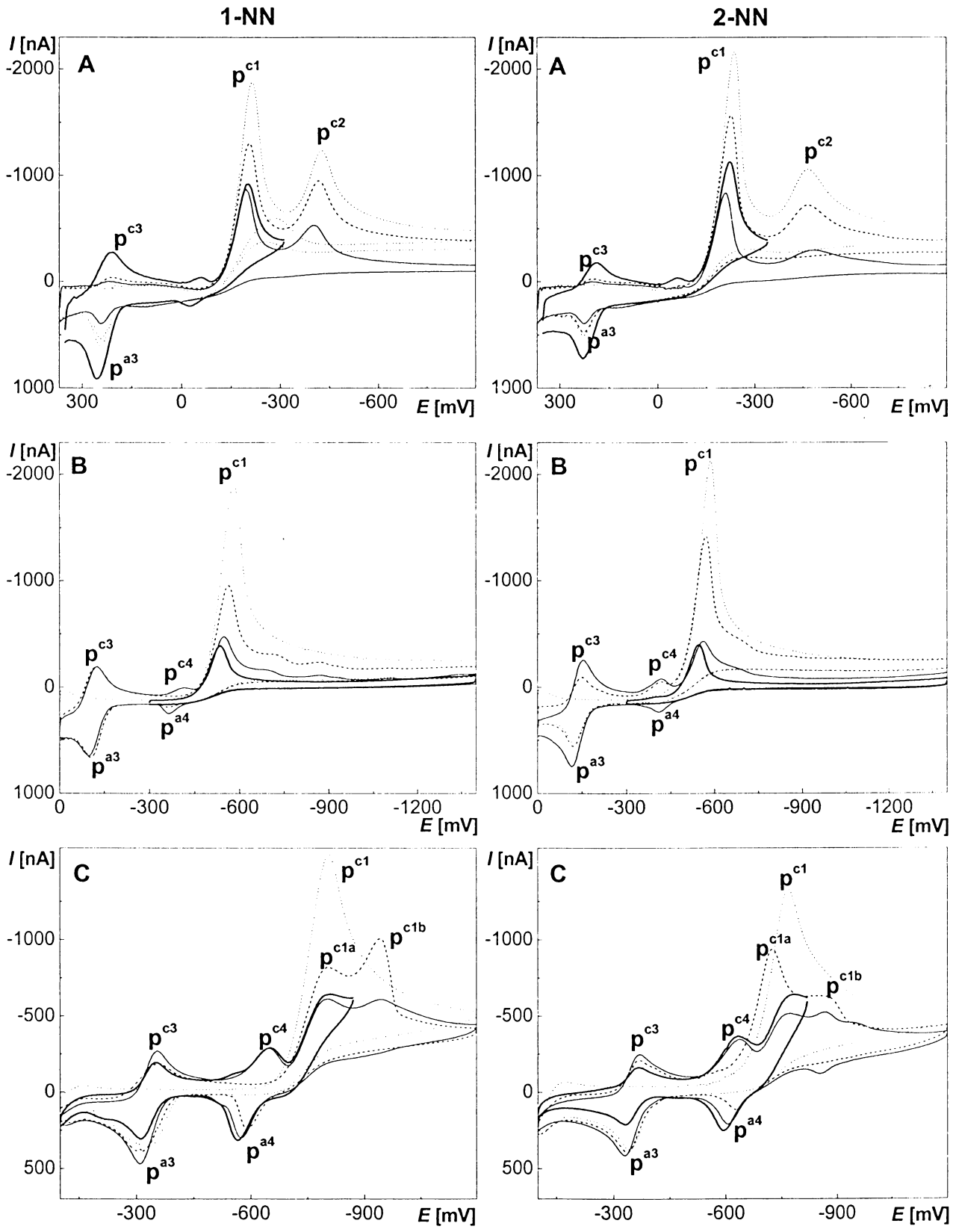

Figure 3.12 *Cyclic voltammograms of 1-NN and 2-NN ($c = 1 \cdot 10^{-4}$ mol L^{-1}) at HMDE in BR buffer - methanol mixture (1:1), pH 2.7 (A), 8.0 (B), and 12.2 (C). The 1st (·····), the 2nd (----) and the 24th (——) scan, scan rate 100 mV s^{-1}. For the shortcut curves, the 24th (——) scan presented. Peak description see in text.*

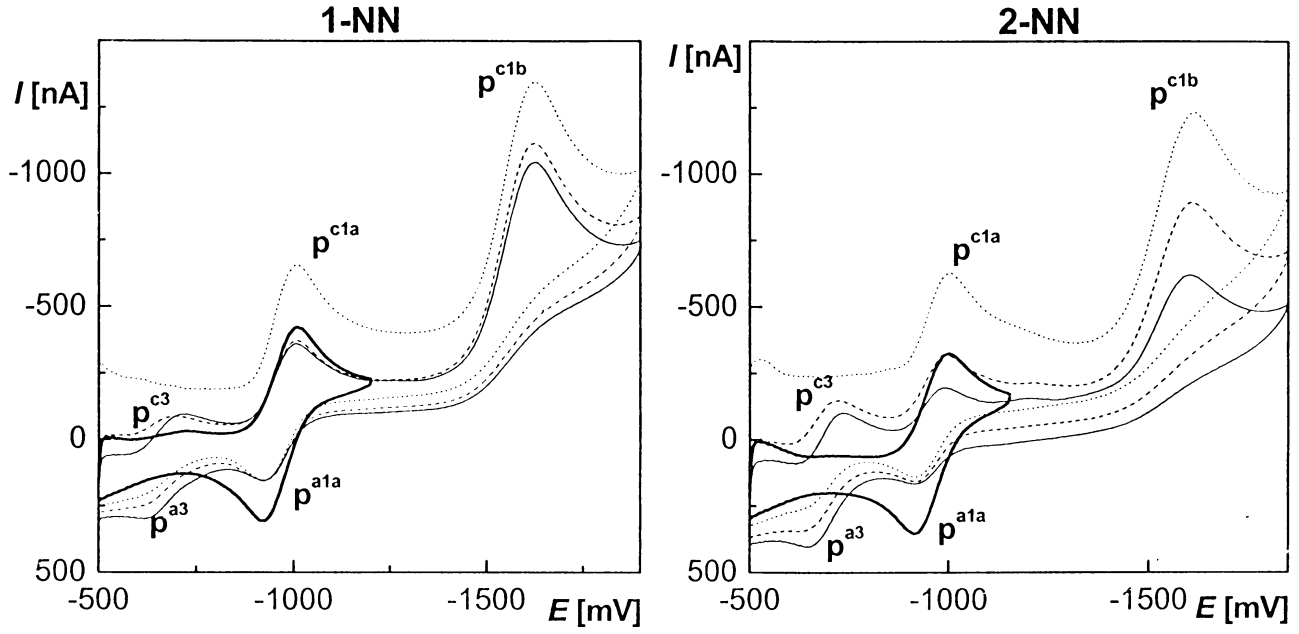

Figure 3.13 *Cyclic voltammograms of 1-NN and 2-NN ($c = 1 \cdot 10^{-4}$ mol L^{-1}) in DMF + 0.1 mol L^{-1} TBAI in the whole potential range (the 1st (·····), the 2nd (----) and the 12th (——) scan) and reversed after the first cathodic peak (the 12th (——) scan), scan rate 100 mV s^{-1}.*

3.3.4 Characterization of the limiting current

Cyclic voltammetry and DC polarography was used to confirm that limiting current is diffusion controlled. DC polarograms of 1- and 2-NN ($c = 1 \cdot 10^{-4}$ mol L^{-1}) were measured in 0.01 mol L^{-1} NaOH - methanol mixture (1:1, pH^f 12.2) at different height of mercury reservoir (h). It can be seen from Fig. 3.14 that the dependence of limiting current of the main reduction wave corresponding with Eq. (3.1) on $h^{1/2}$ is linear and passes through coordinate origin, thus the limiting currents of 1-NN and 2-NN are diffusion controlled.

The cyclic voltammograms of 1-NN and 2-NN ($c = 1 \cdot 10^{-4}$ mol L^{-1}) at HMDE were measured in BR buffer pH 2.0, 7.0 and 12.0 media (1:1 and 9:1) and nonaqueous media of DMF with 0.1 mol L^{-1} TBAI at various scan rates (20, 40, 80, 160, 320, 640, 1280, 2560, and 5120 mV s^{-1}). An example showing the CVs of 1-NN in methanol - BR buffer (1:1), pH^f 12.2 and its evaluation is depicted in Fig. 3.15, corresponding dependences of the cathodic peak currents Ip^{c1}, Ip^{c1a} and Ip^{c1b} on the square root of scan rates follows in Fig. 3.16. These dependences are linear as well as all other dependences of the cathodic peaks currents on the square root of scan rate in media mentioned above, their parameters are summarized in Table 3.6. The linearity and high correlations coefficients (R>0.9900) suggest that these processes corresponding to reduction of the nitro group are diffusion controlled.

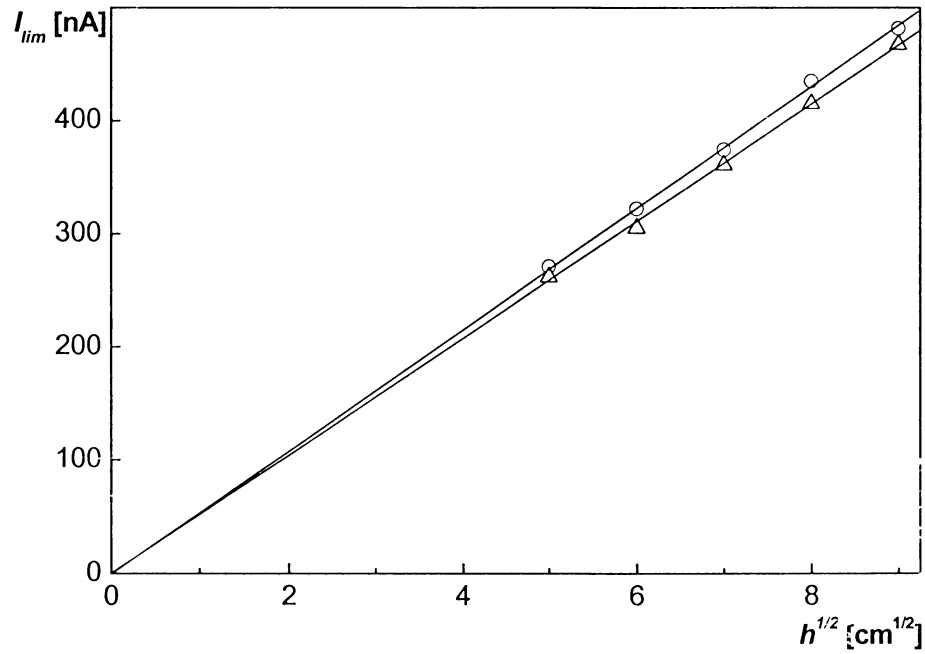

Figure 3.14 *The dependence of the limiting current (I_{lim}) of 1-NN (○) and 2-NN (Δ) ($c = 1 \cdot 10^{-4}$ mol L^{-1}) on $h^{1/2}$. Measured by DC polarography at DME in Britton-Robinson buffer - methanol (1:1, pH 12.2) medium.*

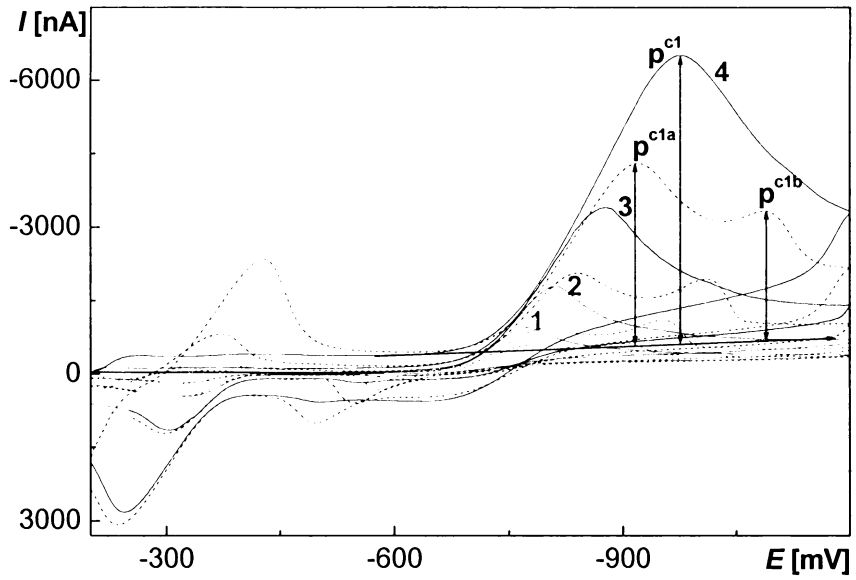

Figure 3.15 *Cyclic voltammograms of 1-NN ($c = 1 \cdot 10^{-4}$ mol L^{-1}) at HMDE in BR buffer - methanol mixture (1:1), pH^f 12.2. The 1st(—) and the 2nd (----) cycle measured at the scan rate of 40 (1), 160 (2), 640 (3) and 2560 (4) mV s^{-1}. Peak descriptions see in text. The vertical black lines indicate the way of peak current evaluation.*

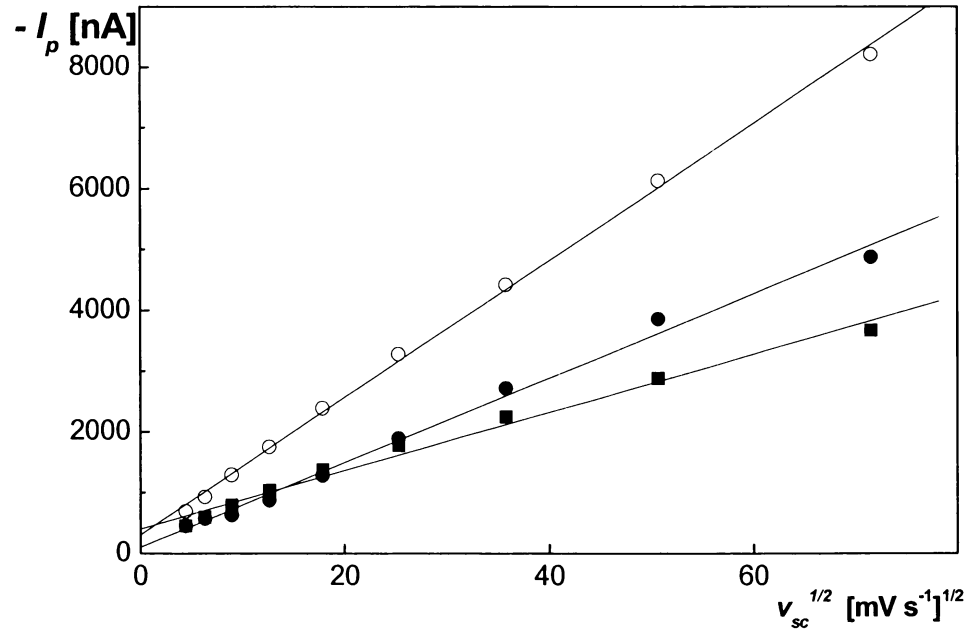

Figure 3.16 *Dependence of the cathodic peak current Ip^{c1} (○), Ip^{c1a} (●), and Ip^{c1b} (■) of 1-NN ($c = 1 \cdot 10^{-4}$ mol L^{-1}) on the square root of scan rate v_{sc}. Measured by cyclic voltammetry at HMDE in methanol - 0.01 mol L^{-1} NaOH (1:1, pH^f 12.2) medium.*

Table 3.6 *Parameters of the linear dependence of the cathodic peaks heights of 1-NN and 2-NN on the square root of scan rate. Peak identity refers to Fig. 3.12.*
Supporting electrolyte: Britton-Robinson buffer - methanol mixture (BRB-MeOH) or 0.1 mol L^{-1} TBAI in DMF.

Supporting electrolyte	Peak identity	Slope [nA $mV^{-1/2} s^{1/2}$]	Intercept [nA]	Correl. coeff.	Slope [nA $mV^{-1/2} s^{1/2}$]	Intercept [nA]	Correl. coeff.
		1-nitronaphthalene			2- nitronaphthalene		
BRB-MeOH	Ip^{c1}	-229.9	-142.4	0.9975	-192.8	-519.9	0.9958
pH^f 2.0 (1:1)	Ip^{c2}	-125.1	-297.0	0.9986	-136.0	-104.1	0.9999
BRB-MeOH	Ip^{c1}	-235.8	-252.2	0.9967	-263.6	-376.3	0.9970
pH^f 2.0 (9:1)	Ip^{c2}	-149.5	-69.4	0.9996	-155.0	-25.2	0.9999
BRB-MeOH pH^f 8.0 (1:1)	Ip^{c1}	-244.4	250.9	0.9999	-287.0	242.1	0.9994
BRB-MeOH pH^f 7.2 (9:1)	Ip^{c1}	-233.7	49.3	0.9991	-338.1	-296.4	0.9982
BRB-MeOH	Ip^{c1}	-112.8	-305.1	0.9992	-116.4	-117.1	0.9998
pH^f 12.2	Ip^{c1a}	-69.5	-103.0	0.9965	-89.8	-57.2	0.9952
(1:1)	Ip^{c1b}	-47.9	-405.5	0.9937	-48.6	-80.1	0.9993
BRB-MeOH	Ip^{c1}	-302.9	-599.1	0.9987	-115.8	-123.1	0.9987
pH^f 12.0	Ip^{c1a}	-165.4	52.1	0.9968	-100.72	111.9	0.9981
(9:1)	Ip^{c1b}	-77.0	-139.3	0.9928	-47.0	-104.8	0.9982
DMF +	Ip^{c1a}	-61.3	-4.8	0.9997	-88.4	-171.6	0.9993
TBAI	Ip^{c1b}	-120.1	-234.7	0.9934	-141.4	-680.11	0.9971

3.4 Conclusions

New electrochemical methods for the determination of 1- and 2-nitronaphthalene were developed applying DC tast polarography and differential pulse polarography at a classical dropping mercury electrode and differential pulse voltammetry and adsorptive stripping voltammetry at a hanging mercury drop electrode. The optimum conditions and achieved limits of determination are summarized in Table 3.7. Nanomolar limits of detection were achieved for AdSV in base media of 0.001 mol L^{-1} LiOH, pH 10.6.

Cyclic voltammetry was used to characterize the reduction mechanism. In mixed methanol - aqueous media it follows the typical pathway of one nitro group containing aromatics, i.e. four electron reduction of the nitro group to the hydroxylamino group (Eq. 3.1) followed by its two electron reduction to amino group in acidic media (Eq. 3.2). In nonaqueous media, the initial one electron reduction of the nitro group to the nitro radical (Eq. 3.4) occurs at more positive potential than the consecutive reductive processes leading to hydroxylamine, thus two peaks are observable at the voltammograms. It was proved by DC polarography and cyclic voltammetry that described processes are diffusion controlled.

Table 3.7 *Optimum conditions and achieved limits of determination (LOD) for polarographic and voltammetric determination of 1- and 2-nitronaphthalene.*

Technique - electrode	Optimum conditions	LOD [mol L^{-1}]
	1-nitronaphthalene	
DCTP - DME	0.01 mol L^{-1} NaOH - MeOH (1:1, pH^f 12.2)	$1 \cdot 10^{-6}$
DPP - DME	0.01 mol L^{-1} NaOH - MeOH (1:1, pH^f 12.2)	$1 \cdot 10^{-7}$
DPV - HMDE	0.01 mol L^{-1} NaOH - MeOH (9:1, pH^f 12.0)	$3 \cdot 10^{-8}$
AdSV - HMDE	0.001 mol L^{-1} LiOH, t_{acc} = 300 s, E_{acc} = –400 mV	$2 \cdot 10^{-9}$
	2-nitronaphthalene	
DCTP - DME	BR buffer - MeOH (1:1, pH^f 8.7)	$2 \cdot 10^{-6}$
DPP - DME	BR buffer - MeOH (1:1, pH^f 8.7)	$2 \cdot 10^{-7}$
DPV - HMDE	0.01 mol L^{-1} NaOH - MeOH (9:1, pH^f 12.0)	$1 \cdot 10^{-8}$
AdSV - HMDE	0.001 mol L^{-1} LiOH, t_{acc} = 120 s, E_{acc} = –400 mV	$2 \cdot 10^{-9}$

3.5 References

1. Shikata M.: *Trans. Faraday Soc.* 21, 42-62 (1925).
2. Shikata M., Tachi I.: *Collect. Czech Chem. Commun.* 10, 368-377 (1938).
3. Vajnstejn J. I.: *Zav. Lab.* 14, 517 - 519 (1948).
4. James J. C.: *Trans. Faraday Soc.* 47, 1240-1246 (1951).
5. Bergmann I., James J. C.: *Trans. Faraday Soc.* 48, 956-964 (1952).
6. Boyd R. N., Reidlinger. A. A.: *J. Electrochem. Soc.* 107, 611-615 (1960).
7. Zahradník R., Boček K.: *Collect. Czech. Chem. Commun.* 26, 1733-1748 (1961).PAH17
8. Jubault M., Peltier D.: *Bull. Soc. Chim.* 4, 1544-1561 (1972).
9. Laviron E., Roullier L.: *J. Electroanal. Chem.* 288, 165-175 (1990).
10. Darchen A., Monet C.: *J. Electroanal. Chem.* 78, 81-88 (1977).
11. Laviron E., Vallat A., Meunier-Prest R: *J. Electroanal. Chem.* 379, 427-435 (1994).
12. Laviron E.: *J. Electroanal. Chem.* 130, 23-29 (1981).
13. Zuman P., Fijalek Z., Dumanovič D., Sužnjevič D.: *Electroanalysis* 4, 783 - 794 (1992).
14. Baizer M. M. (ed.): *Organic electrochemistry: An introduction and guide*, pp. 226-234, Marcel Dekker, New York 1973.
15. Wang J.: *Analytical electrochemistry*, 2nd edition. VCH, Weinheim 2000.
16. Bard A. J.; Faulkner L. R.: *Electrochemical methods*: *Fundamentals and applications*, 2nd edition. John Wiley, New York 2001.
17. Scholz F. (ed.): *Electroanalytical methods : Guide to experiments and applications.* Springer Verlag, Berlin Heidelberg 2002.
18. Wang J.: *Stripping analysis.* VCH, Deerfield Beach 1985.
19. Kasagi M.: *Kogyo Kagaku Zashi* 54, 745-746 (1951). *CA* 47:47235.
20. Imoto E., Motoyama R., Kakiuchi H.: *Bull. Naniwa Univ.* A3, 203-208 (1955). *CA* 49:82886.
21. Bezuglyi V. D., Ogdanets N. D.: *Trudy Komissii Anal. Khim.* 7, 149-154 (1956). *CA* 50:81401.
22. Klopman G., Tonucci D. A., Holloway M., Rosenkranz H. S.: *Mutat. Res.* 126, 139-144 (1984).
23. Quaiserová V.: *MSc Thesis*, Charles University, Faculty of Science, Prague 2001.
24. Sýkora V, in: *Chemickoanalytické tabulky*, SNTL, Prague 1976.
25. Oppenhelmer L., Cappizi T. P., Weppelmann R. M., Metha H.: *Anal. Chem. 55*, 638-643 (1983).
26. Schwartz L. M.: *Anal. Chem.* 55, 1424-1426 (1983).
27. Ebel S., Kamm U.: *Fresenius J. Anal. Chem. 318*, 293-294 (1984).
28. Meloun M., Militký J.: *Statistické zpracování experimentálních dat na osobním počítači.* Finish, Pardubice 1992.

29. Fields M., Valle C., Kane M.: *J. Amer. Chem. Soc.* 71, 421-425 (1949).
30. Mann C. K., Barnes K. K., in: *Monographs in electroanalytical chemistry and electrochemistry* (ed. Bard A. J.), pp. 347. Marcel Dekker, New York, USA 1970.
31. Kastening B.: *Electrochim. Acta* 9, 241-254 (1964).
32. Holleck L., Exner H. J: *Z. Electrochem.* 56, 46-51 (1952).
33. Kastening B., Holleck L.: *Z. Electrochem.* 64, 823-834 (1960).
34. Kastening B., Holleck L. *J. Electroanal. Chem.* 27, 355-368 (1970).
35. McIntire G. L., Chiappardi D. M., Casselberry R. L., Biount H. N.: *J. Phys. Chem.* 86, 2632-2640 (1982).
36. Kemula W., Sioda R.: *Bull. Acad. Pol. Sci.* 11, 395-401 (1963).
37. Kemula W., Sioda R.: *J. Electroanal. Chem.* 7, 233-241 (1964).
38. Krygowski T. M., Stencel M., Z. Galus.: *J. Electroanal. Chem.* 39, 395-405 (1972).
39. Kemula W., Sioda R.: *Naturwissenschaften* 23, 108-109 (1963).
40. Piette L. H., Ludwig P., Adams R. N: *J. Amer. Chem. Soc.* 84, 4212-4215 (1962).
41. Shanmugam K.: *PhD Thesis*, Charles University, Faculty of Science, Prague 2004.

4

Voltammetry of 1- and 2-nitronaphthalene at silver solid amalgam electrode

4.1 Introduction

The investigation on electrochemical performance of various electrode materials over tens of years has confirmed that mercury is the best electrode material for electroanalytical determination of studied NPAHs. However, with respect to strict ecological and safety rules as well as popular prejudices and fears essentially complicating the use of mercury, there is a tendency to substitute it with other non-toxic materials. In the framework of this research, several years ago new types of electrodes based on amalgam materials were introduced. They were designed as follow-ups of previously described electrodes, where the metal surface was covered by mercury [1,2]. The carrier metals included Pt, Au, Ir, Cu or Ag in the form of a wire or a disc. These electrodes proved satisfactory especially thanks to their relatively high hydrogen overvoltage and simple regeneration, including electrochemical pretreatment of their surface. On the other hand, the gradual amalgamation of the metallic support, formation of intermetallic product and some technical difficulties, e.g., with fixing the solid metal in an insulator body caused problems leading to further development of amalgam based electrodes. As a result, the non-toxic solid amalgam electrodes based on amalgamation of soft metal powder (MeSAE) were designed by Prague research group [3]. In the same time, the Trondheim research group developed a solid dental amalgam electrode, which was prepared simply by placing the dental amalgam paste, containing Hg and Ag in weight 1:1 ratio, in a cavity of the electrode holder. So far, this group focuses on the detection of heavy metals [4,5,6,7]. The electrodes prepared by the Prague group feature a variety of metals used for amalgam preparation (e.g., silver, copper, gold, and thallium). They can be used either as mercury-free electrodes after polishing of solid amalgam disc (p-MeSAE) or after modification of their surfaces by mercury film (MF-MeSAE) or mercury meniscus (m-MeSAE). The last two named posses a liquid, ideally smooth and isotropic surface of mercury, exposed to a slow gradual amalgamation process. Among all the metals used, silver seems to perform best of all MeSAE. It was shown that in the absence of specific interactions between the analyte and silver from silver solid amalgam, the DPV peak potentials on m-AgSAE and HMDE are nearly the same [1,2]. Although the solid amalgam electrodes do not reach the quality of HMDE, in many cases they approach it. It was proved by a variety of analytical applications, including the voltammetric determination of heavy metals cations (Cu^{2+}, Pb^{2+}, Cd^{2+}, Zn^{2+}, Fe^{3+}, Ni^{2+}, Tl^{2+}, In^{3+}, Cr^{3+}) and some inorganic anions (NO_3^- , IO_3^-, I^-, Br^-, SCN^-) [1,8,9]. Moreover, m-AgSAE and m-CuSAE were employed for the determination of organic compounds like

nucleic acids [10], cysteine [8], azoaromatics [11], and very low amounts of DNA [12,13] including the detection of its possible damage [14]. Preliminary experiments were done regarding the use of m-AgSAE and m-AuSAE for the analysis of 1-NN, 2-NN, 2-, 3-, and 4- nitrobiphenyl [15], nitro- and m-dinitrobenzene [1,2]. Recently, a DP voltammetric method was proposed for determination of 2-methyl-4,6-dinitrophenol at m-AgSAE with limit of determination $2 \cdot 10^{-7}$ mol L^{-1} (ref. [16]).

After an extended study on the use of modern electroanalytical methods for the determination of 1- and 2-NN on mercury electrodes (chapter 3), this chapter is devoted to study of voltammetric behaviour of studied analytes using m-AgSAE as the most reliable amalgam electrode. Differential pulse voltammetry, cyclic voltammetry and elimination voltammetry with linear scan were used for this purpose. The reduction mechanism, sensitivity and reproducibility were investigated and compared with the situation at mercury electrodes.

4.2 Experimental

4.2.1 Reagents

The stock solution of 1-NN and 2-NN ($c = 1 \cdot 10^{-3}$ mol L^{-1}) was prepared by dissolving 0.0173 g of the substance in 100 mL of methanol or dimethylformamide (DMF). More diluted solutions were prepared by exact dilution of the stock solution with methanol or DMF. All the solutions were stored in the dark. Methanol, DMF, and tetrabutylammoniumiodide (TBAI) were of analytical grade purity (Lachema, Brno, Czech Republic). Britton-Robinson buffers were prepared in a usual way, i.e., by mixing a solution of 0.04 mol L^{-1} in phosphoric acid, 0.04 mol L^{-1} in acetic acid and 0.04 mol L^{-1} in boric acid with the appropriate amount of 0.2 mol L^{-1} sodium hydroxide solution. Chemicals for the preparation of the Britton-Robinson buffers were also obtained from Lachema, Brno, Czech Republic. De-ionized water was produced by Milli-Qplus system (Millipore, USA).

4.2.2 Apparatus

Measurements were carried out using computer controlled Eco-Tribo-Polarograph with Polar Pro software, version 5.1 for Windows 95/98/Me/2000/XP (both Eco-Trend Plus, Prague, Czech Republic) in combination with a three electrode arrangement with a platinum wire auxiliary electrode and silver/silver chloride (1 mol L^{-1} KCl) reference electrode, to

which all the potential values are referred. The working electrode was m-AgSAE with the disc diameter 0.70 mm (area 0.385 mm^2, calculated as the area of a hemisphere with the diameter equal to the disc diameter). The electrode was supplied from Dr. Bogdan Yosypchuk, Institute of Physical Chemistry, Academy of Science, Prague, Czech Republic and consisted of a drawn-out glass tube, the bore of which near the tip was filled with a fine silver powder, amalgamated by liquid mercury and connected to an electric contact [1] (Fig. 4.1 (A)). Afterwards, it was immersed into a small volume of liquid mercury and agitated for 15 seconds to build up the mercury meniscus, which is clearly visible in Fig. 4.1 (B). The m-AgSAE could be used for several weeks without major changes, only its regeneration through mechanical contact with mercury is recommended to be repeated every week. The solution pH was measured with PHM 62 digital pH meter (Radiometer, Copenhagen, Denmark) using combined glass electrode. pH values refer to those of the buffer, pH^f values refer to those of the resulting pH of the mixtures of the buffer with the organic component.

4.2.3 Procedures

Before starting the work, as well as after every pause longer than one hour, the electrochemical activation of m-AgSAE was carried out in 0.2 mol L^{-1} KCl at –2200 mV under stirring of the solution for 300 seconds and then rinsed with distilled water. For DPV measurements, the work with m-AgSAE was carried out at a scan rate of 20 mV s^{-1}, the pulse amplitude of –50 mV, pulse duration of 100 ms, sampling time of 20 ms beginning 80 ms after the onset of the pulse and interval between pulses of 100 ms.

The general procedure to obtain voltammograms was as follows: A required amount of the stock solution of the test substance in methanol or DMF was placed in a 10 mL volumetric flask, an appropriate volume of methanol or DMF was added and the system was diluted to volume with a Britton-Robinson buffer of the required pH. Oxygen was removed from the measured solutions by purging with nitrogen for five minutes under stirring. A prebubbler containing a water-methanol (or DMF) mixture in the same ratio as in the tested solution was placed prior to the polarographic vessel. Regeneration of m-AgSAE lasting about 30 s preceded each measurement; this included the application of 300 polarizing cycles, representing the switching the working potential from E_1 to E_2 for 50 ms. E_1 was selected about 50-100 mV more negative than the potential of the anodic dissolution of the electrode material, E_2 was selected about 50-100 mV more positive than the potential of the hydrogen evolution in the given base electrolyte. Under these conditions, eventual oxides of mercury or

silver are reduced and adsorbed molecules are desorbed. For CV measurements, the regeneration procedure was applied before the first cycle. The appropriate values of the potential and the time of regeneration were inset and modified in the program of the used computer-controlled instrument and regeneration of m-AgSAE could thus be carried out automatically.

The calibration curves were measured in triplicate, the height of the peaks used for evaluation was measured from the straight line connecting the minima before and after the peak, as not stated otherwise. The statistical parameters (i.e. slope, intercept, limit of determination) were calculated according to Oppenhelmer [17], Schwartz [18] and Ebel [19] using statistic software ADSTAT ver. 2.0 (Trilobyte, Czech Republic). The ADSTAT software was also used to test the significance of the intercepts of linear calibration dependences. As these were basically non significant, the intercept values are not listed in Table 4.1 summarizing parameters of calibration dependences.

All the measurements were carried out at laboratory temperature.

4.2.4 Elimination voltammetry with linear scan

The elimination voltammetry with linear scan (EVLS) was used for the elucidation and confirmation of the suggested mechanism on the m-AgSAE and HMDE. This method belongs to the group of methods based on elimination of some particular currents from the registered scans of linear scan voltammetry (DC voltammetry) [20,21,22,23,24]. The EVLS is based on the assumption that the total registered current is composed from various contributions and the EVLS eliminates or conserves its particular contributions or their combinations.

It is assumed that:

1) The registered current is the mathematical sum of particular currents:

$$I = \sum I_j = I_d + I_c + I_k + I_{ir} + \ldots \qquad (4.1)$$

where the I_j are the particular currents (I_d – diffusion, I_c – capacity, I_k – kinetic and I_{ir} – so called irreversible currents).

2) All particular currents I_j are expressible in form:

$$I_j = W_j(v_{sc}).Y_j(E) \qquad (4.2)$$

where the $Y_j(E)$ functions are specific for each current type and are independent on scan rate v_{sc} and $W_j(v_{sc})$ functions are dependent on the scan rate v_{sc} and are totally independent on E (ref. [21]).

$$I_d = v_{sc}^{1/2} Y_d(E);\ I_k = v_{sc}^{0} Y_k(E);\ I_c = v_{sc}^{1} Y_c(E);\ I_{ir} = v_{sc}^{-1/2} Y_c(E) \qquad (4.3)$$

The current function is then constructed and set of m equations for m scan rates is solved. By this way simultaneously some currents can be conserved and some can be eliminated [20-24]. For each EVLS measurement, set of DC voltammograms with different rates of polarization (v_{ref}, $v_{1/2}$, $v_{1/4}$, $2v$) were recorded and digital set of corresponding current values (I_{ref}, $I_{1/2}$, $I_{1/4}$, I_2) was used for calculation.

For the calculation of the following four current functions, one current was conserved and the others were eliminated (the equations are identical with equations (23), (25), (27), and (29) in ref. [21]):

$$f(I_k) = 0; f(I_c) = 0; f(I_r) = I_r$$
$$f(I) = +17.485 \cdot I - 11.657 \cdot I_{1/2} - 5.8284 \cdot I_2 \quad (4.4)$$

$$f(I_r) = 0; f(I_c) = 0; f(I_k) = I_k$$
$$f(I) = -8.2426 \cdot I + 6.8284 \cdot I_{1/2} + 2.4142 \cdot I_2 \quad (4.5)$$

$$f(I_k) = 0; f(I_r) = 0; f(I_c) = I_c$$
$$f(I) = -8.2426 \cdot I + 4.8284 \cdot I_{1/2} + 3.4142 \cdot I_2 \quad (4.6)$$

$$f(I_k) = 0; f(I_{ir}) = 0; f(I_r) = I_r$$
$$f(I) = 6{,}8285 \cdot I - 11{,}657 \cdot I_{1/2} + 4{,}8285 \cdot I_{1/4} \quad (4.7)$$

In the case, when the registered current is not a simple sum of particular currents and when we cannot suppose the validity of eq. (4.1) and/or (4.2), it is possible to perform the same calculations using the theoretical simulations of the processes and thus, on the basis of their comparison, it can be distinguished whether the transported species are before reduction adsorbed or not, or whether the diffusion controlled reaction is preceded by a kinetically controlled reaction. In case of adsorption, characteristic peak - counterpeak form is obtained for a simplified $f(I_d)$ function (according to [24,25]) and counterpeak-peak form for $f(I_c)$ and $f(I_k)$ current functions (according to [26,27]). Using the above given equations (4.4)-(4.7), similar behavior of those functions were obtained (i.e., peak-counterpeak form for $f(I_d)$ and counterpeak-peak form for $f(I_k)$ and $f(I_c)$) and the shape of $f(I_{ir})$ function (see Eq. (4.7)) was similar to $f(I_d)$ function. The forms of elimination voltammograms of diffusion controlled reduction preceded by a kinetically controlled reaction are opposite, i.e., counterpeak-peak for $f(I_d)$, $f(I_{ir})$ functions and peak-counterpeak for $f(I_c)$ and $f(I_k)$ functions.

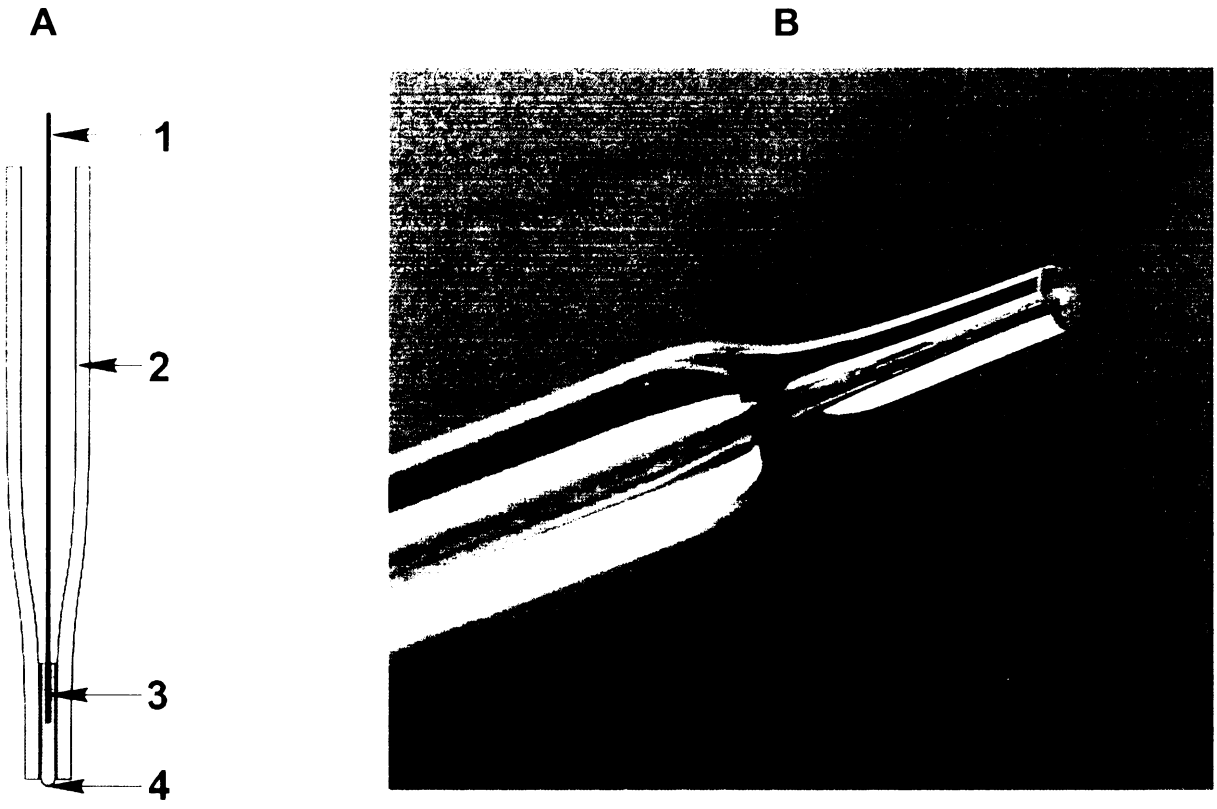

Figure 4.1 *Mercury meniscus modified silver solid amalgam electrode (m-AgSAE):*
A – *Scheme of the electrode body: 1 – electric contact, 2 – glass capillary, 3 – silver powder (amalgam), 4 – mercury meniscus;*
B – *The tip of m-AgSAE with observable mercury meniscus.*

4.3 Results and discussion

4.3.1 Cyclic voltammetry

Similarly to HMDE, cyclic voltammetric experiments were used to characterize the electrochemical behaviour of 1-NN and 2-NN at m-AgSAE in mixed aqueous (Britton Robinson buffer) – nonaqueous (methanol or DMF) media and nonaqueous media of DMF with 0.1 mol L^{-1} TBAI. The CVs of 1-NN and 2-NN in methanol - Britton-Robinson buffer (1:1) media at pH^f 2.7 and 8.0 are depicted in Fig. 4.2, the first, the second and the twelfth cycles are presented. They were recorded from positive to negative potentials, the scan was reversed just before the onset of the background electrolyte decomposition current. On basis of the similarity of the cyclic voltammograms of studied analytes at HMDE (chapter 3.3.3), the mechanism proposed previously for the mercury electrode in Eq. (3.1) - (3.2), chapter 3.1

is assumed: In the first cathodic scan, the cathodic peak p^{c1} can be assigned to the four-electron reduction of the nitro species ($ArNO_2$) to the hydroxylaminoderivative (ArNHOH):

$$ArNO_2 + 4e^- + 4H^+ \rightarrow ArNHOH + H_2O \quad (4.8)$$

In acidic media, this peak is accompanied by an indistinctive peak p^{c2} corresponding to the two electron reduction of the hydroxylaminoderivative to the amino compound ($ArNH_2$):

$$ArNHOH + 2e^- + 2H^+ \rightarrow ArNH_2 + H_2O \quad (4.9)$$

Both these processes are irreversible, as seen from the reverse scan. The anodic peak p^{a3} in this reversed scan reveals the two electron reversible oxidation of the hydroxylamine to a nitroso derivative; the reverse reaction produces p^{c3} in the second cycle:

$$ArNHOH \leftrightarrow ArNO + 2e^- + 2H^+ \quad (4.10)$$

Similarly to HMDE, there is a decrease of p^{c1} and p^{c2} and increase of p^{c3} and p^{a3} current observable upon repetitive cycling, however the changes are not that distinctive. The peak heights at m-AgSAE and calculated current densities are at least seven times lower for the first scan than for HMDE.

In alkaline medium (Fig. 4.3A), in contrast to HMDE, two peaks appear already in the first cathodic scan, presumably corresponding to the one electron reduction to nitro radical anion (p^{c1a}) and its further reduction to hydroxylamine (p^{c1b}) – the same processes assumed for the cathodic peak pair p^{c1a} + p^{c1b} observable from the second cycle of CVs recorded at HMDE (chapter 3.3.3, Eq. (3.4) and (3.12)):

$$ArNO_2 + e^- \leftrightarrow ArNO_2^{\bullet -} \quad (4.11)$$

$$ArNO_2^{\bullet -} + 3e^- + 4H^+ \leftrightarrow ArNHOH + H_2O \quad (4.12)$$

The reversible ArNHOH/ArNO (p^{c3}/p^{a3}) couple can be recognized again in the reverse anodic and second cathodic scan. In addition, an indistinctive peak p^{a1a} is insinuated in the reverse anodic scan, forming a pair with the p^{c1a} peak and corresponding to the reversed oxidation of the nitro radical anion to nitro derivative (Eq. 4.11).

In order to proof the stability of the nitroradical anion and the potential reversibility of the redox system nitroradical anion/nitroderivative (Eq. 4.11), the cathodic sweep was reversed after the first peak p^{c1a} has been traversed. Although the full isolation of $ArNO_2/ArNO_2^{\bullet -}$ (p^{c1a}/p^{a1a}) couple was not observed, a slight increase in the peak current of the nitro radical anion is obvious in Fig. 4.3A. The substantial decrease of the currents of the ArNHOH/ArNO (p^{c3}/p^{a3}) pair gives also evidence about not completed reduction to ArNHOH. Due to the presumably higher stability of the nitro radical anion in an aprotic solvent, the methanol was replaced by DMF. Due to this change the $ArNO_2/ArNO_2^{\bullet -}$

(p^{c1a}/p^{c1b}) couple is more pronounced at the voltammograms (see Fig. 4.3B). It is a proof of decreasing proton availability during the reduction. The full isolation of the $ArNO_2/ArNO_2^{\cdot-}$ pair was achieved in DMF containing 0.1 mol L^{-1} TBAI (Fig. 4.3C) with the current ratio Ip^{c1a}/Ip^{c1b} about one. In this solvent the reduction potential Ep^{c1a} is shifted toward more negative values and $\Delta(Ep^{c1a} - Ep^{c1b})$ increases from about 200 mV (2-NN) and 250 mV (1-NN) in Fig. 4.3A to 670 mV. On the other hand $\Delta(Ep^{c1a} - Ep^{a1a})$ of the $ArNO_2/ArNO_2^{\cdot-}$ couple decreases from 102 mV (1-NN) and 116 mV (2-NN) to about 59 mV for both – a theoretical value for a one-electron diffusion controlled reversible process. Finally, the constant values of the peak potentials in the scan rate range of 20-640 mV s^{-1} suggest that the redox behaviour tends to become reversible.

The peak splitting of p^{c1} to p^{c1a} and p^{c1a} is known also for other solid electrodes, it was observed e.g. in alkaline (0.1 mol L^{-1} NaOH) solutions containing 15% methanol at gold, silver and platinum electrode [28]. At gold and glassy carbon electrodes, the effect of the electrode pretreatment on the reduction mechanism was in addition studied [29], because the condition of the electrode surface plays an important role in the reduction mechanism of nitroaromatics. It may inhibit the protonation steps as well as the electron transfer, due to competitive adsorption at the solid surface or sterically lowered availability of the species for the reaction, both leading to the stabilization of the radical anions and separation of the one electrone reduction step (Eq. 4.11). Although a detailed mechanistic model for m-AgSAE cannot be suggested on the basis of these results alone, the reduction of nitronaphthalenes follows the pattern known for solid electrodes, despite the presence of mercury at the surface of m-AgSAE. It is a proof of a certain inhibition of the electrode kinetic due to the solid, silver containing amalgam surface. The observed linear dependence of peak currents of p^{c1}, p^{c2}, and p^{c1b} on the square root of the scan rate confirms the diffusion control of the observed processes.

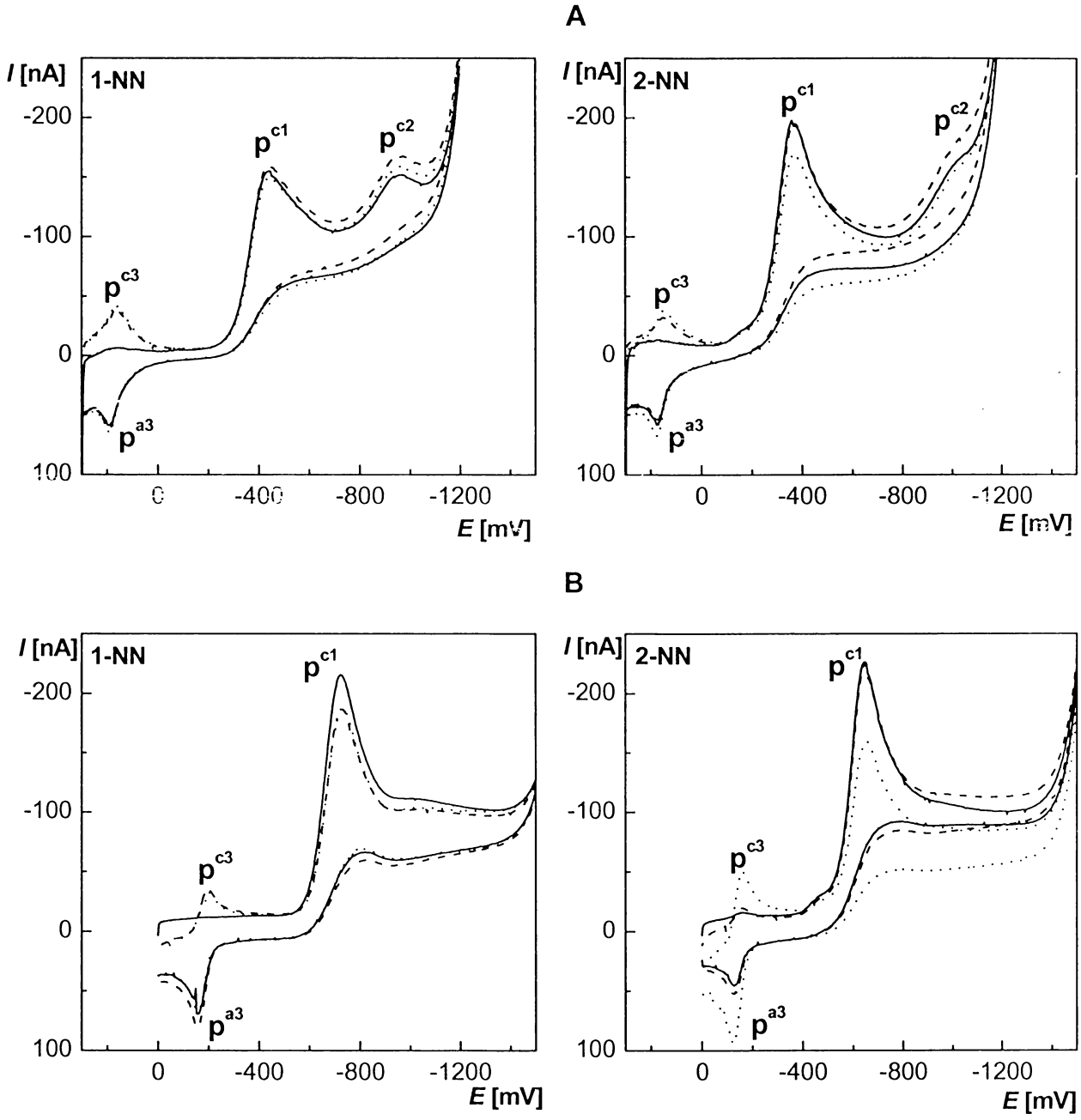

Figure 4.2 *Cyclic voltammograms of 1-NN and 2-NN ($c = 1 \cdot 10^{-4}$ mol L^{-1}) at m-AgSAE in BR buffer - methanol mixture (1:1), pH 2.7 (A) and 8.0 (B). The 1st (——), the 2nd (----) and the 12th (·····) scan, scan rate 100 mV s^{-1}.*

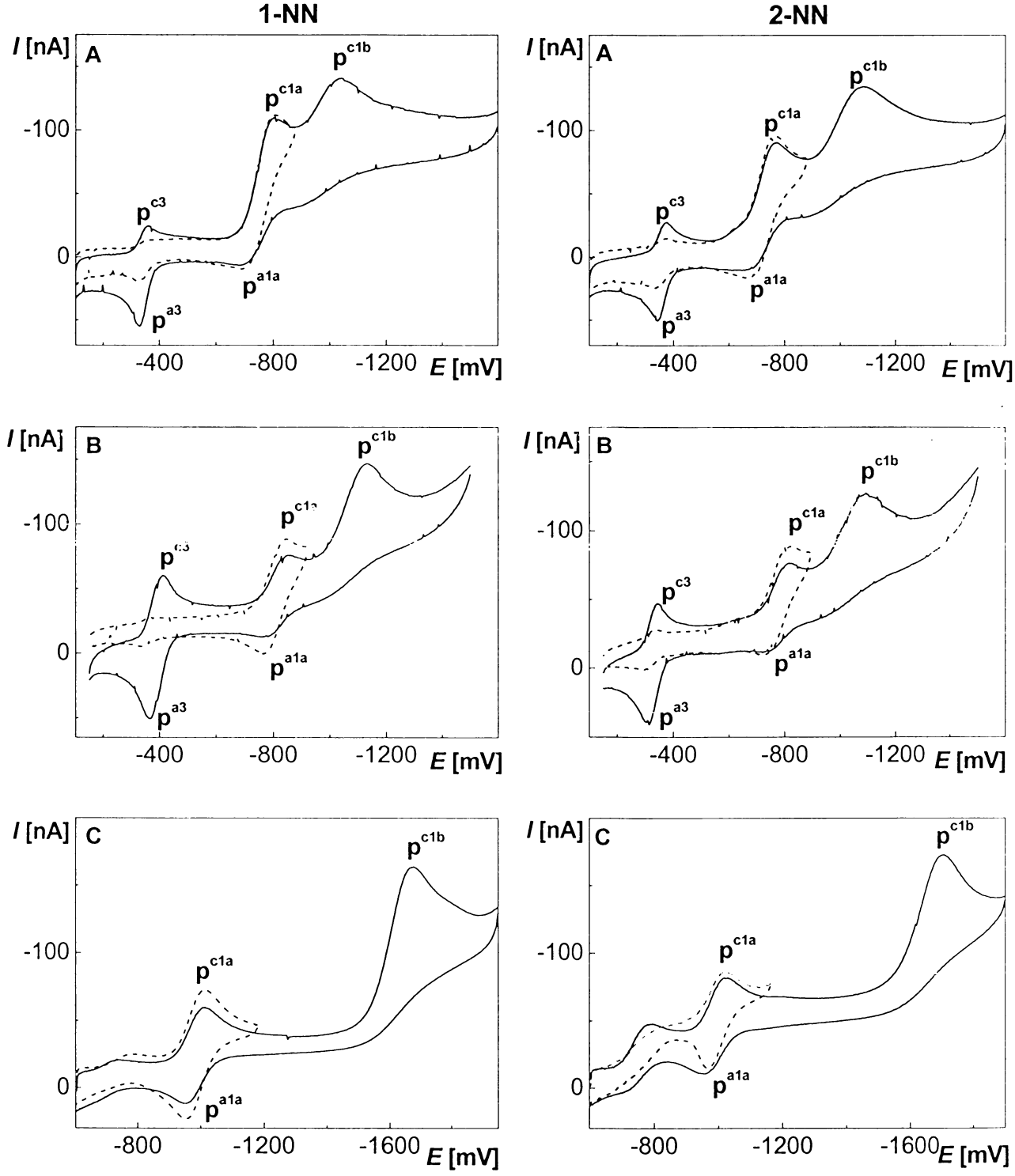

Figure 4.3 *Cyclic voltammograms of 1-NN and 2-NN ($c = 1 \cdot 10^{-4}$ mol L^{-1}) at m-AgSAE in the whole potential range (—) and reversed after the first cathodic peak p^{c1a} (----).*
Base electrolyte: A – mixture of methanol - 0.01 mol L^{-1} NaOH (1:1, pH^f 12.2), B – mixture of DMF - 0.01 mol L^{-1} NaOH (6:4, pH^f 10.8), C – DMF + 0.1 mol L^{-1} TBAI. The 12th scan, scan rate 100 mV s^{-1}. Peak description in text.

4.3.2 Electroanalytical performance of m-AgSAE

4.3.2.1 The influence of pH

The procedures for the detection of possible lowest concentrations of 1-NN and 2-NN at m-AgSAE were optimized using differential pulse voltammetry due to its expected higher sensitivity in comparison to other electroanalytical methods. First, the influence of pH on the DP voltammograms of 1-NN and 2-NN ($c = 1 \cdot 10^{-4}$ mol L^{-1}) was investigated in a mixed Britton-Robinson buffer - methanol (1:1) medium. For 1-NN (2-NN), the voltammograms are depicted in Fig. 4.4A (B) and the dependence of the peak potential on the pH^f for both compounds is shown in Fig. 4.5. The voltammograms exhibit two well developed peaks in acidic, one peak in neutral, and two peaks again in alkaline medium. This electrochemical behaviour in acidic and neutral medium corresponds with our previous studies of 1-NN and 2-NN using differential pulse techniques at DME and HMDE (chapter 3.3.1, 3.3.2 and ref. [30,31]) and the well known reduction pathway of analogical nitroaromatics at mercury electrodes [32,33,34,35] discussed in previous chapter. Therefore, the first peak p^{c1} can be assigned to the irreversible four electron reduction of the nitro group to the hydroxylamino group (Eq. (4.8)). The method of linear regression yielded following relationships for the dependence of the p^{c1} peak potential E_p on pH^f over the region of pH^f 4.1-9.3:

1-NN: E_p [V] = –0.048 pH^f – 0.231 (R = –0.9959) (4.13)

2-NN: E_p [V] = –0.058 pH^f – 0.106 (R = –0.9993) (4.14)

The second peak p^{c2} observable for 1-NN in acidic solutions, at pH^f 2.7-4.9 and for 2-NN at pH^f 2.7, corresponds to the two electron reduction of the hydroxylaminoderivative (ArNHOH) to the amino derivative (Eq. (4.9)):

Different reduction behaviour was observed in alkaline medium at $pH^f > 8.7$. At mercury electrodes, 1-NN and 2-NN yield a well-defined reductive peak corresponding to Eq. (4.13) (Fig. 3.7). At m-AgSAE, two new peaks p^{c1a} and p^{c1b} are produced, in agreement with the CVs recorded at m-AgSAE at pH^f 12.2 (Fig. 4.3A), and presumably corresponding to the one electron reduction of nitronaphthalene to nitro radical anion according to Eq. (4.11) and its consecutive reduction to hydroxylaminonaphthalene (Eq. (4.12)). The peak potential Ep^{c1a} is rather pH-independent above pH^f 10, as the one electron reduction of $ArNO_2$ to $ArNO_2^{\cdot-}$ does not require protons for completion.

4.3.2.2 Calibration dependences, the influence of methanol – buffer ratio

From the analytical point of view, the highest, best developed and most easily evaluable peaks were obtained in neutral or weak alkaline media, where the number of peaks corresponds to the number of nitro groups in the studied compound. Therefore, pH 7.0 of the BR buffer was chosen for further measurements.

From our previous work it follows that the sensitivity of the determination of studied analytes using DPV at HMDE increases about 2.5 times when changing the aqueous phase - methanol ratio from 1:1 to 9:1 (chapter 3.3.2, table 3.4). In this range the ratio of the mixture methanol - BR buffer (pH 7.0) was varied while DP voltammograms at m-AgSAE were recorded. Simultaneously, the pH^f of the methanol - buffer mixture was measured. Fig. 4.6 presents the dependence of the peak potential and peak current of 1-NN on the methanol content. The peak potential shifts towards more positive values and the peak height increases with decreasing content of methanol. For 2-NN, the dependence is similar with the peak potential shift from –590 to –515 mV and peak height increase from –245 to –330 nA. This can be attributed to the decrease of pH^f value from 8.4 to 7.3 and slightly better adsorption of the compounds on the electrode surface in the medium with lower methanol content, as confirmed in next chapter by EVLS. For both extremes, the repeatability was tested by 15 measurements repeated at the concentration of $1 \cdot 10^{-5}$ mol L^{-1}. The values of relative standard deviation obtained for media containing 10 % of methanol (3.8 % for 1-NN, 3.4 % for 2-NN) are higher then those for media containing 50 % of methanol (2.0 %, 1.4 %), nevertheless they are satisfactory for a solid electrode material.

Concentration dependences measured in the range of $2 \cdot 10^{-7}$ ($4 \cdot 10^{-7}$) - $1 \cdot 10^{-4}$ mol L^{-1} for 1-NN (2-NN) in the mixture of Britton-Robinson buffer, pH 7.0 and methanol (9:1, pH^f 7.2) are linear (see table 4.1). Fig. 4.7 represents the DP voltammograms of 1-NN at m-AgSAE in the lowest concentration range measured. The height of the peak in this case was evaluated after subtraction of the background current. The limits of determination are $3 \cdot 10^{-7}$ mol L^{-1} and $5 \cdot 10^{-7}$ mol L^{-1} for 1-NN and 2-NN. In contrast to HMDE, further attempts to decrease these limits by adsorptive accumulation of studied compounds on the electrode surface were not successful even in media containing less than 0.1 % of methanol.

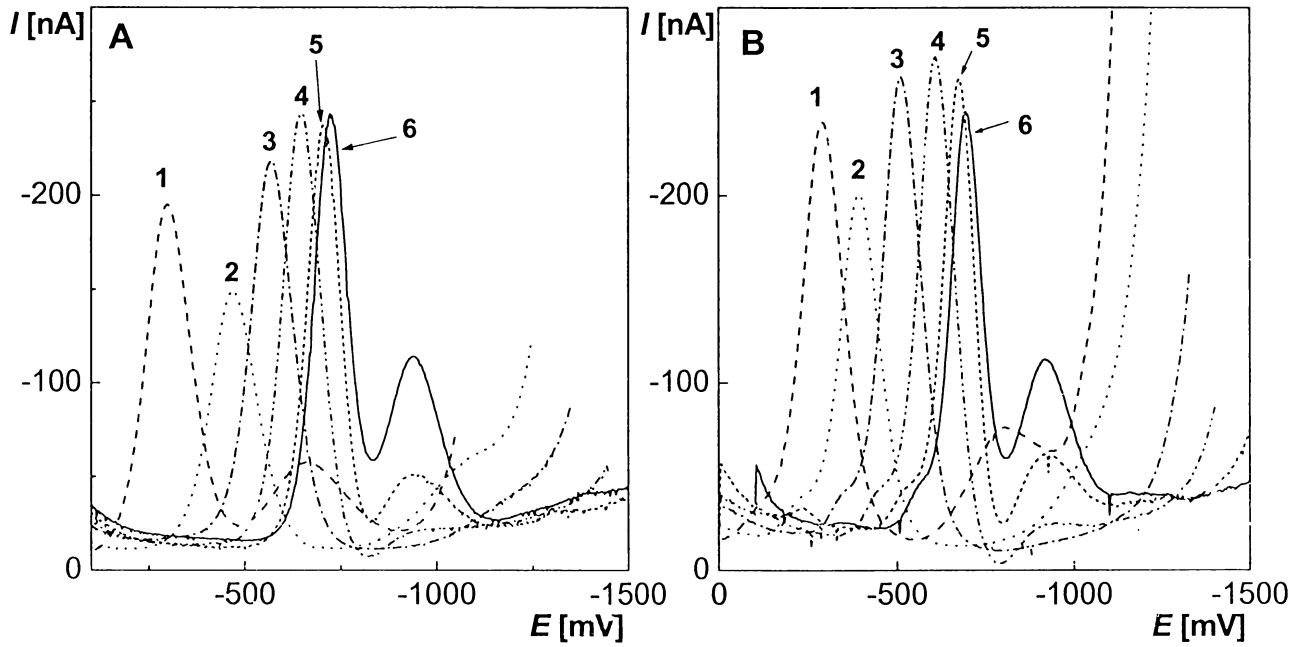

Figure 4.4 *Selected DP voltammograms of 1-NN (A) and 2-NN (B) ($c = 1 \cdot 10^{-4}$ mol L^{-1}) at m-AgSAE in a BR buffer - methanol mixture at pH^f (1) 2.7, (2) 4.9, (3) 7.0, (4) 8.7, (5) 10.3, (6) 12.2.*

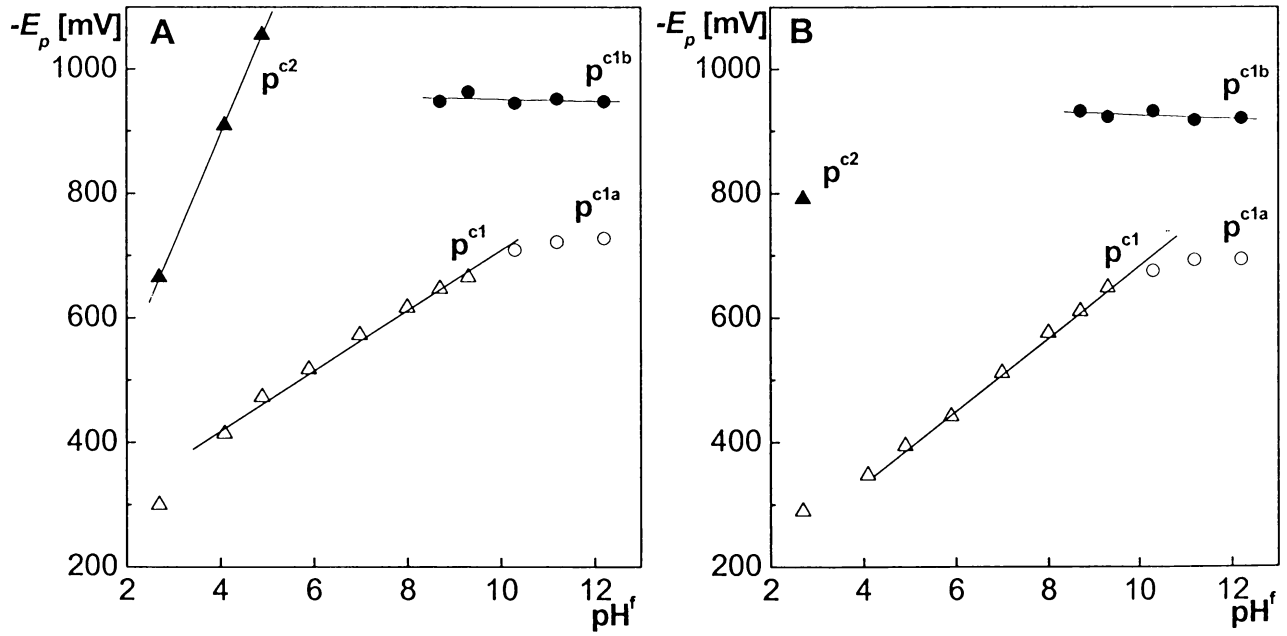

Figure 4.5 *The dependence of peak potential E_p of 1-NN (A) and 2-NN (B) ($c = 1 \cdot 10^{-4}$ mol L^{-1}) on pH^f measured by DPV at m-AgSAE. Base electrolyte BR buffer - methanol mixture (1:1).*

p^{c1} (Δ) – the first peak in acidic and neutral media, p^{c2} (▲) – the second peak in acidic media, p^{c1a} (○) and p^{c1b} (●) – the first and second peak in alkaline media

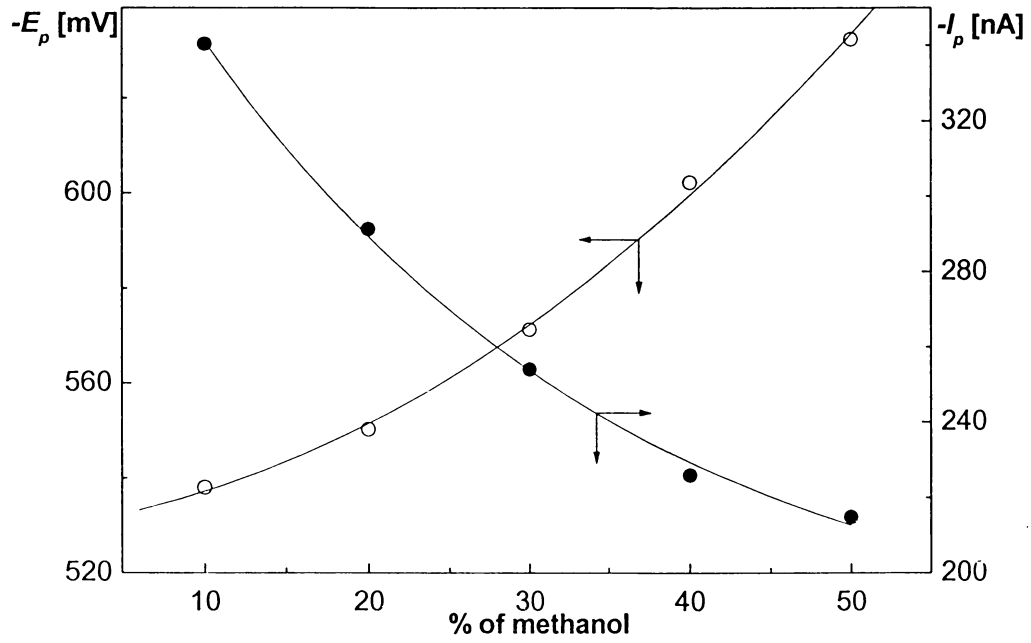

Figure 4.6 *The dependence of peak potential E_p (○) and peak current I_p (●) of 1-NN ($c = 1 \cdot 10^{-4}$ mol L^{-1}) on methanol content in BR buffer (pH 7.0) - methanol mixture. Measured by DPV at m-AgSAE.*

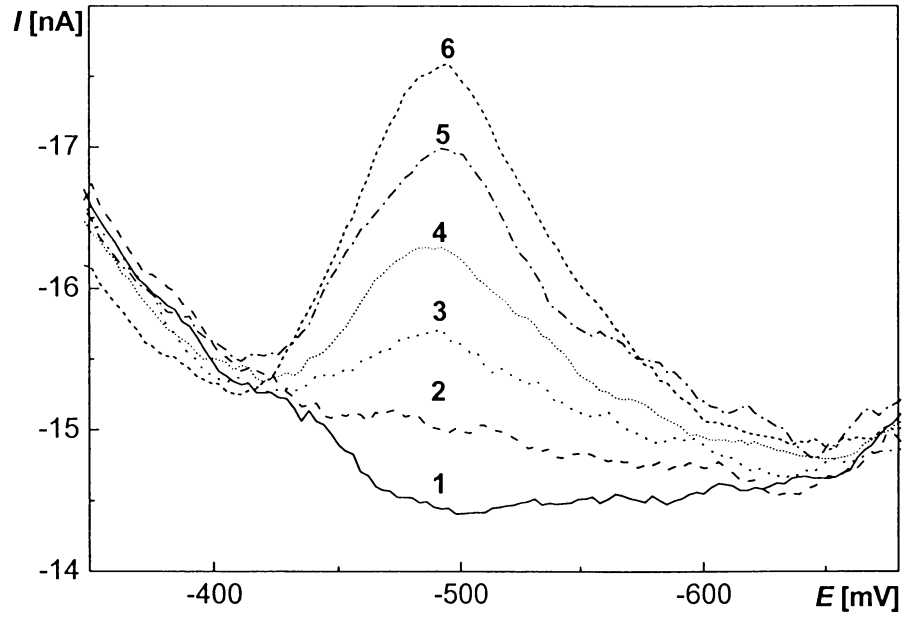

Figure 4.7 *Differential pulse voltammograms of 1-NN at m-AgSAE in a mixture BR buffer - methanol (9:1, pH 7.2). Concentration of 1-NN [μmol L^{-1}]: (1) supporting electrolyte, (2) 0.2, (3) 0.4, (4) 0.6, (5) 0.8, (6) 1.0.*

Table 4.1 *Parameters of the calibration straight lines for the determination of 1-NN and 2-NN using DPV at m-AgSAE in a BR buffer - methanol mixture (9:1, pH^f 7.2).*

Analyte	Concentration [mol L^{-1}]	Slope [mA mol^{-1} L]	Correlation coefficient	LOD [mol L^{-1}]
1-NN	$(2 - 10)\cdot10^{-5}$	3.24 ± 0.07	0.9991	---
	$(2 - 10)\cdot10^{-6}$	3.01 ± 0.08	0.9982	---
	$(2 - 10)\cdot10^{-7}$	3.22 ± 0.07	0.9994	$3\cdot10^{-7}$
2-NN	$(2 - 10)\cdot10^{-5}$	3.19 ± 0.09	0.9982	---
	$(2 - 10)\cdot10^{-6}$	3.23 ± 0.07	0.9999	---
	$(4 - 10)\cdot10^{-7}$	2.78 ± 0.10	0.9950	$5\cdot10^{-7}$

4.3.3 Comparison of electrochemical behaviour of 1- and 2-nitronaphthalene at HMDE and m-AgSAE

The pH study and the cyclic voltammetric experiments described in chapters 3.3.3 (HMDE) and 4.3.1 (m-AgSAE) revealed that the reduction mechanism is similar in acidic and neutral media involving four electron reduction of the nitro group to the hydroxylamine group (Eq. (3.1), p^{c1}) with its consecutive two electron reduction to the amine (Eq. (3.2), p^{c2}) in acidic media. In alkaline media the reduction proceeds as an integral four electron reduction step at lower pH values at HMDE, however, at m-AgSAE it is separated into one electron reduction to the nitro radical (Eq. (4.11), p^{c1a}) and further three electrone reduction to hydroxylamino derivative (Eq. (4.12), p^{c1b}). These reduction peaks are observable in nonaqueous media of DMF with 0.1 mol L^{-1} TBAI at both electrodes. In comparison to mercury electrodes in methanol - buffer mixtures (1:1), both compounds are at m-AgSAE reduced at more negative potentials, as documented in Fig. 4.8. This difference is about 130 mV for acidic and 70 mV for neutral media, in alkaline media a slight difference can be observed only for 1-NN, when comparing the four electron reduction peak p^{c1} at HMDE (Eq. 3.1) and one electrone reduction peak p^{c1a} at m-AgSAE (Eq. 4.11). This potential difference is responsible for the slightly lower slope of the linear dependence of reduction potential of p^{c1} on pH^f obtained for m-AgSAE (Eq. (4.13) and (4.14)) in comparison with HMDE (Eq. (3.5) and (3.6)). In the nonaqueous media (considering peak potentials estimated from the first scan of cyclic voltammograms depicted at Fig 3.13 (HMDE) and Fig 4.3C

(m-AgSAE)) the peak maximum corresponding to the one electron reduction of nitro group to the nitro radical (p^{c1a}) occurs around the potential of –1010 mV at both electrodes, the consecutive reduction to hydroxylamine (p^{c1b}) occurs at –40 mV (1-NN) and –80 mV (2-NN) more negative potential at m-AgSAE than HMDE. These results indicate that the potential of the first fast electron uptake (Eq. (4.11), p^{c1a}) is independent on the electrode material, however, the consecutive three electron reduction (Eq. 4.12) including the rate determining step of the reduction (the uptake of the second electron, forming a nitrosoanion) is hindered at the solid amalgam surface in comparison to the smooth liquid mercury surface of HMDE, thus more negative potential is required to complete the reduction at m-AgSAE.

Further, it follows from Fig. 4.8 that slightly lower potential for reduction of 2-NN than 1-NN is demanded. It can be attributed to different electronic and steric effects in the structures of both derivatives. While the electron density on the N-atom of the nitro group is lower for 1-NN than 2-NN [36], favoring easier reduction of the first one, the fact that nitronaphthalenes are reduced in the opposite order indicates that the steric effect plays a more important role. From the literature it follows that 2-NN is a planar molecule while the nitro group of 1-NN on C1 is forced out of the aromatic plane by the peri-hydrogen [37,38,39]. Therefore it seems that the reduction of 1-NN requires higher energy due to partially aliphatic character of its nitro group. This is in agreement with the fact that the aliphatic nitrocompounds are reduced at potentials about 400-600 mV more negative than aromatic ones. For 1-NN and 2-NN at m-AgSAE the difference is only about 20-50 mV in the whole pH range measured, which can be attributed to the opposite effect of the electronic densities and steric effect described above. Also the tendency of the electrode surface to bring the stericly hindered derivatives into coplanarity lowers the reduction potentials of non-planar nitroderivatives. For chemical reductions in bulk solution without this effect, the doubled value of the rate constant for reduction with titanous chloride was reported for 2-NN in comparison to 1-NN [36]. The planar design of 2-NN facilitates presumably also its adsorption at the electrode surface, which results in shorter accumulation time t_{acc} compared to 1-NN using AdSV (chapter 3.3.2).

When comparing the electroanalytical performance of both electrodes, the limits of determination reached by DPV at m-AgSAE (LOD = $3 \cdot 10^{-7}$ for 1-NN, $5 \cdot 10^{-7}$ mol L^{-1} for 2-NN) are at least one order of magnitude higher than limits reached by DPV at HMDE (LOD = $3 \cdot 10^{-8}$ and $1 \cdot 10^{-8}$ mol L^{-1} for 1-NN and 2-NN, respectively), nevertheless they are only slightly higher than for DPP at DME (LOD = $1 \cdot 10^{-7}$ and $2 \cdot 10^{-7}$ mol L^{-1} for 1-NN and 2-NN), and lower in comparison to DC tast polarography at DME (LOD = $1 \cdot 10^{-6}$ and

$2 \cdot 10^{-6}$ mol L^{-1}). Unfortunately, m-AgSAE does not enable the accumulation of the studied compounds on the electrode surface to enhance the sensitivity.

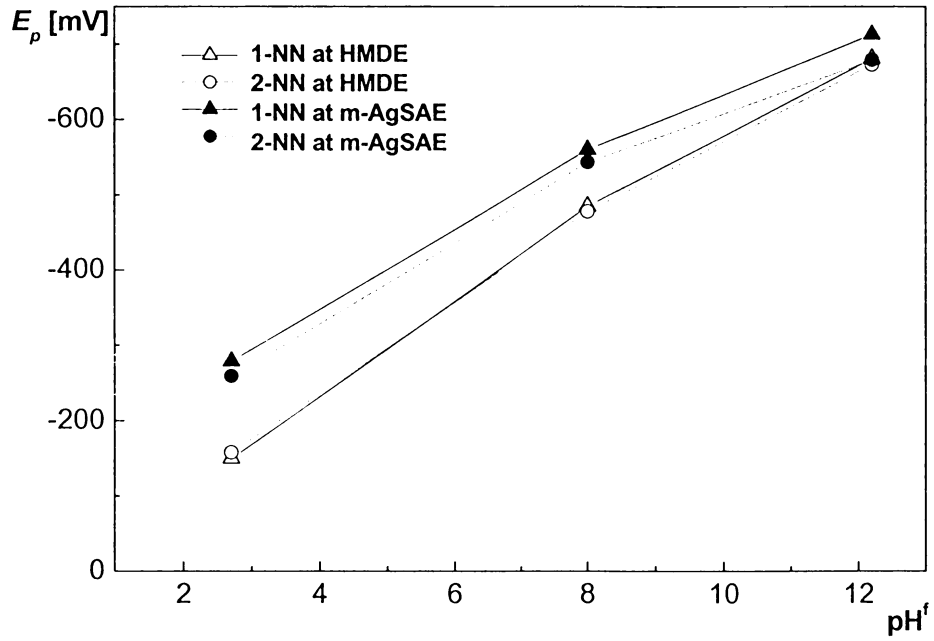

Figure 4.8 *The dependence of peak potential E_p of 1-NN (triangles) and 2-NN (circles) ($c = 1 \cdot 10^{-4}$ mol L^{-1}) on pH^f measured by DPV at HMDE (hollow symbols) and m-AgSAE (full symbols). Base electrolyte BR buffer - methanol mixture (1:1).*

4.3.4 Elimination voltammetry with linear scan

Elimination voltammetry with linear scan (EVLS) was used for further characterization of processes on the electrode surface of HMDE and m-AgSAE and to the calculation of the coefficient αn [21]. Symbol α represents charge transfer coefficient and n is a number of exchanged electrons during the reduction. This calculation is based on the difference between the peak potential, which was measured at the reference scan rate (80 mV s^{-1} for the first, 160 mV s^{-1} for the second set of scan rates) and of the peak potential, which was obtained after the elimination of the individual currents measured by DC voltammetry. Two sets of scan rates (20, 40, 80, 160 mV s^{-1} and 40, 80, 160, 320 mV s^{-1}) were used and elimination curves were calculated from equations 4.4, 4.5, and 4.6 (equal with equations (23), (25) and (27) in ref. [21]). The analyzed solutions contained $1 \cdot 10^{-4}$ mol L^{-1} of 1-NN or 2-NN in methanol - BR buffer mixture (pH 2.0 or 6.0) or 0.01 mol L^{-1} NaOH, ratio 1:1 and 1:9.

It follows from the elimination curves that both compounds offer three elimination peaks at HMDE for the main $4e^-$ reduction of the nitrogroup, summarized in Eq. (3.1) (see Fig. 4.9A1 and B1). A kinetically controlled reaction, (e.g., protonisation of the nitroradical anion) precedes its diffusion controlled reduction at adsorbed state. It is derived from the presence of a characteristic peak - counterpeak pair in voltammograms calculated accordingly to Eq. (4.4) and counterpeak - peak pair obtained using Eq. (4.5) and (4.6) following (proof of an adsorption), and opposite counterpeak-peak positions for the same equations (proof of kinetically controlled reaction) preceding the reference DC peak [23,25]. The adsorption trend increases with decreasing pH and content of methanol in solutions, the strongest adsorption was revealed at pH^f 2.2, BR buffer - methanol ratio 9:1 (Fig. 4.9A1). It is a difference to elimination voltammograms calculated for m-AgSAE (Fig. 4.9A2 and B2). They exhibit mainly one peak, i.e., the reduction is diffusion controlled; a weak adsorption could be recognized only in solutions with lower content of methanol (see Fig. 4.9A2). This fact suggests that the competitive adsorption of methanol proceeds faster at the surface of m-AgSAE than at HMDE and so impedes the adsorption of analyte. The difference in reduction potentials of studied compounds at both electrodes mentioned above can be attributed to this fact.

The αn coefficient was calculated for reductions at m-AgSAE in methanol - 0.01 mol L^{-1} NaOH, ratio 1:1. For the first, one electron reduction step (Eq. (4.11)), the results are ambiguous, probably because of partially overlapping of the one electron reduction (Eq. (4.11)) with the subsequent three electron reduction (Eq. (4.12)) in this media. For this second step, the αn coefficient is 0.52 (1-NN) and 0.61 (2-NN). It leads to conclusion that in this step a one electron, rate determining reduction of the nitroradical anion to the nitrosoanion occurs with $\alpha = 0.52$ (0.61). Further two electron reduction of nitrosoanion to ArNHOH is a fast process which can not be monitored by EVLS.

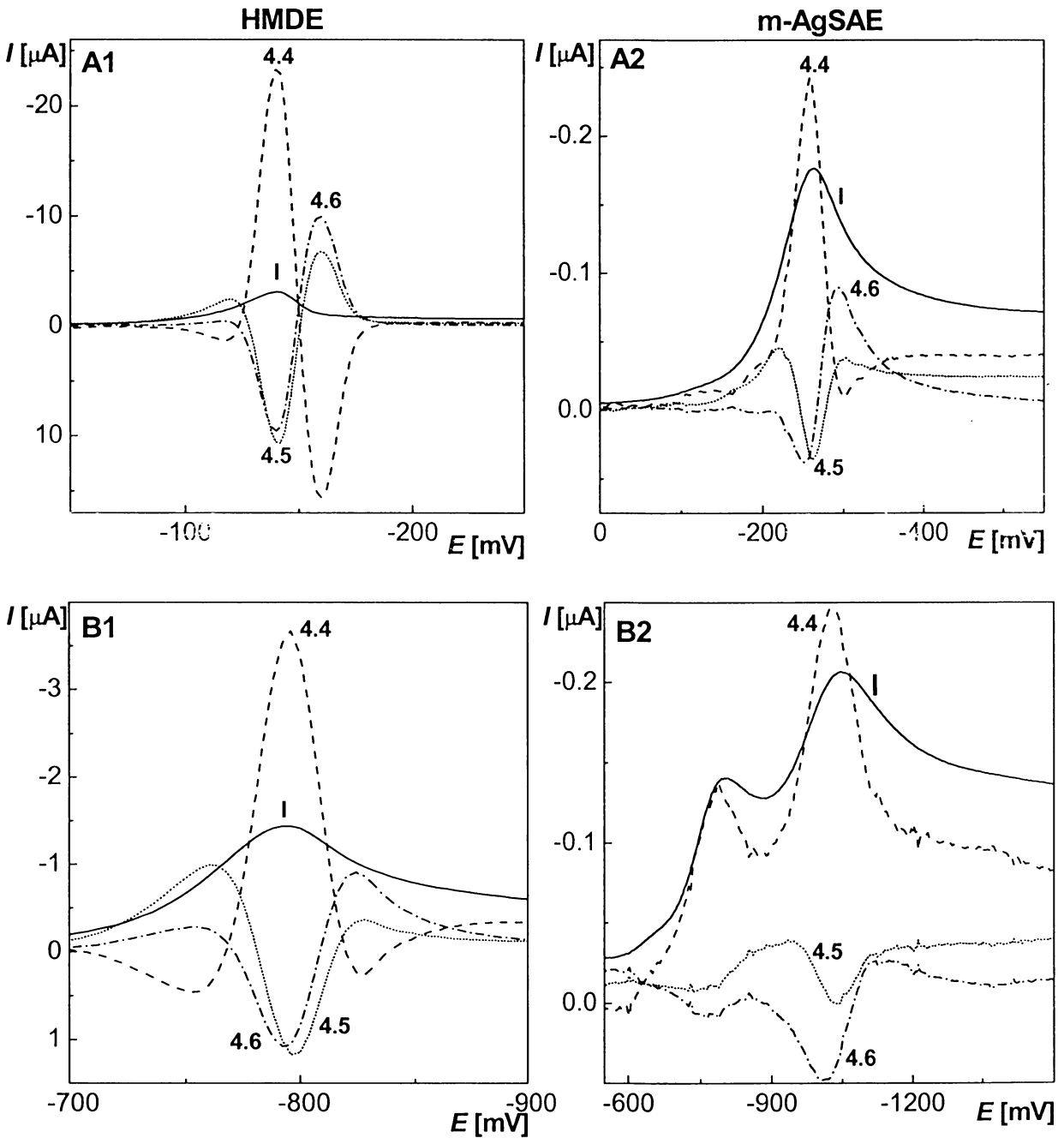

Figure 4.9 *DC and elimination voltammograms of 2-NN ($c = 1 \cdot 10^{-4}$ mol L^{-1}) at HMDE (1) and m-AgSAE (2) in a mixture of Britton-Robinson buffer - methanol (A) (9:1, pH^f 2.2) and 0.01 mol L^{-1} NaOH buffer - methanol (B) (1:1, pH^f 12.2). DC voltammograms at reference scan rate 80 mV s^{-1} (I, (——)), elimination voltammograms calculated according to Eq. 4.4 (---), 4.5 (·····), and 4.6 (·-·-·).*

4.4 Conclusions

It has been shown that m-AgSAE in combination with modern voltammetric techniques is a suitable sensor for the determination of submicromolar concentrations of 1-NN and 2-NN. The reduction mechanism in acidic and neutral media corresponds to the well known mechanism of nitro-group containing aromatics at mercury electrodes with the main signal corresponding to the four-electron reduction of the nitro to the hydroxylamino group. In alkaline media this reduction occurs in two separated steps with the first one being a one electron reduction of the nitro group to the nitro anion radical – a mechanism recognized earlier at silver and other solid electrodes. A DP voltammetric method for the determination of studied compounds with LOD $3 \cdot 10^{-7}$ and $5 \cdot 10^{-7}$ mol L^{-1} for 1-NN and 2-NN, respectively, was developed, which is about one order of magnitude higher than limits reached by DPV at HMDE. Thus, it can be concluded that the m-AgSAE with regard to the electrochemical behavior of 1-NN and 2-NN combines some properties of the solid silver and liquid mercury electrodes. It shows a good reproducibility and sensitivity and therefore represents an effective and simple alternative to mercury electrodes.

4.5 References

1. Yosypchuk B., Novotný L.: *Electroanalysis* 14, 1733-1738 (2002).
2. Yosypchuk B., Novotný L.: *Crit. Rev. Anal. Chem.* 32, 141-151 (2002).
3. Yosypchuk B., Novotný L.: *Chem. Listy* 94, 1118-1120 (2000).
4. Mikkelsen Ø., Schrøder K. H.: *Anal. Lett.* 33, 3253-3269 (2000).
5. Mikkelsen Ø., Schrøder K. H.: *Anal. Chim. Acta* 458, 249-256 (2002).
6. Mikkelsen Ø., Schrøder K. H.: *Electroanalysis* 15, 679-687 (2003).
7. Mikkelsen Ø., Schrøder K. H.: *Electroanalysis* 16, 386-390 (2004).
8. Yosypchuk B., Novotný L.: *Electroanalysis* 14, 1138-1142 (2002).
9. Yosypchuk B., Novotný L.: *Electroanalysis* 15, 121-125 (2003).
10. Yosypchuk B., Heyrovský M., Paleček E., Novotný L.: *Electroanalysis* 14, 1488-1493 (2002).
11. Barek J., Dodova E., Navrátil T., Yosypchuk B., Novotný L., Zima J.: *Electroanalysis* 15, 1778-1781 (2003).
12. Jelen F., Yosypchuk B., Kouřilová A., Novotný L., Paleček E., *Anal. Chem.* 74, 4788-4793 (2002).
13. Yosypchuk B., Fojta M., Havran L., Heyrovský M., Paleček E.: *Electroanalysis* 18, 186-194 (2006).
14. Kuchariková K., Novotný L., Yosypchuk B., Fojta M.: *Electroanalysis* 16, 410-414 (2004).
15. Pecková K., Barek J., Dřevínek M., Navrátil T., Novotný L., Yosypchuk B., Vaingátová S., Zima J., in: *Book of abstracts, US-CZ Workshop on electrochemical sensors* (eds. Barek J., Drašar P.), Prague, Czech Republic, June 19-22, 2001, p. 32. Czech Chemical Society 2001.
16. Fischer J., Barek J., Yosypchuk B., Navrátil T.: *Electroanalysis* 18, 127-130 (2006).
17. Oppenhelmer L., Cappizi T. P., Weppelmann R. M., Metha H.: *Anal. Chem.* 55, 638-643 (1983).
18. Schwartz L. M.: *Anal. Chem.* 55, 1424-1426 (1983).
19. Ebel S., Kamm U.: *Fresenius J. Anal. Chem.* 318, 293-294 (1984).
20. Trnková L., Dračka O.: *J. Electroanal. Chem.* 413, 123-129 (1996).
21. Dračka O.: *J. Electroanal. Chem.* 402, 19-28 (1996).
22. Šestáková I., Navrátil T.: *Bioinorg. Chem. Appl.* 3, 43-53 (2005).
23. Sander S., Navrátil T., Novotný L.: *Electroanalysis* 15, 1513-1521 (2003).
24. Trnková L., Dračka O.: *J. Electroanal. Chem.* 348, 265-271 (1993).
25. Trnková L., Kizek R., Dračka O.: *Electroanalysis* 12, 905-911, (2000).
26. Trnková L., *Talanta* 56, 887-894 (2002).
27. Brdička R., Wiesner K., *Collect. Czech. Chem. Commun.* 12, 138-149 (1947).
28. Holleck L., Kastening B., Vogt H.: *Electrochim. Acta* 8, 255-263 (1963).
29. Rubinstein I.: *J. Electroanal. Chem.* 183, 379-386 (1985).
30. Pecková K., Barek J., Zima J.: *Chem. Listy* 95, 709-712 (2001).
31. Pecková K., Barek J., Moreira J. C., Zima J.: *Anal. Bioanal. Chem.* 381, 520-525

(2005).
32. Kemula W., Krygowski T. M., in: *Encyclopedia of the Electrochemistry of the Elements - Organic Section*, vol. 13, p. 77 (eds. Bard A. J., Lund H.). Marcel Dekker, New York 1979.
33. Kolthoff I. M., Elving P. J., in: *Treatise on Analytical Chemistry*, Part II, Vol.16, p. 188. Wiley, New York 1980.
34. Fry A. J., in: *Chemistry of Amino, Nitroso and Nitro Compounds and Their Derivatives*, p. 319 (ed. Patai S.). Wiley, Chichester 1982.
35. Zuman P., Fijalek Z., Dumanovič D., Sužnjevič D.: *Electroanalysis* 4, 783-794 (1992).
36. Zahradník R., Boček K.: *Collect. Czech. Chem. Commun.* 26, 1733-1748 (1961).
37. Miller D. W., Evans F. F., Fu P. P.: *Spectrosc. Int. J.* 4, 91-94 (1985).
38. Lin S.-T., Jih Y.-F., Fu P. P.: *J. Org. Chem.* 61, 5271-5273 (1996).
39. Balakrishnan P., Boykin D. W.: *J. Org. Chem.* 50, 3661-3663 (1985).

5

Extraction-voltammetric determination of 1- and 2-nitronaphthalene

5.1 Introduction

Both studied nitronaphthalenes are partially soluble in water, which is a unique property among others NPAHs. For 1-NN and 2-NN, the solubility in water (20°C) is 34 mg L^{-1} ($2.0 \cdot 10^{-4}$ mol L^{-1}) and 26 mg L^{-1} ($1.5 \cdot 10^{-4}$ mol L^{-1}) [1], respectively. Thus, these compounds may potentially pass over from aerosol particulate and gaseous phase through river sediments into water [2]. They were found together with 1,3- and 1,5-dinitronaphthalene e.g. in river water close to a plant producing dinitronaphthalenes in Japan [3] (see Table 2.3). To the relatively high water solubility of 1-NN and 2-NN was also ascribed the fact that these compounds (as the only NPAHs) were found in the edible interior part after several NPAHs were applied on the apple peel [4]. Other possible sources of NPAHs include wastewater [2], nitronaphthalenes were found in wastewater from oil/water separating tanks of gasoline stations and in used crankcase oil [5]. More often, NPAHs are found in complex matrix samples, therefore preliminary separation and preconcentration is often used to achieve low detection limits for target analytes [1,6]. This sample preparation step is often accomplished by extraction techniques, based on enrichment of the analyte of interest on liquid (liquid-liquid extraction) or solid (solid phase extraction) phases [6]. Therefore, an extraction-voltammetric determination of 1-NN and 2-NN in water samples may represents a useful tool for the detection of their low concentrations or may serve as a cheap screening method of their presence.

In this chapter, the voltammetric methods at HMDE optimized in chapter 3 were used for determination of 1-NN and 2-NN in model samples of drinking and river water. These analytes were detected either directly in water samples or liquid-liquid extraction (LLE) and solid phase extraction (SPE) were used for preliminary extraction and preconcentration of studied analytes. DP voltammetry at HMDE was chosen as analytical ending, because it is sufficiently sensitive, fast and the adsorption of impurities contained in matrix does not influence the determination as in the case of AdSV.

5.2 Experimental

5.2.1 Reagents

Stock solutions of 1-NN and 2-NN ($c = 1 \cdot 10^{-3}$ mol L^{-1}) in methanol were prepared. More diluted solutions were prepared by exact dilution of the stock solution with methanol.

All the solutions were refrigerated and stored in the dark. Methanol, sodium hydroxide, hexane and dichloromethane were of analytical grade purity (Lachema, Czech Republic). The river water, used for extraction, was taken in the river Vltava in the centre of the city Prague, filtered using S4 sintered glass and used within one week after sampling. The drinking water (pH ~ 5) was taken immediately before the use in the chemistry building of Faculty of Science, Charles University in Prague, Hlavova 8, Prague 2.

5.2.2 Apparatus

Measurements were carried out using a computer driven EcoTribo Polarograph with PolarPro software, version 2.0 (both EcoTrend, Prague, Czech Republic) in combination with a HMDE type UMμE (EcoTrend), a platinum wire auxiliary electrode and silver/silver chloride (1 mol L^{-1} KCl) reference electrode, to which all the potential values are referred. For DPV at HMDE, the maximum drop size attainable obtained by opening the valve for 100 ms, with a surface of 0.864 mm^2, a polarization rate of 20 mV s^{-1}, and the modulation amplitude of –50 mV were used. All spectra were measured in quartz cuvettes (optical path length 1 cm) vs. hexane in diode array spectrophotometer HP 8453 (Hewlett Packard, Netherlands) giving the spectra in electronic format. Rotating vacuum evaporator Rotavapor R-114 equipped with water bath B-480 (both Büchi, Flawil, Schwitzerland), an universal automatic shaker type 327 (Premed, Poland) and vacuum manifold (Burdick & Jackson, USA) were used. An SPE column LiChrolut RP-select B (catalog number K90154159, Merck, Darmstadt, Germany), which is a SPE column filled with 500 mg of RP-18 phases bonded on silica gel, was used for SPE. The solution pH was measured using Conductivity & pH meter Jenway 4330 (Jenway, England). pH values refer to those of the buffer, pH^f values refer to those of the resulting pH of the mixtures of the buffer with the organic component.

5.2.3 Procedures

For the direct determination of 1-NN and 2-NN in water, the water sample was spiked with appropriate amounts of the studied analyte solution in methanol, 9 mL of the sample was placed in a 10 mL volumetric flask and it was diluted to volume by 0.1 mol L^{-1} NaOH. After deaeration with N_2 (5 min) DP voltammograms were recorded immediately.

For the extraction methods, distilled water was used for preliminary experiments as a model matrix. With exclusion of the distilled water samples for LLE described below, the extraction efficiencies (Table 5.2 and 5.3) and reproducibility were calculated for model water

samples containing $1 \cdot 10^{-7}$ mol L^{-1} of 1-NN or 2-NN. The final volume of measured solution was always 10 mL, thus tenfold and hundredfold preconcentration of the studied analyte was achieved when starting with 100 and 1000 mL of the sample, respectively. The recoveries were calculated from the ratio I_p/I_p^o, where I_p is the height of the peak of the analyte of interest after extraction with hexane or solid phase extraction and I_p^o is the height of peak in a reference solution prepared by the addition of the standard solution of studied analyte to the blank solution. All recoveries and reproducibility were calculated from four repetitive extractions.

For the DP voltammetric determination of 1-NN and 2-NN in distilled water samples after LLE with hexane the procedure was as follows: 10 mL of the model sample of distilled water containing $1 \cdot 10^{-6}$ mol L^{-1} of added 1-NN or 2-NN was extracted for 10 minutes with 2 mL of hexane using an automatic shaker, the organic phase was evaporated using a rotating vacuum evaporator or other methods to dryness, the residue was dissolved in 5 mL or 1 mL of methanol using automatic Vortex shaker and sonication, 9 mL of 0.01 mol L^{-1} NaOH was added and after deaeration the DP voltammogram at HMDE was recorded. The drinking or river water samples were spiked with an appropriate amount of studied analyte, extracted with 10 mL of hexane and the above described procedure was applied.

The procedure for DP voltammetric determination of 1-NN or 2-NN in model samples of distilled, drinking or river water after SPE was as follows: An SPE column was connected to a vacuum manifold and activated by washing with 3 mL of methanol and 3 mL of de-ionized water, which was allowed to pass through the cartridge without the use of vacuum. Afterwards, the model water sample spiked with different amounts of 1-NN or 2-NN was sucked through the column using volumetric flasks as sample reservoirs and PTFE tubing as connector of the reservoirs and SPE columns (Figure 5.1). Adsorbed analyte was then eluted with 5 or 1 mL of methanol, the solution was made-up to 10.0 mL with 0.01 mol L^{-1} NaOH and after deaeration DP voltammogram was recorded. The blank samples were handled according to the above described procedures. Following the sample application, the cartridges were washed with 3 mL of methanol and distilled water and dried under the vacuum for 5 min. The cartridges were re-used three times when working with distilled and drinking water samples.

Calibration curves were measured in triplicate, the height of the peaks used for evaluation was measured from the straight line connecting the minima before and after the peak. The statistical parameters (e.g. slope, intercept, limit of determination) were calculated according to Oppenhelmer [7], Schwartz [8] and Ebel [9] using statistic software ADSTAT ver. 2.0

(Trilobyte, Czech Republic). The significance of the intercepts of linear calibration dependences was tested by ADSTAT, the non-significant intercepts are omitted in Table 5.1, 5.2 and 5.4 summarizing parameters of calibration dependences.

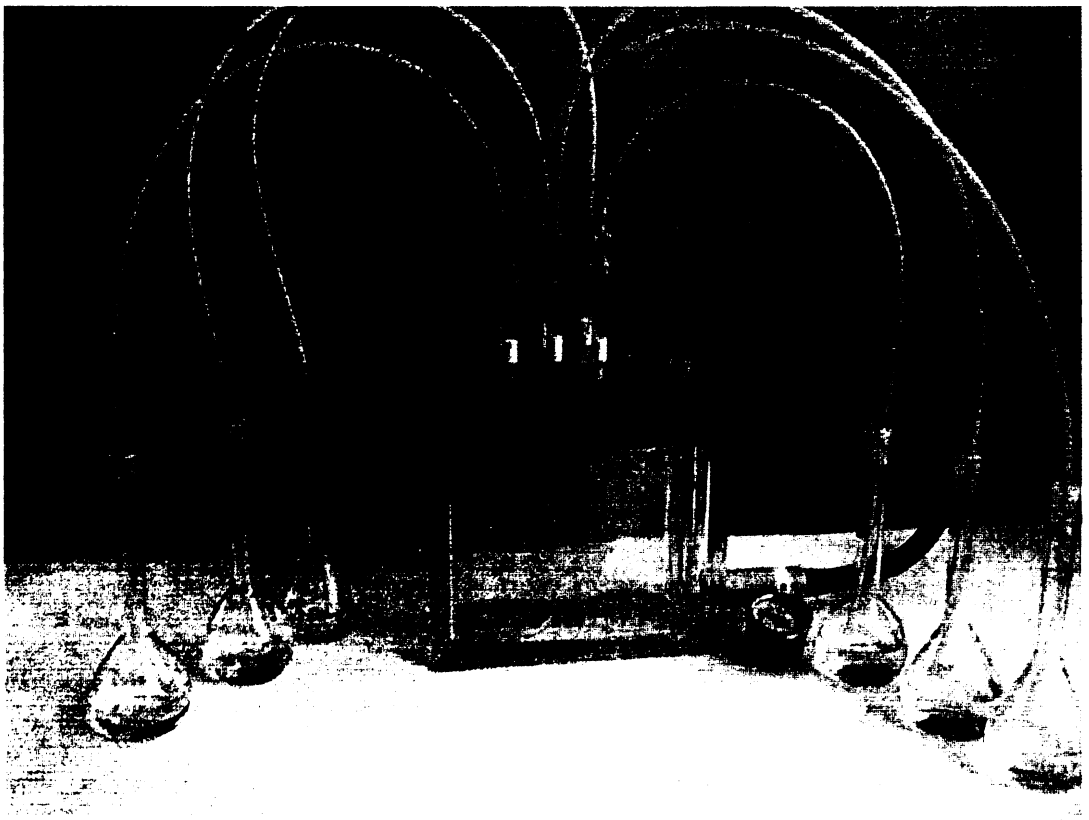

Figure 5.1 *Setup for simultaneous application of six samples on SPE columns using PTFE tubing adapters for connecting the sample reservoirs and extraction columns on a vacuum manifold.*

5.3 Results and discussion

5.3.1 Direct DP voltammetric determination of 1- and 2-nitronaphthalene in water samples

With respect to the time consuming extraction procedures, we tried to determine 1-NN and 2-NN directly in the drinking and river water. As 1 mL of 0.1 mol L^{-1} NaOH was used to dilute 9 mL of the sample, the final pH of the investigated solutions was near to 12.0 – the optimum pH for their DP voltammetric determination. As seen from Table 5.1, where the parameters of calibration curves are given, the sensitivity of this direct determination is comparable with the previous DP voltammetric experiments carried out with de-ionized water

(chapter 3.3.2, Table 3.4). Also the limits of determination lie within the same concentration range and are ~$3 \cdot 10^{-8}$ mol L^{-1}. The DP voltammograms for the lowest attainable concentration range for 1-NN determination in drinking water are depicted in Fig. 5.2. It is obvious, that the curve of the blank sample (1) is complicated by peaks of present interferents. They accumulated at the electrode surface at great extent when applying accumulation potential of –400 mV, thus these attempts to determine lower amounts of target analytes by AdSV failed. To lower the determinable amount of 1-NN and 2-NN, preconcentration using liquid-liquid or solid phase extraction was necessary.

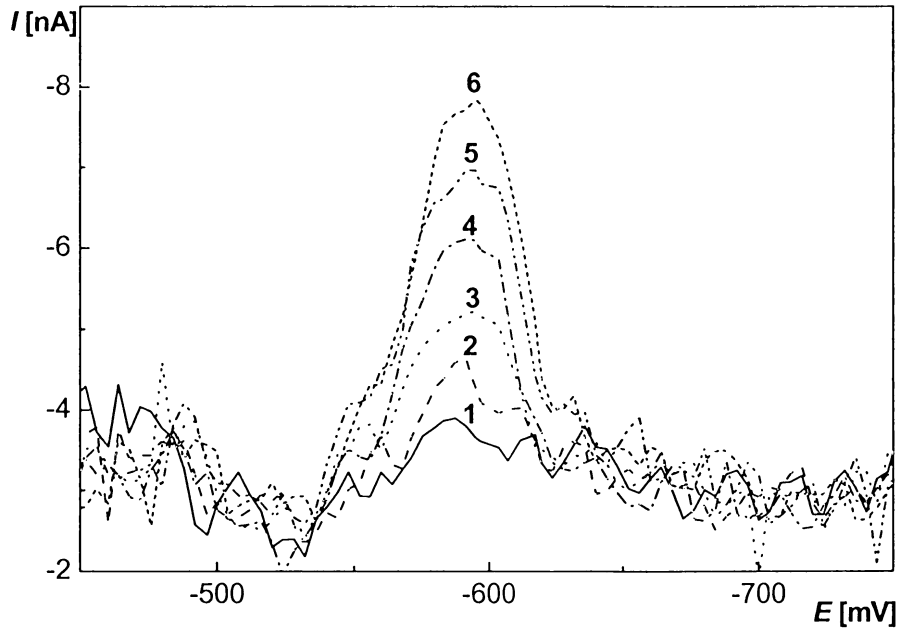

Figure 5.2 *DP voltammograms of 1-NN of direct determination in drinking water. Base electrolyte 0.01 mol L^{-1} NaOH in drinking water, pH 11.9. Concentration of 1-NN in drinking water: 0 mol L^{-1} (1), $2 \cdot 10^{-8}$ mol L^{-1} (2), $4 \cdot 10^{-8}$ mol L^{-1} (3), $6 \cdot 10^{-8}$ mol L^{-1} (4), $8 \cdot 10^{-8}$ mol L^{-1} (5), $1 \cdot 10^{-7}$ mol L^{-1} (6).*

Table 5.1 *Parameters of the calibration straight lines for the direct DP voltammetric determination of 1- and 2-nitronaphthalene in drinking and river water.*

Model sample	Concentration [mol L^{-1}]	Slope [mA mol^{-1} L]	Correlation coefficient	LOD [mol L^{-1}]
		1-nitronaphthalene		
Drinking water	$(2\text{-}10)\cdot10^{-8}$	40.87 ± 0.53	0.9998	$2\cdot10^{-8}$
River water	$(2\text{-}10)\cdot10^{-8}$	38.75 ± 1.52	0.9934	$3\cdot10^{-8}$
		2-nitronaphthalene		
Drinking water	$(2\text{-}10)\cdot10^{-8}$	38.89 ± 0.92	0.9988	$2\cdot10^{-8}$
River water	$(2\text{-}10)\cdot10^{-8}$	41.31 ± 2.94	0.9925	$4\cdot10^{-8}$

5.3.2 Liquid-liquid extraction - DP voltammetric determination of 1- and 2-nitronaphthalene in water samples

The procedures for extraction of 1-NN and 2-NN to hexane were optimized with model samples in distilled water. The results for 1-NN were rather ambiguous, as seen from Fig. 5.3. First, 10 mL of distilled water sample with 1-NN concentration of $1\cdot10^{-6}$ mol L^{-1} was extracted with 2 mL of hexane. The maximum recovery of four times repeated extraction was 58.2 %. When hexane was replaced with dichloromethane, even lower and unrepeatable recoveries with the maximum of 34.3 % were achieved. These lower values in comparison to hexane may be due to difficult separation of dichloromethane from water phase. Three hypotheses were tested to explain the low extraction yields. First, the decrease of 1-NN signal can not be ascribed to compounds present in the residue after the evaporation of the extract, as documented in Fig. 5.3: The height of the DPV peak of 1-NN obtained after direct addition of 1-NN to the blank sample (curve 2) is only slightly lower than the DPV peak of 1-NN in base electrolyte not containing the hexane residue (curve 3). Second, it was confirmed by UV-VIS spectrophotometry that the extraction of 1-NN to hexane proceeds quantitatively, as documented in Fig. 5.4. The absorbance of the curve maximum (λ = 326 nm) of the 1-NN spectrum measured after its extraction to hexane is about 97 % of the absorbance value of the spectrum measured after 1-NN was added to the hexane, which was shaked with water before (blank sample). Third, the attention was paid to the possible loss of 1-NN during the

evaporation step. Therefore, the spectrum of 1-NN ($c = 5 \cdot 10^{-5}$ mol L^{-1}) in hexane was recorded, after the hexane was blowed away by nitrogen directly from the spectrophotometric cuvette, the residue was dissolved in 2 mL of hexane and a new spectrum was recorded. Resulting spectra are depicted in Fig. 5.5. It follows from the comparison of the curves (1) and (3) that 1-NN molecules pass over partially into the gaseous phase, because the absorbance of the 1-NN solution obtained after hexane evaporation and its re-addition is only as high as 10 % of the absorbance value before evaporation. Other methods were used for hexane evaporation, i.e. the water bath or the Kuderna-Danish evaporator, which enables the evaporation of the organic phase while the residue is continuously preconcentrated in the tip of the special vessel used. It guarantees easier dissolution of the residue. The lowest loss of 1-NN was observed when using vacuum rotating evaporator (Fig. 5.5, curve 2); nevertheless, the maximum absorbance was only 40% in comparison with the absorbance of the not evaporated sample (curve 1) and satisfactory repeatability was not achieved for the whole extraction procedure even when the evaporation was conducted at constant temperature of the water bath (25°C) at constant time. Thus, LLE could not be used for the determination of 1-NN in water samples.

Surprisingly, for 2-NN the recoveries for the same test extraction as for 1-NN (i.e. extraction of the studied analyte ($c = 1 \cdot 10^{-6}$ mol L^{-1}) from 10 mL of distilled water sample with 2 mL of hexane) was 88.1 % with relative standard deviation of 7.2 %. It was confirmed by the UV-VIS spectrophotometry that 2-NN molecules do not evaporate using rotating vacuum evaporator at that greet extent as 1-NN – the absorbance at $\lambda = 303$ nm of the 2-NN solution ($c = 5 \cdot 10^{-5}$ mol L^{-1}) obtained after hexane evaporation and re-addition is 85.0 % (RSD 5.4 %, n = 3) of the absorbance value before evaporation. Thus, LLE was applied on model drinking water samples spiked with 2-NN. Conditions specified in Table 5.2 were used. The recovery was found to be 90 % (58 %) with RSD 6.1 % (8.9 %) for the extraction with 10 mL of hexane from 100 mL (1000 mL) of the drinking water and it can not be increased either by multiple extractions or by the increase of the solvent volume. The lower recoveries for the extraction from 1000 mL in concentration range of $(4\text{-}10) \cdot 10^{-10}$ mol L^{-1} can be ascribed to the loss of 2-NN during the extraction and evaporation step due to relative low amount in the solution. Moreover, the recovery of the extraction-voltammetric determination of $1 \cdot 10^{-8}$ mol L^{-1} 2-NN in 100 mL river water was even lower (maximum about 40%) and the results were not repeatable, because in addition to the evaporation, interactions between the compound and impurities in the polluted river water affect the whole procedure. Therefore, calibration dependences were measured only for the determination of 2-NN in the drinking

water (parameters in Table 5.2) and LODs as low as $4 \cdot 10^{-10}$ mol L^{-1} for extraction from 1000 mL of drinking water were achieved.

The fact that LLE including the evaporation step is not applicable for 1-NN shows that when developing determination methods for NPAHs in real matrices, a special attention should be paid to the evaporation step, which is usually included in the methods. The analogical extraction procedure to our one succeeded e.g. in an extraction-voltammetric determination of 9-nitroanthracene [10] and 4-nitrobiphenyl [11] in river water samples. In agreement with our results, low recoveries (56 % 1-NN, 51 % 2-NN) and poor reproducibility were reported by Mocko [12] for the determination of 1-NN and 2-NN in drinking water samples using LLE to cyclohexane:diisopropylether (9:1, v/v) mixture followed by evaporation and HPLC with fluorescence detection. On the other hand, Sekyra et al. [13] published a GC-MS method for analysis of polluted ambient air samples from Teplice, Czech Republic, collected on combined quartz and polyurethane foam filters. The extraction and purification steps included three times the evaporation with rotating vacuum evaporator and reported recoveries are 79.9 % (RSD 10.7 %) and 86.5 % (RSD 17.8 %) for 1- and 2-NN, respectively. This high yields can be due to the fact that the extracts were evaporated for short time, as no evaporation to dryness was needed. Moreover, the authors report higher recoveries for other NPAHs including 9-nitroanthracene (91.0 %, RSD 22.4 %). These ambiguous results show that precise and sometimes time-consuming work is necessary when developing analytical methods for NPAHs determination in complex matrices.

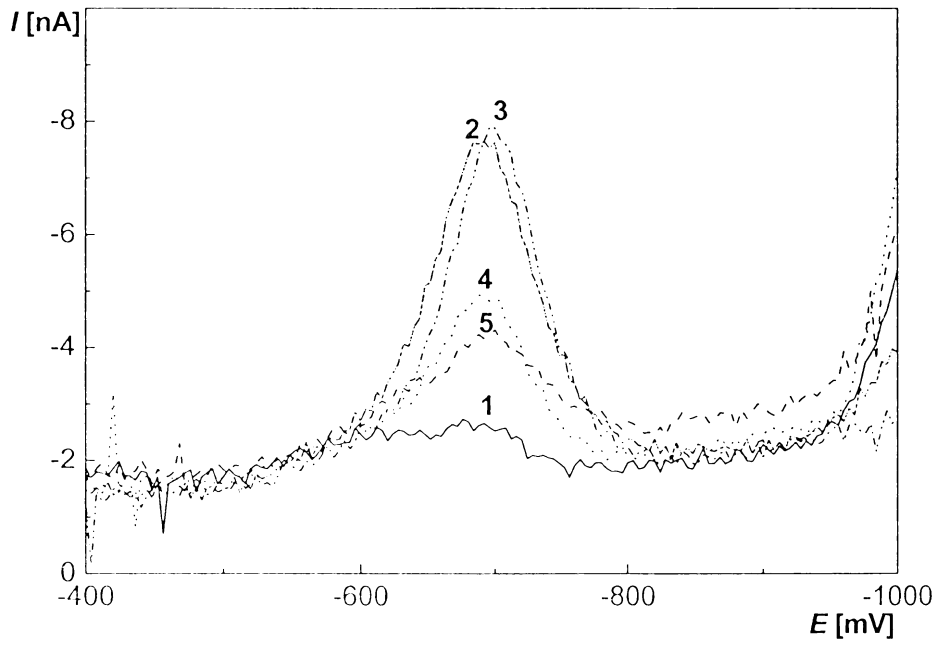

Figure 5.3 *DP voltammograms of 1-NN ($c = 1\ 10^{-6}$ mol L^{-1}) after extraction from 10 mL of distilled water to 2 mL of hexane (dichlormethane): Blank sample (1), direct addition of 1-NN to the blank sample (2), 1-NN in base electrolyte (0.01 mol L^{-1} NaOH - methanol, 1:1, pH 12.2) not containing the hexane residue (3); the curves obtained after extraction to hexane (4) and dichloromethane (5).*

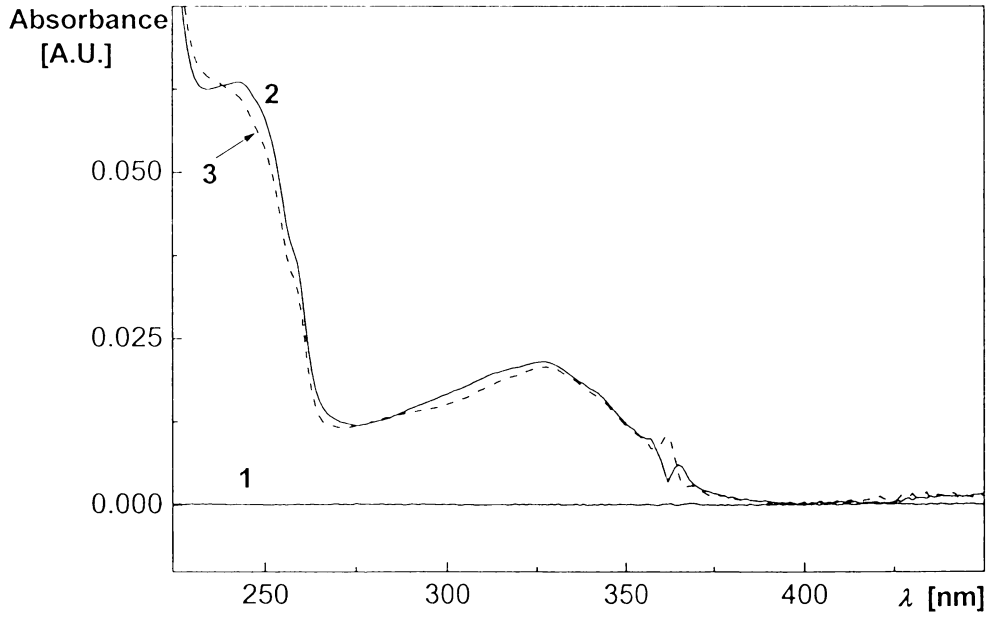

Figure 5.4 *Spectrophotometric control of the extraction of 1-NN from distilled water to hexane. Spectra measured against hexane in 1.0 cm cuvettes. Spectrum of hexane (1); 1-NN in hexane after addition of 10 µL stock solution of 1-NN ($c = 1 \cdot 10^{-3}$ mol L^{-1}) to 2 mL of hexane (2); 1-NN in hexane after its extraction from 10 mL of distilled water (c (1-NN) = $1 \cdot 10^{-3}$ mol L^{-1})) to 2 mL of hexane (3).*

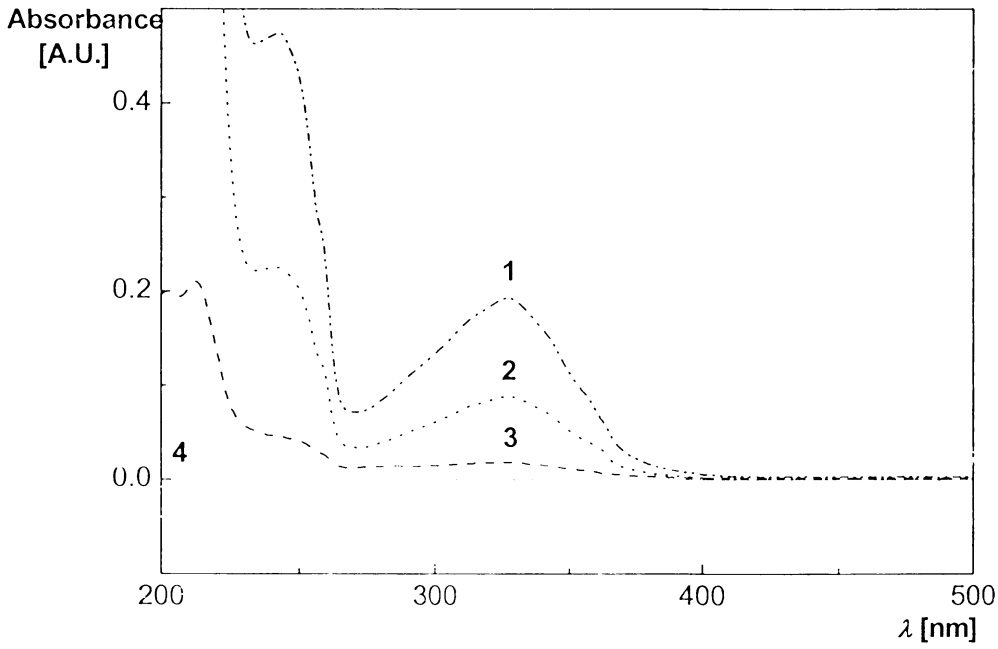

Figure 5.5 *Spectrophotometric monitoring of the evaporation of 1-NN in hexane. Spectra measured against hexane in 1.0 cm cuvettes. Spectrum of the stock solution of 1-NN ($c = 5 \cdot 10^{-5}$ mol L^{-1}) in hexane (1); spectrum of 1-NN after evaporation of 2 mL $5 \cdot 10^{-5}$ mol L^{-1} solution of 1-NN in hexane and re-dissolution of the residue in 2 mL of hexane, the evaporation realized with rotating vacuum evaporator (2) and blowing of nitrogen (3); spectrum of hexane (4).*

Table 5.2 *Parameters of calibration straight lines for DP voltammetric determination of 2-nitronaphthalene after its extraction from model samples of drinking water to 10 mL of hexane. The residue was dissolved in 1 mL of methanol – base electrolyte 0.01 mol L^{-1} NaOH - methanol, 9:1, pH[f] 12.0.*

Sample volume [mL]	Concentration [mol L^{-1}]	Recovery (RSD[a]) [%]	Slope [mA mol^{-1} L]	Correlation coefficient	LOD [mol L^{-1}]
100	$(2 - 10) \cdot 10^{-9}$	90.5 (6.1)	258.0 ± 24.3	0.9870	$5 \cdot 10^{-9}$
1000	$(4 - 10) \cdot 10^{-10}$	58.3 (8.9)	2004 ± 95	0.9977	$4 \cdot 10^{-10}$

[a] Relative standard deviation

5.3.3 Solid-phase extraction - DP voltammetric determination of 1- and 2-nitronaphthalene in water samples

Further, the possibility to determine trace amounts of 1-NN and 2-NN in spiked drinking and river water using DP voltammetry in combination with solid phase extraction was investigated. Based on the literature survey [6], the SPE was carried out on the octadecyl bonded silica as sorbent material. The procedures were optimized with distilled water samples, conditions specified in Table 5.3 were used. It follows from this table that achieved recoveries are in general higher for 2-NN than for liquid-liquid extraction and the method is applicable also for extraction of 1-NN. The reproducibility of the developed method is satisfactory, with relative standard deviation below 5.8 % for all samples.

For the elution of model samples of 1-NN and 2-NN in distilled water first 5 mL of the eluent (methanol) were used and further diluted to 10 mL with 0.01 mol L^{-1} NaOH. Under these conditions, the expected LODs for the measured solution for DPV determination are around $3 \cdot 10^{-7}$ mol L^{-1} (compare Table 3.4, chapter 3.3.2), i.e. two orders of magnitude lower when starting with 1000 mL of the sample assuming 100% recoveries. When using 1 mL of eluent and further dilution with 0.01 mol L^{-1} NaOH to 10 mL, optimum conditions for DPV determination of 1-NN and 2-NN are achieved and about ten times lower LODs than for elution with 5 mL are expected. It follows from Table 5.3, that resulting recoveries for both elution volumes are comparable, higher than 87 %, thus elution with 1 mL was used for samples of drinking and river water. It was found that the height of the DPV peak is also dependent on the volume of the water sample passed through the column, as depicted at Figure 5.6. There is observable decrease of the DPV peak of 1-NN , if it is added to the blank solution after passing 1000 mL (Fig. 5.6B) of drinking water in comparison 100 mL (Fig. 5.6A) samples. This is probably due the increased presence of the surface active impurities when passing higher volumes of sample. This effect was even more obvious when working with high volumes of distilled water, which was prepared by water purification using active carbon cartridges, rich on organic material. Presumably, there are still some neutral organic contaminants present in the water affecting the peak heights. These impurities are probably preconcentrated at SPE column as well. Nevertheless, the recoveries for drinking water samples were > 95 % for 1-NN and slightly lower (> 72 %) for 2-NN, which has potentially more exposed nitro group and may have been less retained on the RP-18 phase of the SPE column than 1-NN having more compact structure. The DP voltammograms corresponding to the lowest attainable concentration range $(2\text{-}10) \cdot 10^{-10}$ mol L^{-1} for drinking water samples of

2-NN are depicted in Fig. 5.7, the parameters of calibration curves for SPE-DPV determination of 1-NN and 2-NN in water samples are summarized in Table 5.4. The inconsistency in the slope values of the calibration straight lines for different volumes of samples extracted is in agreement with the peak decrease for higher sample volumes described above.

For river water samples, the recoveries are slightly lower than in the case of drinking water. Possible explanation is again the presence of surface active substances decreasing the height of DPV peak which are not completely removed by SPE. Nevertheless, the dependence of the height of the DPV peak of studied analytes on its concentration in river water is linear in the concentration range of $(2\text{-}10)\cdot10^{-9}$ mol L^{-1} (see Table 5.4). Attempt to lower the determination limits by passing 1000 mL river water through the SPE column was not successful, because it resulted in an increase of the peaks of electrochemical active impurities on recorded voltammograms and in substantial decrease of the sample flow rate, and therefore unacceptable prolongation of analysis time.

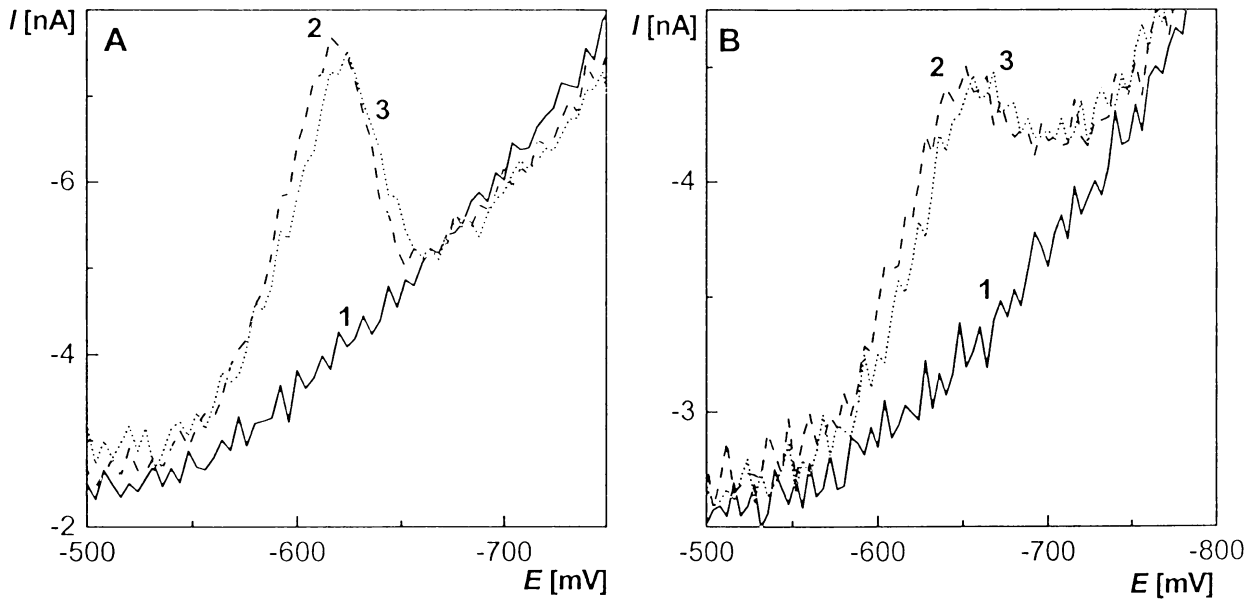

Figure 5.6 *DP voltammograms of 1-NN ($c = 1\cdot10^{-7}$ mol L^{-1}) in 0.01 NaOH – methanol medium (9:1, pH 12.0) after solid phase extraction of 1-NN from 100 mL (A) and 1000 mL (B) of drinking water.*

Blank sample (1), direct addition of 1-NN to the blank sample (2), extraction of 1-NN from the water sample (3).

Table 5.3 *Extraction conditions, recovery and repeatability for solid phase extraction - DP voltammetric determination of 1-nitronaphthalene (1-NN) and 2-nitronaphthalene (2-NN) in distilled, drinking and river water samples.*

Model sample	Analyte concentration [mol L^{-1}]	Sample volume [mL]	Eluent volume [mL]	Sample flow rate [mL min^{-1}]	Recovery (RSD[a]) [%] 1-NN	Recovery (RSD[a]) [%] 2-NN
Distilled water	$1 \cdot 10^{-7}$	50	5	2	98.1 (1.8)	94.2 (2.8)
	$1 \cdot 10^{-8}$	500	5	5	94.3 (3.9)	87.1 (4.9)
	$1 \cdot 10^{-7}$	100	1	2	95.8 (2.4)	93.7 (3.1)
Drinking water	$1 \cdot 10^{-8}$	100	1	2	95.5 (2.0)	94.2 (2.8)
	$1 \cdot 10^{-9}$	1000	1	5	95.7 (4.0)	71.4 (5.8)
River water	$1 \cdot 10^{-8}$	100	1	2	93.0 (3.2)	83.1 (4.1)

[a] Relative standard deviation

Table 5.4 *Parameters of the calibration straight lines for the DP voltammetric determination of 1-nitronaphthalene and 2-nitronaphthalene in drinking and river water after solid phase extraction.*

Model sample	Sample volume [mL]	Analyte concentration [mol L^{-1}]	Slope [mA mol^{-1} L]	Correlation coefficient	LOD [mol L^{-1}]
1-nitronaphthalene					
Drinking water	100	$(2 - 10) \cdot 10^{-9}$	295.6 ± 19.1	0.9938	$2 \cdot 10^{-9}$
	1000	$(2 - 10) \cdot 10^{-10}$	881.1 ± 60.6	0.9930	$2 \cdot 10^{-10}$
River water	100	$(2 - 10) \cdot 10^{-9}$	189.0 ± 9.8	0.9960	$2 \cdot 10^{-9}$
2-nitronaphthalene					
Drinking water	100	$(2 - 10) \cdot 10^{-9}$	294.5 ± 9.6	0.9984	$3 \cdot 10^{-9}$
	1000	$(2 - 10) \cdot 10^{-10}$	1377 ± 47	0.9983	$3 \cdot 10^{-10}$
River water	100	$(2 - 10) \cdot 10^{-9}$	152.8 ± 8.1	0.9963	$3 \cdot 10^{-9}$

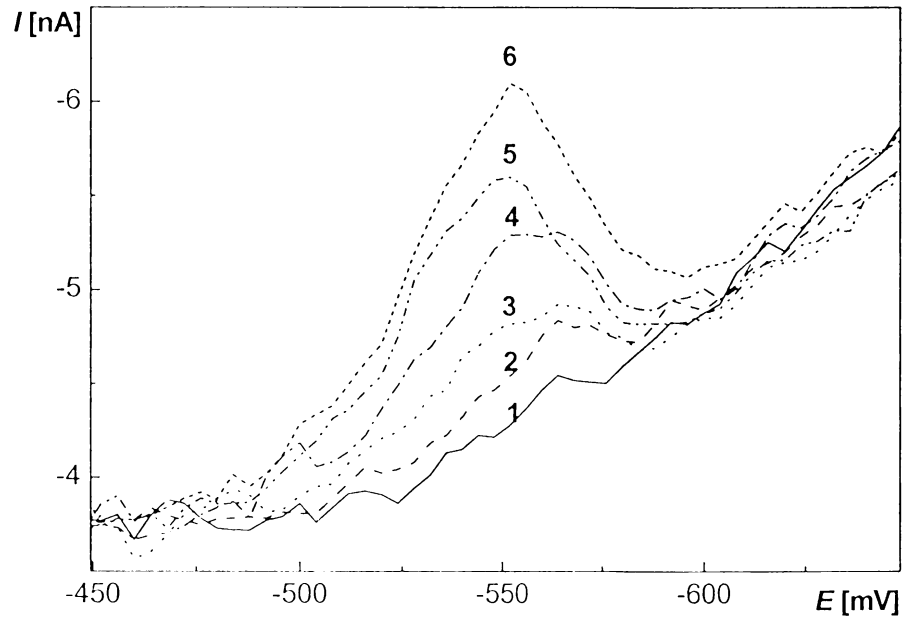

Figure 5.7 *Differential pulse voltammograms of 2-NN after solid phase extraction from 1000 mL of drinking water containing 0 (1), $2 \cdot 10^{-10}$ mol L^{-1} (2), $4 \cdot 10^{-10}$ mol L^{-1} (3), $6 \cdot 10^{-10}$ mol L^{-1} (4), $8 \cdot 10^{-10}$ mol L^{-1} (5), $1 \cdot 10^{-9}$ mol L^{-1} (6) of the analyte.*

5.4 Conclusions

A method for determination of trace amounts of 1-NN and 2-NN in drinking and river water samples was developed. The direct determination of studied analytes by DP voltammetry at HMDE is possible after addition of 0.1 mol L^{-1} NaOH to the water samples in the same concentration range as when using DPV under the optimized condititions. Limits of determination as low as ~ $2 \cdot 10^{-8}$ mol L^{-1} and ~ $4 \cdot 10^{-8}$ mol L^{-1} were achieved for drinking and river water samples, respectively. For further decrease of determination limits in drinking water a preliminary separation and preconcentration of studied analytes is necessary. Liquid-liquid extraction is applicable only on drinking water samples of 2-NN, 1-NN passes over partially into the gaseous phase during the evaporation step, resulting in low and unrepeatable recoveries. On the other hand, DP voltammetric determination after solid phase extraction using LiChrolut RP-Select B columns for analyte preconcentration and 1 mL of methanol for its elution is a reliable method for the determination of both analytes, characterized by high recoveries and reproducibility. For drinking water samples, recoveries higher than 95 % for 1-NN and 71.4 % 2-NN were obtained with maximum relative standard deviation of 5.8 % for

the determination of 2-NN, when starting with 1000 mL of the sample. The limits of determination ($2 \cdot 10^{-10}$ mol L^{-1} (1-NN) and $3 \cdot 10^{-10}$ mol L^{-1} (2-NN)) are nearly one order of magnitude lower than when using HPLC-UV detection after SPE on the same cartridges [14]. For river water samples, the preconcentration could be carried out from maximum 100 mL of the sample and determination limits $2 \cdot 10^{-9}$ mol L^{-1} (1-NN) and $3 \cdot 10^{-9}$ mol L^{-1} were achieved. Further possibilities to decrease the LODs, e.g. by eluate evaporation and decrease of the volume of voltammographed solution, were not tested, as evaporation step would have to be included.

5.5 References

1. Al-Bashir B., Hawari J., Leduc R., Samson R.: *Water Res.* 28, 1817-1826 (1994).
2. Moreira J. C., Barek J.: *Quim. Nova* 18, 362-367 (1995).
3. Takahashi Y., Nakagawa J., Hosokawa N., Asano M., Morita M.: *Kankyo Kagaku* 5, 207-214 (1995). *CA* 123:349623.
4. Ziegler W., Penalver L. G., Preiss U., Wallnöfer P. R.: *Adv. Food. Sci.* 21, 54-57 (1999).
5. Manabe Y., Kinouchi T., Wakisaka K., Tahara I., Ohnishi Y.: *Environ. Mutagen* 6, 669-681 (1984).
6. Bruzzoniti M. C., Sarzanini C., Mentasti E.: *J. Chromatogr. A* 902, 289-309 (2000).
7. Oppenhelmer L., Cappizi T. P., Weppelmann R. M., Metha H.: *Anal. Chem.* 55, 638-643 (1983).
8. Schwartz L. M.: *Anal. Chem.* 55, 1424-1426 (1983).
9. Ebel S., Kamm U.: *Fresenius J. Anal. Chem.* 318, 293-294 (1984).
10. Barek J., Pumera M., Muck A., Kadeřábková M., Zima J.: *Anal. Chim. Acta* 393, 141-146 (1999).
11. Štěpán R., Mejstřík V., Zima J.: *Sensors* 3, 43-60 (2003).
12. Quaiserová V.: *MSc Thesis*, Charles University, Faculty of Science, Prague 2001.
13. Sekyra M., Leníček J., Bednárková K., Beneš I.: *Chem. Listy* 94, 924-930 (2000).
14. Mocko V.: *PhD Thesis*, Charles University, Faculty of Science, Prague 2004.

6

Electrochemical and spectrophotometrical monitoring of photolytical degradation of 1- and 2-nitronaphthalene

6.1 Introduction

Nitro derivatives of polycyclic aromatic hydrocarbons constitute one of the largest groups of chemical carcinogens and mutagens [1,2] as highlighted in chapter 2.2.2. Even extremely low concentration of carcinogens can increase the occurrence of cancer [3]. The monitoring of these contaminants in the environment and evaluation of their biological impacts on humans and other organisms increases the number of laboratories working with these hazardous substances. Therefore, the development of methods suitable for their destruction and decontamination of laboratories is strongly recommended by International Agency for Research on Cancer [4,5]. Simultaneously, the ultra sensitive methods for destruction monitoring are needed.

Several methods have proved to be effective for the destruction. Biological treatment uses microorganism to metabolize the pollutants, however, it is applicable only in aqueous solutions and a large number of compounds are not biodegradable or cannot be destroyed by biological treatment due to their toxicity [6]. Other possibility of destruction includes addition of a chemical like oxidants (H_2O_2 or O_3) [7] or catalyst (TiO_2) to the decontaminated solution [8]. A powerful technique for oxidizable PAH derivatives involves oxidation with potassium permanganate in sulphuric acid medium [5], the procedure protocol for NPAHs requires preliminary reduction of the analyte, e.g by zinc powder. For 4-nitrobiphenyl solution in acetic acid, this method revealed destruction efficiency higher than 99.8 % [9] and the degradation products were found to be non-mutagenic [10]. 1-NN, 2-NN, 1-AN and 2-AN decomposed with efficiencies higher than 99.5 %, which was confirmed by HPLC-UV used for destruction monitoring [11]. However, the method is unsuitable for wastes containing oxidizable solvents, e.g. methanol and ethanol.

The research on alternative methods has led in last two decades to the development of photochemical methods for the oxidative degradation of pollutants. In general, the use of UV/visible radiation can lead to the degradation by two main processes [12]: (i) excitation of the substrate and its subsequent decomposition (photolysis) and (ii) generation of highly oxidizing species able to attack the substrate. The latter is primarily based on the generation of hydroxyl radicals (Advanced Oxidation Procedures (AOP)) and include substrate treatment with UV/H_2O_2 [12,13,14], UV/TiO_2 [15], $UV/H_2O_2/O_3$ [7,16], and $UV/H_2O_2/Fe^{2+}$ or Fe^{3+} (photo assisted Fenton reaction [17]), among others. Compared to chemical methods of destruction, photochemical methods based on degradation of aromatic PAH skeletons by UV light provide

easier operation procedures, less complicated sample handling, result in smaller amount of waste mixtures and could therefore replace chemical degradation methods.

Chromatographic analysis is usually employed for the study of the course of destruction and estimation of destruction efficiency. However, UV/VIS spectroscopy and differential pulse voltammetry at HMDE succeeded as a fast and cheap alternative to HPLC and GC methods in the destruction monitoring of selected antineoplastic drugs, nitrogen containing heterocycles [18], and aromatic amines. Muck used differential pulse polarography at DME for monitoring of methanolic 1-nitropyrene solution after UV irradiation in a laboratory made reactor [19]. The same system has been used in this study in order to develop a safe and efficient destruction procedure for 1-NN and 2-NN, based on the UV irradiation of their solutions in methanol. For the monitoring of destruction efficiency, UV/VIS spectroscopy and differential pulse voltammetry at HMDE were used. An attempt was also made to characterize the destruction products by electrochemical methods and GC-MS.

6.2 Experimental

6.2.1 Reagents

The stock solutions of 1-NN and 2-NN ($c = 1 \cdot 10^{-3}$ mol L^{-1}) were prepared in methanol (Merck, gradient grade purity). More diluted solutions were prepared by exact dilution of the stock solution with methanol. The chemicals involved in identification of destruction products 1,5-dinitronaphthalene (98 %), 1-nitropyrene (97 %), 9-nitroanthracene (98 %), 1,4-naphthoquinone (97 %), 1-aminonaphthalene (99 %), 2-aminonaphthalene (95 %), 1-hydroxynaphthalene (99 %), 2-hydroxynaphthalene (99 %), and naphthalene (99 %) were purchased from Sigma-Aldrich and their stock solutions ($c = 1 \cdot 10^{-3}$ mol L^{-1}) were prepared in methanol. All the solutions were stored refrigerated in the dark. Methanol, sodium hydroxide and hydrogen peroxide were of analytical grade purity (Lachema, Czech Republic). De-ionised water was produced by Milli-Q_{plus} system (Millipore, USA).

6.2.2 Apparatus

For UV irradiation, a laboratory made photochemical reactor was used with a 300 W Hg mid-pressure lamp emitting full UV spectrum (Fig. 6.1). For electrochemical monitoring experiments, a computer driven EcoTriboPolarograph with PolarPro software, version 4.0 (both EcoTrend, Prague, Czech Republic) in combination with a hanging mercury drop

electrode (HMDE) of the type UMμE (EcoTrend), or classical dropping mercury electrode (DME), a platinum wire auxiliary electrode and silver/silver chloride (1 mol L^{-1} KCl) reference electrode was used. The parameters of the classical DME used in DC tast polarography were as follows: At a mercury reservoir height of h = 49 cm, the flow rate was m = 0.76 mg s^{-1} and the drop time was τ = 9.5 s. Work with the DME was carried out at a polarization rate of 4 mV s^{-1} and controlled drop time of 1 s. For DPV at HMDE, the maximum drop size attainable obtained by opening the valve for 100 ms, with a surface of 0.864 mm^2, a polarization rate of 20 mV s^{-1}, and the modulation amplitude of –50 mV were used. The oxygen was removed from solutions by purging with nitrogen for 10 minutes. A pre-bubbler with a methanolic solution of the same water - methanol ratios as in the analyzed solutions were placed prior the voltammetric vessel. The electrochemical curves were recorded three times. Spectra were measured in quartz cuvettes (optical path length 0.1 cm) in spectrophotometer Pye Unicam SP-400 UV/VIS (Cambridge, UK). Rotating vacuum evaporator Rotavapor R-114 equipped with water bath B-480 (both Büchi, Flawil, Schwitzerland) was used. pH of the solutions was measured by Conductivity and pH meter 4330 (Jenway, Great Britain) with a combined glass electrode. All experiments were carried out at laboratory temperature. pH values refer to those of the buffer, pH^f values refer to those of the resulting pH of the mixtures of the buffer with the organic component.

GC-MS analyses were carried out on a Shimadzu 17 A gas chromatograph with 30 m x 0.25 mm capillary column (35 % phenyl and 65 % polydimethyl siloxane) and interfaced with Shimadzu QP 5050 A MS-engine. The GC conditions were as follows: carrier gas helium; column head pressure 60 kPa; injector temperature 310 °C; oven isothermal 250 °C temperature and interface temperature 270 °C. All samples were run in triplicate. Data acquisition was delayed until 4 min after injection; samples were monitored in scan mode under the control of GC-MS solution version 1.02D. The MS spectra of degradation products were compared to spectra recorded in NIST MS library [20].

6.2.3 Procedures

The procedure for monitoring of photodegradation of 1-NN and 2-NN by UV-VIS spectroscopy was as follows: $5 \cdot 10^{-4}$ mol L^{-1} solutions of 1-NN and 2-NN were prepared in methanol. 100 mL of this solution was transferred to the inner glass shell of the reactor. The mercury lamp was placed in the center of the reactor and the solution was irradiated either in presence of oxygen (air saturated) or oxygen was removed by purging nitrogen for 10 minutes

and further the solution was kept under nitrogen atmosphere during irradiation. A water cooler was used and an aluminum foil covered the glass body of the reactor for eye protection from UV light. Blank methanolic solution was irradiated in the same way. In one hour intervals, 1 mL of the irradiated sample was transferred in quartz cuvettes (optical path length 0.1 cm) and UV-VIS spectrum versus methanol between 500 and 200 nm was recorded.

The procedure for electrochemical monitoring of photodegradation of 1-NN and 2-NN by DPV at HMDE was as follows: 50 mL of $5 \cdot 10^{-4}$ mol L^{-1} solutions of 1-NN and 2-NN in methanol was placed to the inner glass shell of the reactor and the solution was irradiated. In given time intervals, 1 mL of the irradiated solution was made up with 0.01 mol L^{-1} NaOH in a 10 mL volumetric flask. The mixture was transferred into an electrochemical vessel, deareated by passing nitrogen (5 min) and DP voltammograms were recorded. Blank methanolic solution was handled in the same way, the DP voltammograms were recorded also for the standard $5 \cdot 10^{-4}$ mol L^{-1} solution of 1-NN and 2-NN without the irradiation. Methanolic solutions of 1,5-dinitronaphthalene, 1-nitropyrene, 9-nitroanthracene, and 1,4-naphthoquinone used for comparison during destruction products characterizations were treated identically.

Standard addition method has been used for the evaluation of the efficiency of the destruction. To the 10 mL solution in the polarographic vessel prepared by the addition of 0.01 mol L^{-1} NaOH to 1 mL of the irradiated sample of 1-NN (2-NN) were subsequently added 2, 5 and 10 μL of $1 \cdot 10^{-4}$ mol L^{-1} solutions of 1-NN (2-NN) in methanol. These standard additions corresponded to the 0.04 %, 0.1 %, and 0.2 % of the originally present amount of 1-NN (2-NN)

For GC-MS analysis, the irradiated solution was ten times preconcentrated by evaporation (vacuum rotating evaporator) of 10 mL of the solution and re-dissolution of the residue in 1 mL of water followed by injection using SPME fiber (100 μm polydimethylsiloxane fiber, Supelco). Direct injection of irradiated solution was also used.

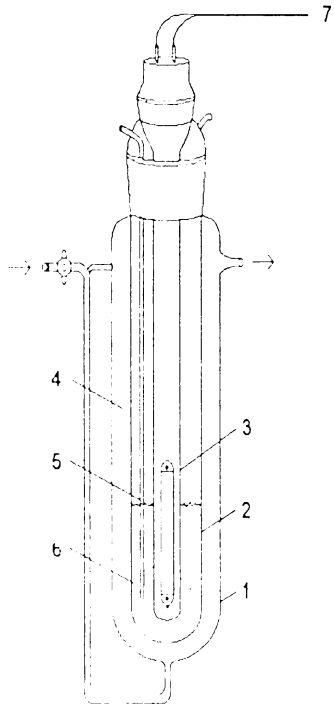

Figure 6.1 *UV irradiation reactor: 1 – outer glass shell, 2 – inner glass shell, 3 – silica glass tube with Hg lamp, 4 – water cooler, 5 – pressure equilibrating, inlet of nitrogen, 6 – photolysed solution, 7 – high voltage supply.*

6.3 Results and discussion

6.3.1 Monitoring of photolytical degradation of 1- and 2-nitronaphthalene by UV-VIS spectroscopy

The absorption spectrum of 1-NN is characterized by three well resolved vibrational absorption bands in the UV-VIS region: ~326, ~ 245 and ~210 nm. Similarly, 2-NN shows maximum absorbance at ~348, ~303, ~260, ~209 nm (Fig. 3.2 chapter 3.2.4). The bands with maximum at 326 nm and 348 nm for 1-NN and 2-NN, respectively, were chosen to monitor the photolytical degradation, because they are well resolved and lie within the near VIS region.

The course of the photolytical degradation of 1-NN and 2-NN in methanol is documented in Fig. 6.2A and 6.3A. It shows the UV-VIS spectra of irradiated solution of $5 \cdot 10^{-4}$ mol L^{-1} 1-NN and 2-NN in methanol in one hour intervals. The distinct absorbance maxima of studied compounds fade already during the first hour of irradiation, nevertheless a new broadband spectrum of increasing absorbance in direction of the decreasing wavelength is formed. This spectrum is the results of residual absorbance of the studied analyte and its

degradation products. The destruction efficiency was calculated as the quotient of absorbance value of the irradiated solution and the absorbance of the solution before irradiation, measured at the absorbance maximum. After six hours of irradiation, the destruction efficiency was lower than 80 % (1-NN) and 71 % (2-NN), as obvious from Figure 6.4. To accelerate the photodegradation, 0.5 mL of 30% H_2O_2 was added to 100 mL of the studied solution before irradiation. The final H_2O_2 concentration was 48.7 mmol L^{-1}. The accelerating effect of hydrogen peroxide consists in photolytic formation of reactive hydroxyl radicals, which attack the naphthalene nucleus. The degradation proceeds faster and leads to lower absorbance of the broad band spectrum, as obvious from Fig. 6.2B and Fig. 6.3B, thus the destruction efficiency decreases on ~ 95.5 % for both analytes, as summarized in Fig. 6.4.

Figure 6.2 *UV-VIS spectra for monitoring of the UV photolysis of 1-nitronaphthalene (initial concentration $5 \cdot 10^{-4}$ mol L^{-1}, solution volume 100 mL) in methanol (A) and in methanol with addition of 0.5 mL 30 % H_2O_2 (B). Spectra measured in 0.1 cm quartz cuvettes versus methanol. The suffix by „t" indicates hours of irradiation, t_0 corresponds to the spectrum of 1-nitronaphthalene before irradiation.*

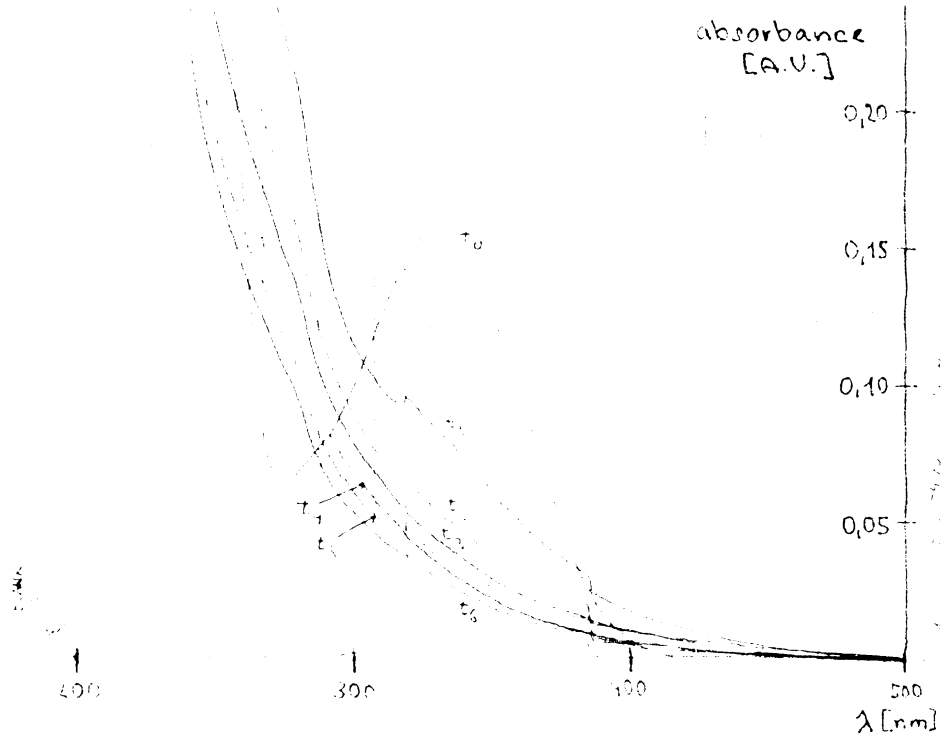

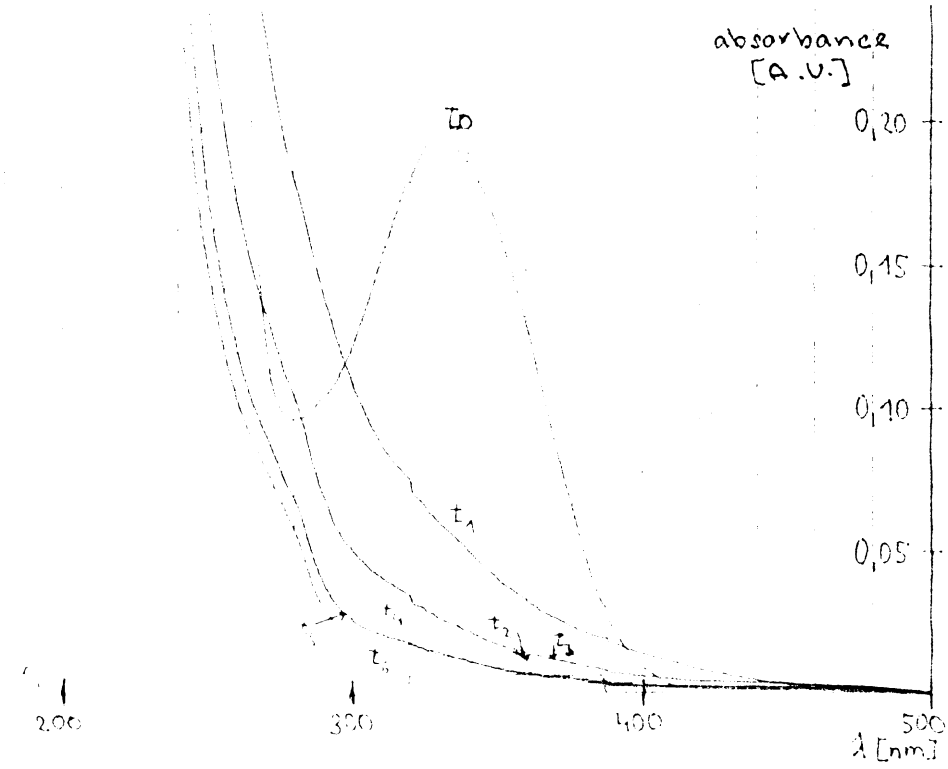

Figure 6.3 *UV-VIS spectra for monitoring of the UV photolysis of 2-nitronaphthalene (initial concentration $5 \cdot 10^{-4}$ mol L^{-1}, solution volume 100 mL) in methanol (A) and in methanol with addition of 0.5 mL 30 % H_2O_2 (B). Spectra measured in 0.1 cm quartz cuvettes versus methanol. The suffix by „t" indicates hours of irradiation. t_0 corresponds to the spectrum of 2-nitronaphthalene before irradiation.*

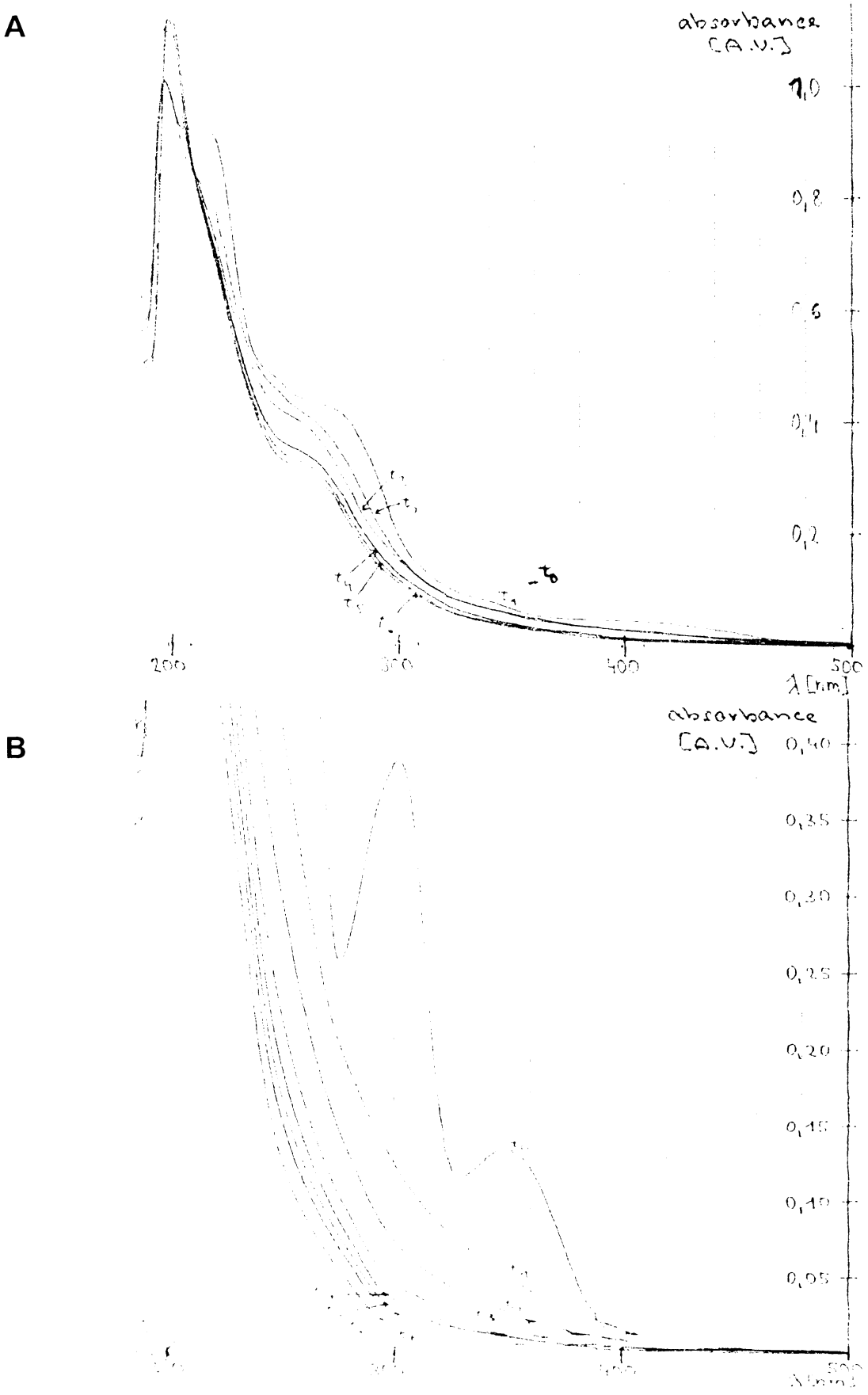

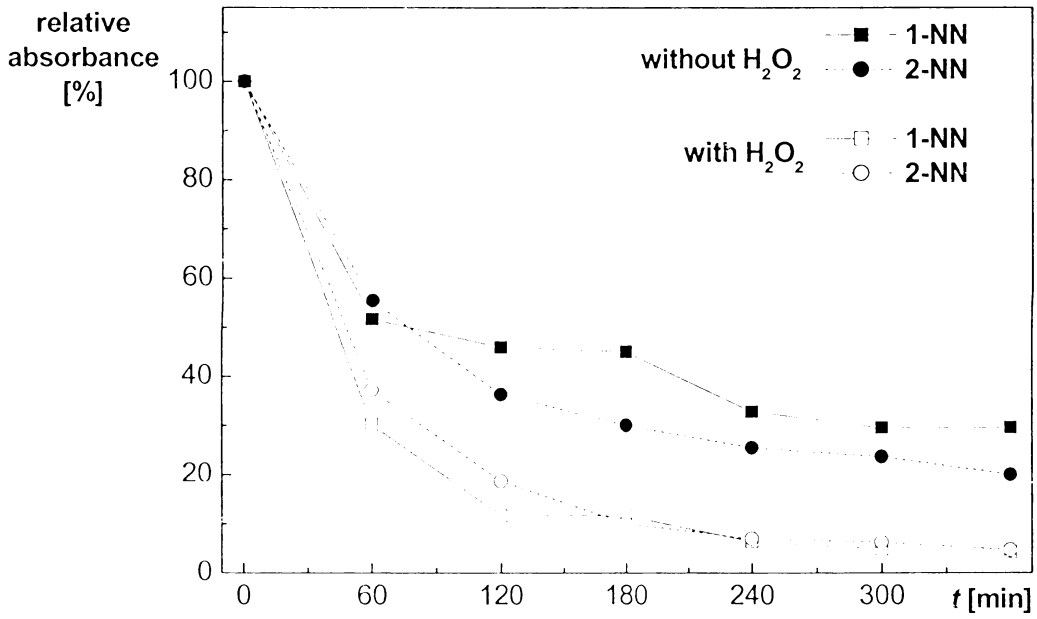

Figure 6.4 *The dependence of the relative absorbance of the solution of 1-nitronaphthalene ($c = 5 \cdot 10^{-4}$ mol L^{-1}) and 2-nitronaphthalene ($c = 5 \cdot 10^{-4}$ mol L^{-1}) in methanol (full symbols) and in methanol with addition of 0.5 mL 30% H_2O_2 (hollow symbols) on the time of its irradiation. Spectra measured in 0.1 cm quartz cuvettes versus methanol. Relative absorbance calculated as quotient of absorbance value of the irradiated solution and the absorbance of the solution before irradiation, measured at the absorbance maximum (326 nm for 1-NN, 348 nm for 2-NN).*

6.3.2 Electrochemical monitoring of photolytical degradation of 1- and 2-nitronaphthalene by differential pulse voltammetry at hanging mercury drop electrode

The electrochemical behaviour of 1-NN and 2-NN at mercury electrodes has been in detail described elsewhere (chapter 3). For DPV at HMDE, quantitative experiments showed linear signal response over more than three concentration orders of magnitude with LODs ~ $2 \cdot 10^{-8}$ mol L^{-1}. This method was selected for monitoring of the photochemical degradation of 1-NN and 2-NN. 1 mL of the irradiated solution was diluted to 10 mL with 0.01 mol L^{-1} NaOH for the DP voltammetric scan, so that the optimum conditions for determination of both studied compounds (compare Table 3.4) were achieved. In Fig. 6.5, the DP voltammograms recorded during the irradiation of $5 \cdot 10^{-4}$ mol L^{-1} solution of 1-NN in methanol are depicted. While the peak of 1-NN at –610 mV is decreasing, a new peak is growing at its expense at –130 mV. This belongs to a destruction product, because no peaks

were observed at the curves of irradiated blank methanol solution. The same trend was observed for 2-NN, the dependence of the peak heights of both nitronaphthalenes and their degradation product on the time of irradiation is depicted in Fig. 6.6. No peak of 1-NN (2-NN) was observed after 120 minutes (150 min) of irradiation. The faster degradation of 1-NN is in agreement with experiments simulating direct photolysis of gaseous phase nitronaphthalenes. It was realized that the rate constant of photolysis k_{phot} for the reaction: $ArNO_2 + h\nu \rightarrow$ products, can be estimated from following equation [21]:

$$\ln\left\{\frac{[ArNO_2]_{t0}}{[ArNO_2]_t}\right\} = k_{phot}(t - t_0) \qquad (6.1)$$

where $[ArNO_2]_{t0}$ is the concentration of the nitro aromatics at time t_0 and $[ArNO_2]_t$ the corresponding concentration at time t. Thus, plots of $(\ln\{[ArNO_2]_{t0}/[ArNO_2]_t\})$ against $(t - t_0)$ should be straight lines with a slope of k_{phot} and a zero intercept. Reported rate constants k_{phot} of 1-NN photolysis in gas phase are four times [21] or one order of magnitude [22,23] higher than for 2-NN, when model experiments were carried out under sunlight. Moreover, 2-NN was stable towards photolysis in a different experiment using an artificial blacklight irradiation in an indoor Teflon chamber, while 1-NN decomposed fast [24].

In aqueous phase, studies were carried out with solutions of selected nitroaromatics including 1-NN and 2-NN in acetonitrile, which were irradiated with incandescent sunlamp and after 480 minutes of irradiation, 42 % of 1-NN and more than 95 % of 2-NN were present in the solution [25]. For this Thesis, the calculation of k_{phot} using data presented in Fig. 6.6 results in k_{phot}(1-NN) = 0.0602 ± 0.0056 min^{-1} (R = 0.9875) and k_{phot}(2-NN) = 0.0521 ± 0.0024 min^{-1} (R = 0.9958), representative plot of Eq. (6.1) is shown in Fig. 6.7. The lower difference between k_{phot} value for 2-NN and 1-NN photodegradation in this case in comparison with the gaseous phase is probably due massive attack of oxygen containing radicals present in methanolic solution. In gaseous phase, the nonequivalent stability of nitronaphthalenes towards photodegradation was subscribed to the differences in the planarity of nitronaphthalenes, discussed earlier in chapter 4.3.2. While 2-NN is a planar molecule, the nitro group of 1-NN is forced out of the molecular plane due to the steric interaction with the peri proton. In this arrangement, in the excited state the interaction of the nitro group with the aromatic π system is increased [26,27,28]. This favors intramolecular nitro to nitrite rearrangement of the excited state, to which the photochemistry of nitroaromatics has been attributed [29,30].

In order to evaluate the efficiency of the destruction method, standard addition method has been used. Standard additions corresponding to 0.04 %, 0.1 % and 0.2 % of 1-NN

originally present are shown in Figure 6.8, the curve recorded after 120 min of irradiation exhibits no 1-NN peak. Thus, it can be concluded that more than 99.96 % of 1-NN were successfully removed by UV photolysis. For 2-NN, standard addition corresponding to 0.2 % of originally present amount was obvious after 180 min of irradiation, thus the destruction efficiency was at least 99.8 % for this compound.

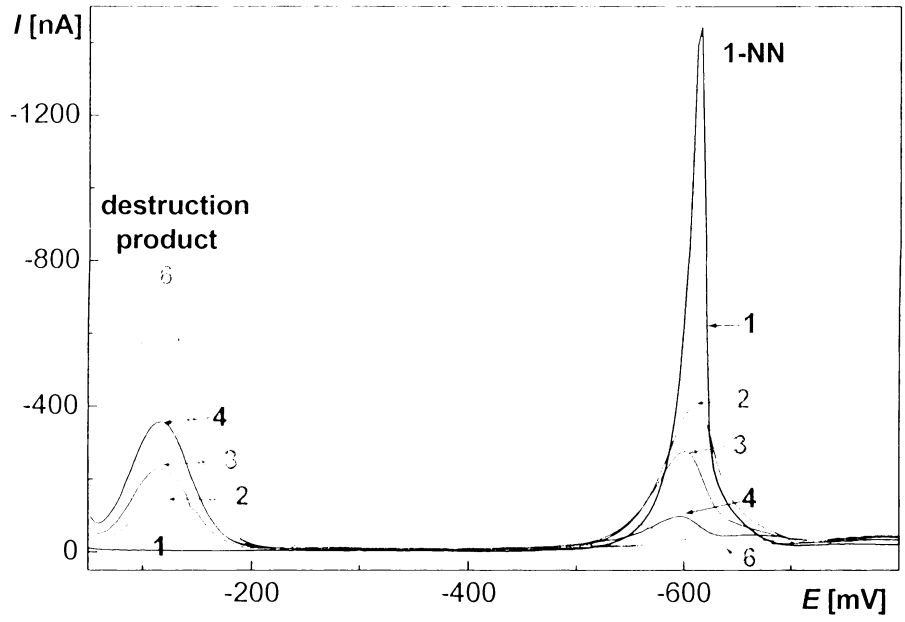

Figure 6.5 *DP voltammograms for monitoring of the UV photolysis of 1-NN in methanol. Supporting electrolyte 0.01 mol L^{-1} NaOH - methanol (irradiated solution) 9:1, pH 12.0 The 1-NN solution (c = $5 \cdot 10^{-4}$ mol L^{-1}) before irradiation (1) and after 15 min (2), 30 min (3), 60 min (4), 90 min (5) and 120 min (6) of UV irradiation in the reactor.*

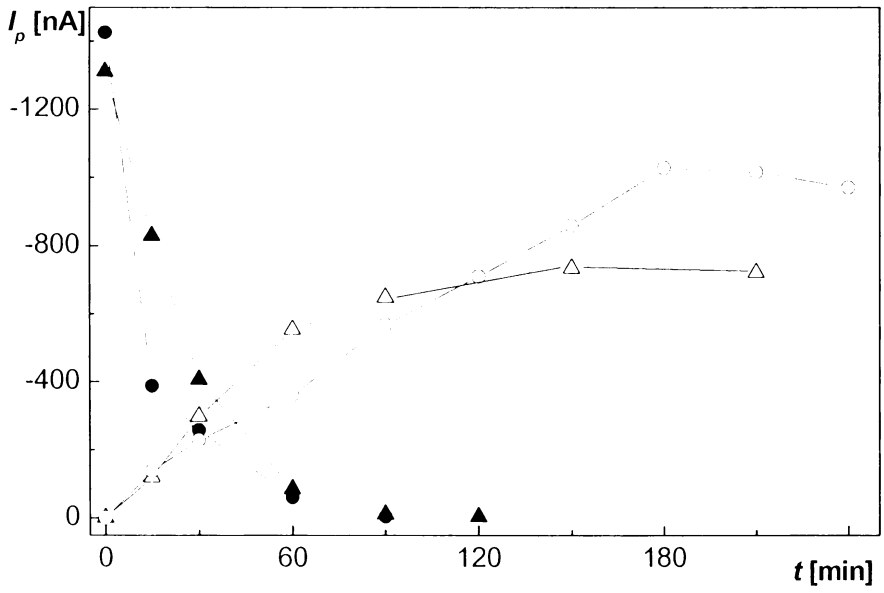

Figure 6.6 *Dependence of the peak height I_p of 1-NN (●) and its destruction product (○) and of 2-NN (▲) and its destruction products (Δ) on the time of UV irradiation. Measured by DPV at HMDE in 0.01 mol L^{-1} NaOH - methanol (irradiated solution) 9:1, pH 12.0), initial concentration of 1-NN and 2-NN was $5 \cdot 10^{-4}$ mol L^{-1}.*

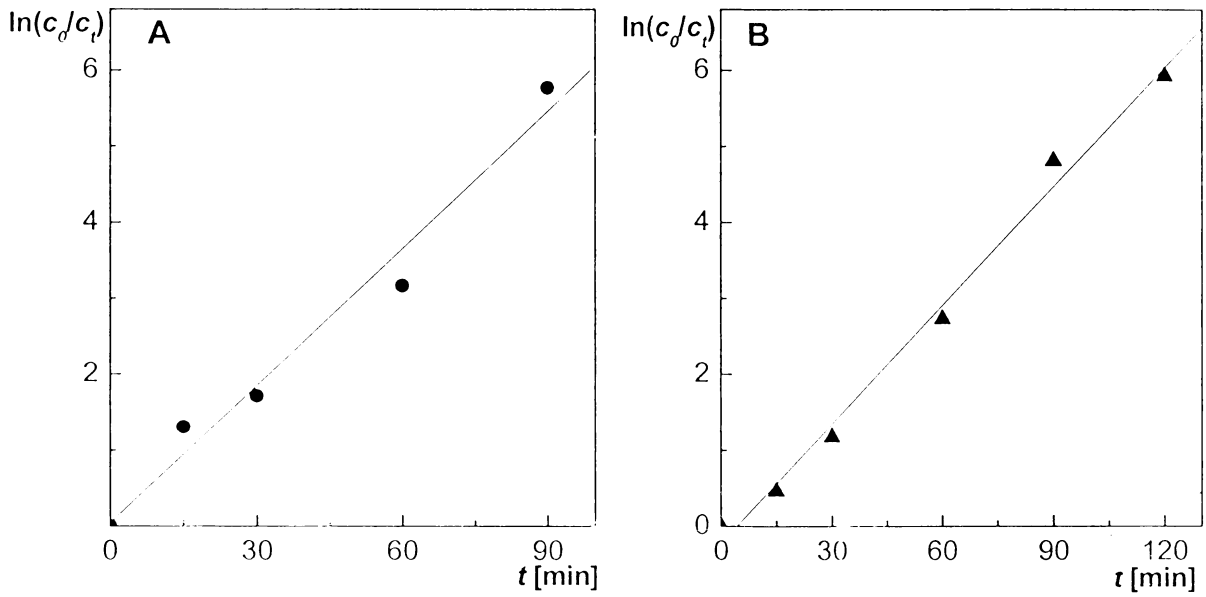

Figure 6.7 *Plot of Eq. (6.1) for 1-NN (A,●) and 2-NN (B,▲) photolytical degradation. The coefficient c_0/c_t was calculated as I_{p0}/I_{pt} ratio, where I_{p0} is the height of the DPV peak of 1-NN (2-NN) before beginning and I_{pt} after t min of UV irradiation.*

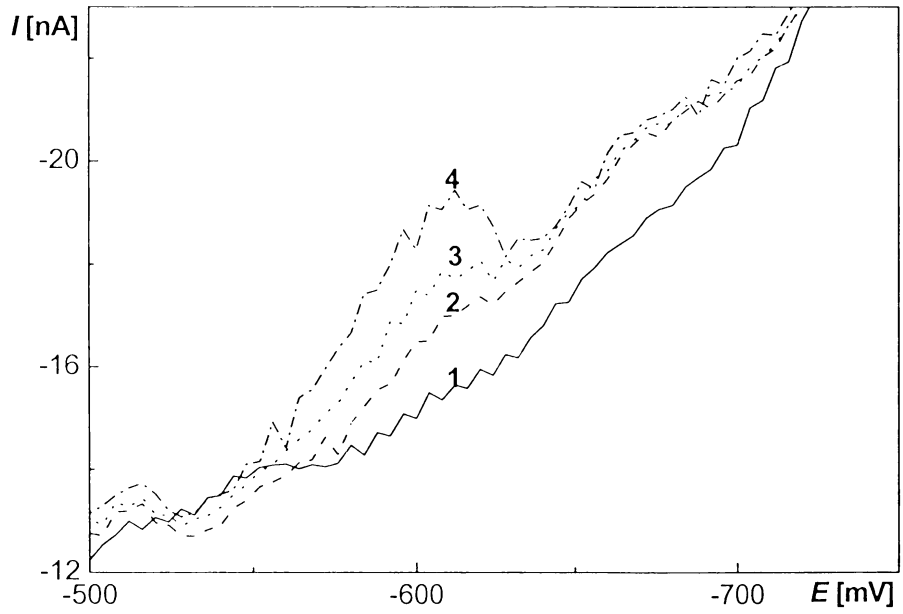

Figure 6.8 *DP voltammograms for monitoring of the UV photolysis of 1-NN in methanol, recorded in a mixture of irradiated solution with 0.01 mol L^{-1} NaOH (1:9, pH 12.0). $5 \cdot 10^{-4}$ mol L^{-1} 1-NN after 120 min irradiation in the reactor (1) and the same irradiated solution with standard addition of 1-NN corresponding to 0.04 % (2), 0.1 % (3) and 0.2 % (4) originally present.*

6.3.3 Products of photodegradation

This chapter is inspired by the presence of a peak of a destruction product with peak potential about –130 mV obvious after DP voltammetric analysis of irradiated solutions of 1-NN and 2-NN (Figure 6.5). The identification of degradation products is always a difficult task due to their number and variety. It is useful tool for understanding the mechanism of NPAHs photolytic degradation. This process is in particular important in understanding the fate of NPAHs in the atmosphere. While for most of relatively volatile NPAHs (formed from two ring PAHs), including 1-NN, the dominant atmospheric loss process is the gas-phase photolysis, for 2-NN other pathways, i.e. the OH-attack may be also important [22,23]. As the experiments conducted with NPAHs in gaseous phase prevail, the experiments in solution or adsorbed to solid surface are easier to conduct and can bring useful information according the photodegradation mechanism and relationship between the nitro group orientation and photodegradation [25].

To understand at least partially the structure of degradation products, several other experiments were conducted with irradiated solutions using electrochemical methods and GC-MS. In a previous study of Muck [19], 1-nitropyrene (1-NP) in methanol was irradiated and HPLC-MS was used to analyze the irradiated solution. Three methoxypyrene isomers, hydroxymethylpyrene, nitrosopyrene and 1-hydroxypyrene were identified as degradation products when low energy UV irradiation was applied on 1-NP methanolic solution purged by oxygen. After massive irradiation (6 hours) using the same experimental setup as in this study, the aromatic pyrene system was destroyed to polar fragments and no other peak except 1-NP was observable at DP voltammetric curves recorded in a mixture of Britton-Robinson buffer pH 12 with irradiated solution (1:9). These curves were recorded in a potential window starting at –200 mV, if the irradiation was repeated in our experimental setup, DP voltammetric peak increasing with the time of irradiation appeared at –140 mV. Non from the above mentioned 1-nitropyrene destruction products matches with this redox potential, because nitrosopyrene is reducible at more negative and monohydroxyderivatives of pyrene are oxidizable at more positive potentials than the mentioned –140 mV. A new peak appeared also when irradiating methanolic solutions of 1,5-dinitronaphthalene (peak potential of the degradation product E_{DP} = –145 mV), 9-nitroanthracene (E_{DP} = –115 mV) and 1-nitrobenzene (E_{DP} = –50 mV) in our experimental setup. In Figure 6.9 and 6.10 the DC tast polarograms and cyclic voltammogram recorded during the UV irradiation of methanolic solution of 2-NN are depicted. The anodic current of the destruction product at the first figure indicates an

oxidation process, the logarithmic analysis of the best developed wave with $E_{1/2} = -155$ mV (curve 7) revealed that 1.94 electrons are exchanged. The cyclic voltammograms reveal the reversibility of the redox systems with potential difference of ~55 mV between the cathodic and anodic peak maximum. These cyclic voltammograms matches with CVs of 1,4-napthoquinone recorded in the same supporting electrolyte – a mixture of 0.01 mol L^{-1} NaOH with methanol (9:1). The oxidation process recognized by DC tast polarography indicates the presence of a diol moiety rather than the quinone structure, e.g. the presence of 1,4-dihydroxynaphthalene. The redox couple 1,4-naphthalenediol - 1,4-naphthoquinone exchanges 2 electrons, which is in a good agreement with results of logarithmic analysis for the unknown destruction product reported above. Substances with quinone structure are common products of NPAHs photolysis [31,25], e.g. 1,4-naphthoquinone was together with 2-nitro-1-hydroxynaphthalene identified as a gas-phase photolysis relatively stable product of 1-NN after outdoor sunlight and indoor blacklamp irradiation [31], 2-methyl-1,4- naphthoquinone was found a degradation product when irradiating 2-methyl-1-nitronaphthalene in acetonitrile with a sunlamp [25]. The possible mechanism of the photo induced quinone formation from NPAHs was explained first for 9-nitroanthracene in acetone - after UV irradiation, the nitro group of the excited NPAHs rearranges to nitrite, which dissociates to nitrogen(II)oxide and 9-anthryloxyradical. Further reactions lead to antraquinone with higher yields in presence of oxygen in comparison to when it was absent [30]. However, in an alcoholic solvent, the quinone group can suffer hydrogen donation from the solvent, 1,4-naphthalenediol was reported as product of 1,4-naphtoquinone photoredution in 25% methanol [32], 2-propanol or ethanol [33] under nitrogen atmosphere, in presence of oxygen the quinone decayed to phthalic acid and its derivatives (dimethylphthalate, ethylmethylphthalate). When we repeated the UV irradiation under nitrogen (oxygen absence), the degradation of 1-NN and 2-NN was substantially slower and the DPV peak height of the destruction product gave the maximum of –37 nA (2-NN) and –20 nA (1-NN). The dihydroxyl moiety oxidizable to quinone structures could be present between the destruction products of all tested nitroaromatics and in view of reported results on photodegradation of 1-NN in gaseous phase, 1,4-naphthalenediol is the most probable one for this compound.

GC-MS was further used for characterization of degradation product, however, dinaphtols can not be detected using this technique until they are derivatized [34,35]. The solutions irradiated in presence and absence of oxygen were analyzed, corresponding GC-MS spectra are depicted in Fig. 6.11A and B. A large number of products were found in the first

case, which confirms the greater efficiency of photodegradation in the presence of oxygen containing radicals. However, the large number of products in absence of oxygen confirms the complexity of photodegradation mechanism consisting of various radical reactions. Based on the MS spectra recorded after GC separation and injection of several standards (naphthalene, 1- and 2- aminonaphthalene, 1- and 2- hydroxynaphthalene), the compounds summarized in Table 6.1 are presumably present in irradiated solutions. Some of the naphthalene derivatives found after irradiation under nitrogen are analogous to pyrene derivatives obtained by low energy UV irradiation of 1-nitropyrene mentioned earlier in this chapter. All identified products contain the naphthalene aromatic ring, which confirms the low efficiency of degradation. On the other hand, the products obtained in air saturated samples are characterized by decay of the nitro group bearing benzene ring. Typically, its fragments are photo oxidized forming an acid and possibly further methylated. Some of the destruction products, i.e. phthalic acid (or its anhydride, these product were dominant in solutions when using direct injection of irradiated solutions to GC (chromatograms not shown), 3H(1)isobenzofuranon, dimethylphthalate) were earlier identified after naphthalene irradiation in a smog chamber containing NO and OH radicals [36,37,38] or in photodegradation of 1,4-naphthoquinone in 2-propanol as mentioned above [33]. There are many other reaction products of 1-NN and 2-NN photodegradation, their identification would be of benefit to infer a detailed conversion pathway.

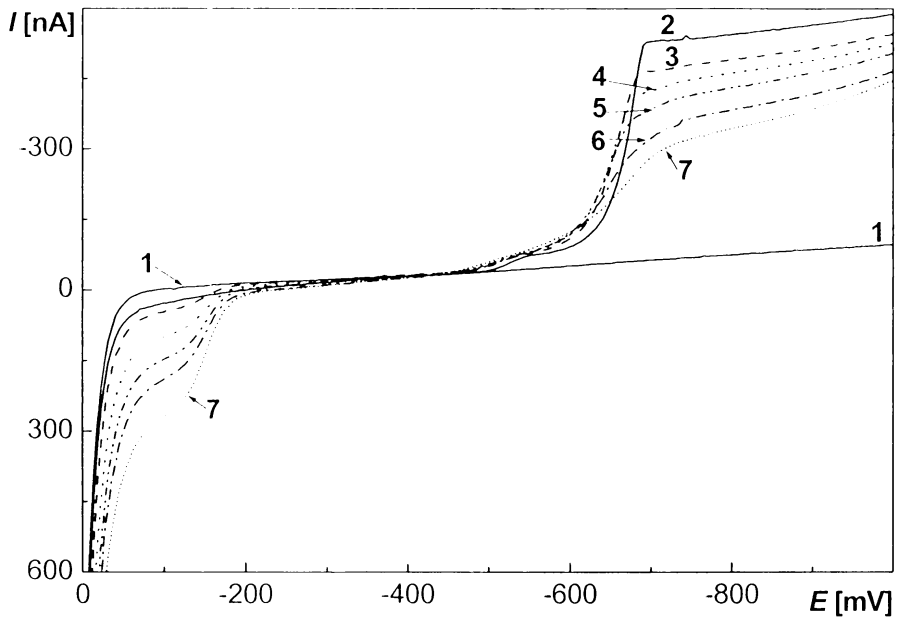

Figure 6.9 *DC tast polarograms recorded during UV photolysis of 2-NN in methanol. Supporting electrolyte 0.01 mol L^{-1} NaOH - irradiated solution 9:1, pH 12.0. Blank methanol (1), and 2-NN solution (c = $5 \cdot 10^{-4}$ mol L^{-1}) before irradiation (2) and after 30 min (3), 60 min (4), 90 min (5), 120 min (6) and 180 min (7) of UV irradiation in the reactor (lower radiation intensity of the Hg lamp than Fig. 6.5).*

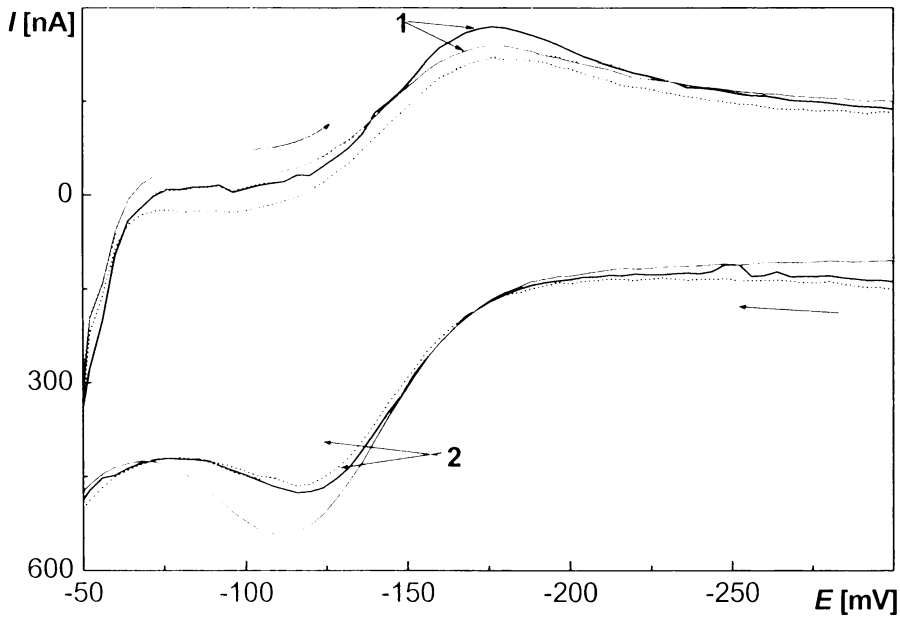

Figure 6.10 *Cyclic voltammograms recorded after 60 min UV photolysis of 2-NN in methanol in 0.01 mol L^{-1} NaOH - irradiated solution 9:1, pH 12.0 (black curves) and cyclic voltammograms of 1,4-naphthoquinone (c = $5 \cdot 10^{-3}$ mol L^{-1}) in 0.01 mol L^{-1} NaOH - methanol 9:1, pH 12.0 (red curves). The first (1, full lines) and the second (2, dashed lines) cycle presented, scan rate 500 mV s^{-1}.*

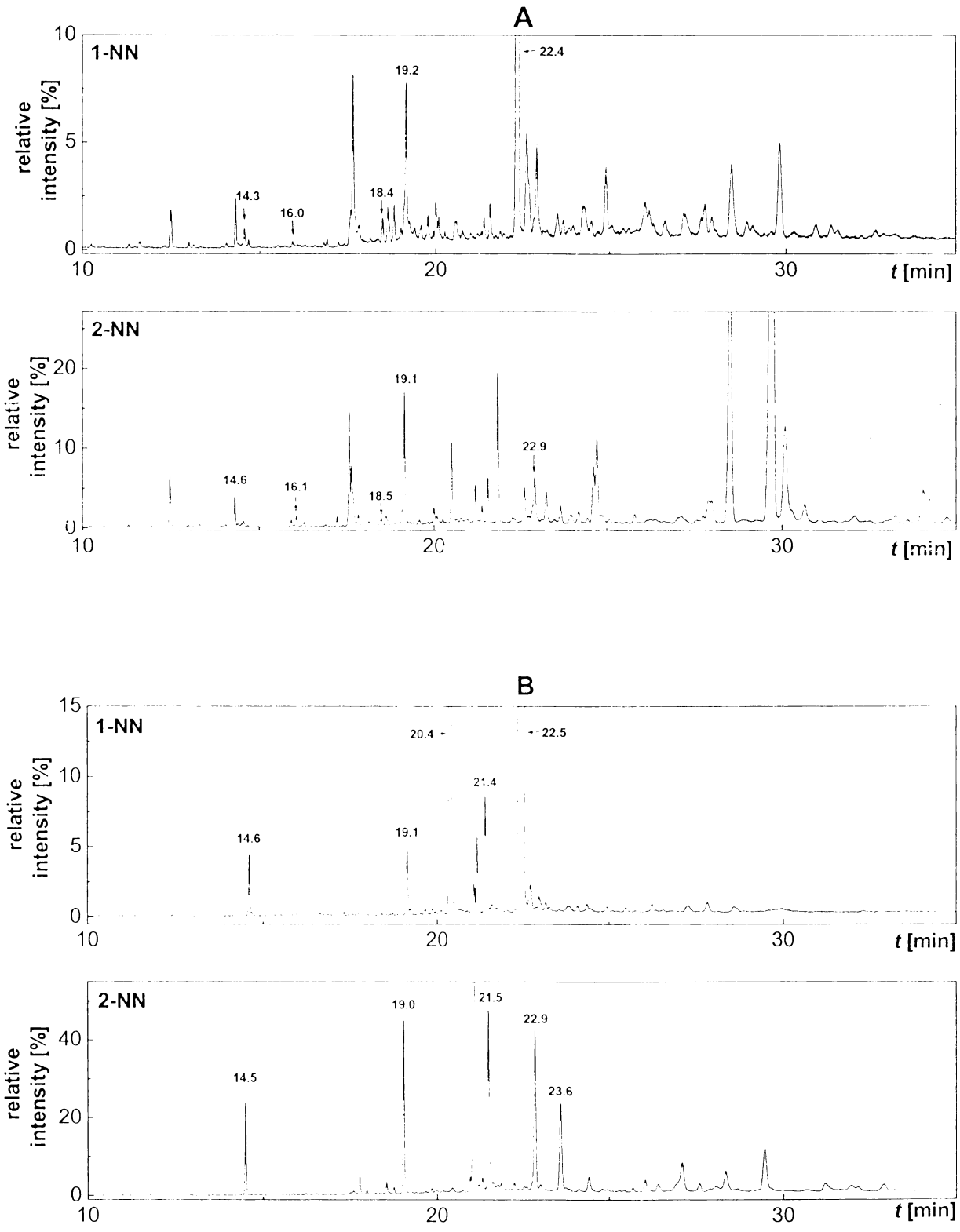

Figure 6.11 *GC-MS chromatograms of $5 \cdot 10^{-4}$ mol L^{-1} 1-NN and 2-NN in methanol after 3 hours of irradiation under atmospheric conditions (A) and under nitrogen atmosphere (B). TIC, large scale.*

Table 6.1 *Identified products of 1-NN and 2-NN photolytical degradation.*

1-nitronaphthalene		2-nitronaphthalene	
Product	**Retention time [min]**	**Product**	**Retention time [min]**
Presence of oxygen			
Naphthalene	14.3	Naphthalene	14.6
Phthalic acid (anhydride)	16.1	Phthalic acid (anhydride)	16.1
1(3H) Isobenzofuranon	18.4	1(3H) Isobenzofuranon	18.5
Dimethylphthalate	19.2	Dimethylphthalate	19.1
1-nitronaphthalene	22.4	2-nitronaphthalene	22.9
Absence of oxygen			
Naphthalene	14.6	Naphthalene	14.5
Methoxynaphthalene [a]	19.1	Methoxynaphthalene [a]	19.0
Hydroxynaphthalene [a]	20.4	Aminonaphthalene [a]	21.5
Aminonaphthalene [a]	21.4	2-nitronaphthalene	22.9
1-nitronaphthalene	22.5	Methoxynaphthaleneamine [a]	23.6

[a] isomers not distinguishable

6.4 Conclusions

The efficiency of the photolytical degradation for safe destruction of 1-NN and 2-NN in methanol was evaluated. Methods based on spectrophotometry and DPV at HMDE were used for monitoring of the UV degradation process. Lower values (80 % 1-NN, 71 % 2-NN) were obtained for UV spectrophotometry due to the increasing absorbance of the destruction residuals in the range of 400-200 nm. However, after addition of hydrogen peroxide and water the decomposition proceeds with efficiency higher than ~ 95 %. More suitable for the monitoring is the DPV at HMDE, no peak of 1-NN and 2-NN is observable after 120 min and 150 min of irradiation in air saturated solutions, respectively. The standard addition method revealed more than 99.8 % efficiency of the photolysis of both analytes. However, many destruction products are formed as demonstrated by GC-MS. In general, the UV irradiation of oxygen containing solutions proceeds faster than in absence of it, the naphthalene nucleus is destroyed and more polar compounds containing benzene ring are formed. By electrochemical methods, a compound containing probably diol moiety was identified. The irradiation under nitrogen leads mainly to changes in the substitution of the naphthalene nucleus. However, the toxicity of the resulting solutions should be subject to further mutagenicity experiments.

6.5 References

1. World Health Organisation: *Selected Non-heterocyclic Polycyclic Aromatic Hydrocarbons*, IPCS Environmental Health Criteria 202. WHO, Geneva 1998.
2. World Health Organisation: *Selected Nitro- and Nitro-Oxy-Polycyclic Aromatic Hydrocarbons*, IPCS Environmental Health Criteria 229. WHO, Geneva 2003.
3. http://*www.iarc.fr*, accessed 18. 12. 2005.
4. Montesaro R. (Ed.): *Handling Chemical Carcinogens in the Laboratory - Problems of Safety*. Vol. 33, IARC Press, Lyon 1979.
5. Castegnaro M. (Ed.): *Laboratory Decontamination and Destruction of Carcinogens in Laboratory Wastes: Some Aromatic Amines and 4-Nitrobiphenyl*. Vol. 64, IARC Press, Lyon 1985.
6. Smith M. R.: *Biodegradation* 1, 191-206 (1990).
7. Beltran F. J., Gonzalez M., Gonzalez J. F.: *Water Res.* 31, 2405-2414 (1997).
8. Tinnucci L., Borgarello E., Minero C., Pelizetti E., in: *Photocatalytic purification and treatment of water and air* (ed. Ollis D. F., Al-Ekabi H.), p. 585. Elsevier Science Publisher BV, Amsterdam 1993.
9. Barek J., Berka A., Müller M., Procházka M., Zima J.: *Collect. Czech. Chem. Commun.* 51, 1604-1608 (1986).
10. Castegnaro M., Malaveille C., Brouet I., Michelon J., Barek J.: *Amer. Ind. Hyg. Assoc. J.* 46, 187-191 (1985).
11. Mocko V.: *PhD Thesis*, Charles University, Faculty of Science, Prague 2004.
12. Legrini O., Oliveros E., Braun A. M.: *Chem. Rev.* 30, 671-678 (1993).
13. Lopez J. L., García Einschlag, F. S., Gonzalez M. C., Capparelli A. L., Oliveros E., Hashem T. M., Braun A. M.: *J. Photochem. Photobiol. A - Chem.* 137, 177-184 (2000).
14. Ho P.: *Environ. Sci. Technol.* 20, 260-267 (1986).
15. Fujishima A., Rao T. N., Tryk D. A.: *J. Photochem. Photobiol. C - Photochem. Rev.* 1, 1-21 (2000).
16. Glaze W. H.: *Environ. Sci. Technol.* 21, 224-230 (1987).
17. Bossmann S. H., Oliveros E., Göb S., Siegwart S., Dahlen E. P., Payawan L., Jr., Straub M., Wörner M., Braun A. M.: *J. Phys. Chem. A* 102, 5542-5550 (1998).
18. Barek J., Mejstřík V., Zima J.: *Chem. Listy* 87, 322-331 (1993).
19. Muck A.: *PhD Thesis*, Charles University, Faculty of Science, Prague 2002.
20. Stein S., Mirokhin Y., Tchekhovskoi D., Mallard G.: *NIST MS Search Program*. Version 2.0, USA 2003.
21. Phousongphouang P. T., Arey J.: *J. Photochem. Photobiol. A-Chem* 157, 301-309 (2003).
22. Feilberg A., Kamens R. M., Strommen M. R., Nielsen T.: *Atmos. Environ.* 33, 1231-1243 (1999).

23. Feilberg A., Kamens R. M., Strommen M. R., Nielsen T.: *Polycycl. Arom. Comp.* 14-15, 151-160 (1999).
24. Atkinson R., Aschmann S. M., Arey J., Zielinska B., Schuetzle D.: *Atmos. Environ.* 23, 2679-2690 (1989).
25. Warner S. D., Farant J. P., Butrel I. S.: *Chemosphere* 54, 1207-1215 (2004).
26. Balakrishnan P., Boykin D. W.: *J. Org. Chem.* 50, 3661-3663 (1985).
27. Lin S.-T., Jih Y.-F., Fu P. P..: *J. Org. Chem.* 61, 5271-5273 (1996).
28. Miller D. W., Evans F. F., Fu P. P.: *Spectrosc. Int. J.* 4, 91-94 (1985).
29. Chapman O. L., Griswold A. A., Hoganson E., Lenz G., Reasoner J. W.: *J. Pure Appl. Chem.* 9, 585-590 (1964).
30. Chapman O. L., Heckert D. C., Reasoner J. W., Thackaberry S. P.: *J. Am. Chem. Soc.* 88, 5550-5554 (1966).
31. Yang D. T. C., Chou A., Chen E., Chiu L.-H., Ni Y.: *Polycycl. Arom. Comp.* 5, 201-208 (1994).
32. Poapě F.: *Collect. Czech. Chem. Comm.* 15, 399-613 (1950).
33. Ide A., Ueno Y., Takaichi K., Watanabe H.: *Agric. Biol. Chem.* 43, 1387-1394 (1979).
34. Wu R. N., Waidyanatha S., Henderson A. P., Serdar B., Zheng Y. X., Rappaport S. M.: *J. Chromatogr. A* 826, 206-213 (2005).
35. Samantha S. K., Chakraborti A. K., Jain R. K.: *Appl. Microbiol. Biotechnol.* 53, 98-107 (1999).
36. Lane D. A., Fielder S. S., Towmsend S. J., Bunce N. J., Zhu J., Liu J., Wiens B., Pond P.: *Polycycl. Arom. Comp.* 9, 53-59 (1996).
37. Bunce N. J., Liu L., Zhu J., Lane D. A.: *Environ. Sci. Technol.* 31, 2252-2259 (1997).
38. Sasaki J., Aschmann S. M., Kwok E. S. C., Atkinson R., Arey J.: *Environ. Sci. Technol.* 31, 3173-3179 (1997).

7

Amperometric detector with microcylindrical electrode for HPLC

7.1 Introduction

Over the past three decades, the development of electrochemical detection for HPLC has represented one of the most active and successful movements in electroanalytical chemistry. During this period, amperometry has become the most commonly employed electrochemical detection method thanks to its sensitivity, versatility and relative selectivity. A number of various construction arrangements of amperometric detectors appear every year in the literature [1,2,3]. It is generally accepted that they should be designed to meet two basic requirements [2]:

a) From the chromatographic point of view the detector effective volume should be sufficiently low so as not to contribute to the additional peak broadening.

b) From the electrochemical point of view the electrode system should have geometry permitting the existence of a homogenous electric field between the indicator and counter electrode and also permitting close position of the reference electrode, which is necessary for the potential stability. Moreover, the counter electrode should be separated from the detection space so that the reaction products formed at its surface cannot interfere with the detection.

It is practically impossible to fabricate a detector that fully meets both these requirements, because the considerably large detection space for proper arrangement of all the electrodes is unacceptable due to the additional peak broadening. In high performance separation methods the chromatographic demands are often preferred over the electrochemical ones, as the low detection volume is more important. Nevertheless the effort to fulfill also the electrochemical demands leads often to complicatedly designed detectors with numerous specially machined components.

In this chapter an amperometric detector based on a microwire electrode is described and tested. Its construction is similar to that of an platinum amperometric tubular detector (TD) constructed earlier in our laboratory [4]. They consist from a working electrode placed directly into the Teflon tube joined to the column outlet, the reference and auxiliary electrode are placed close to it in an overflow vessel without any further special fixing. In such a simple configuration, the electrochemical demands mentioned above are almost ignored nevertheless a reliable detection is possible. For the tubular mode of detection it was confirmed on the detection of several genotoxic derivatives of polycyclic aromatic hydrocarbons (PAHs) (e.g. amino and hydroxyderivatives of biphenyl, hydroxyphenanthrenes and aminoquinolines) [5,6,7].

It this work, we focused on the new arrangement with platinum microwire working

electrode. The constructed platinum microcylindrical detector (Pt-μCD) was employed for the HPLC-ED determination of amino and hydroxy derivatives of naphthalene, namely 1-aminonaphthalene, 2-aminonaphthalene, 1-hydroxynaphthalene, and 2-hydroxynaphthalene. The optimized separation conditions of studied derivatives were taken from Mocko [8]. In this work and in the work of Cvačka [4] the previously mentioned platinum tubular detector was employed for their detection, so in this work we focused on the comparison of analytical parameters of both types of detectors.

7.2 Experimental

7.2.1 Fabrication of the detector

The working electrode was made by fixing of a thin platinum wire in the Teflon tubing (1/16" o.d., 0.010" i.d., Alltech) across to the flow of mobile phase. For its easier placement, the tubing was first pierced with a sharp needle and the wire was then cautiously draught through the resulting aperture. The part of the wire, which is exposed to the electrolyte solution, is a cylinder and its area is given by the diameter of the wire used and by its length, which corresponds to the inner diameter of the Teflon tube. Hot gun glue was used for further fixing of the wire inside the Teflon tubing and a heat shrinkable plastic tube was drawn over it to ensure the full isolation of the wire contact. The tube was immersed in an overflow vessel containing an electrolyte solution (mobile phase) in which an Ag/AgCl (1 mol L^{-1} KCl) reference electrode and platinum auxiliary electrode have been placed. The experimental arrangement of all electrodes is depicted in Fig. 7.1, the detailed scheme focuses on the Teflon tube with the working electrode. The photo of the tip of this part (Fig. 7.2) shows that the wire was placed near to the outlet.

The newly prepared platinum microcylindrical electrode was activated in $5 \cdot 10^{-2}$ mol L^{-1} H_2SO_4 by switching ten times between the potential −0.3 and +1.4 V, applying the potential always for 10 seconds.

The electrode area is 0.08 mm^2 and was calculated as the area of a cylinder jacket with length of i.d. 0.010" (= 0.254 mm) and diameter corresponding to the wire diameter (d = 0.1 mm).

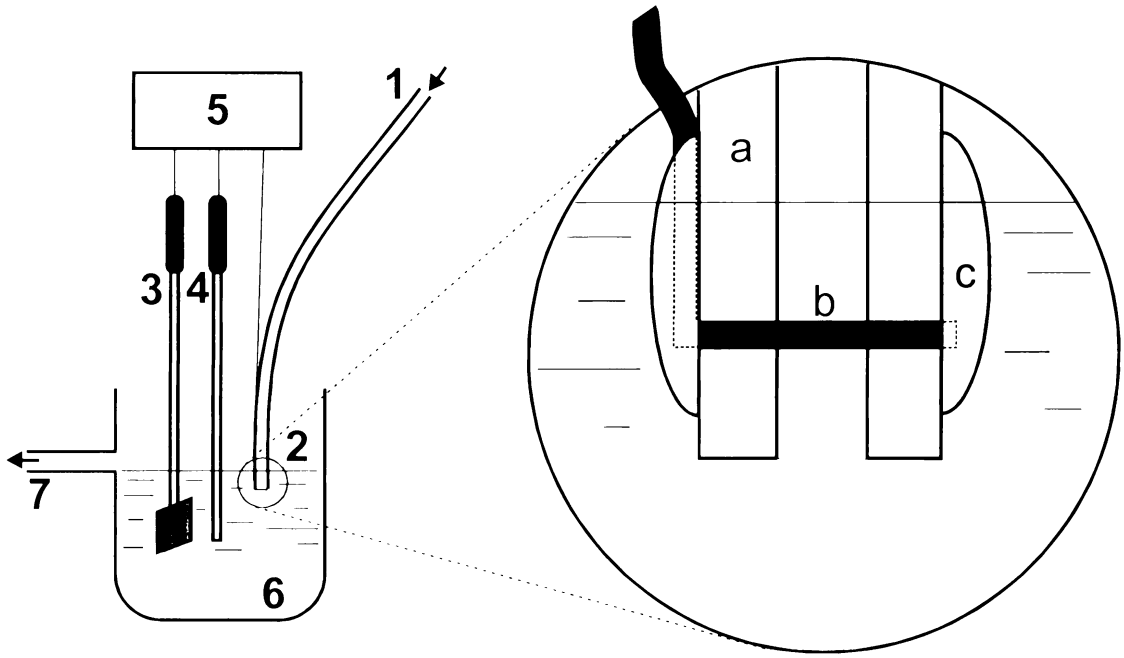

Figure 7.1 *Scheme of the detector with microcylindrical electrode (the individual parts are not depicted on the same scale). 1 – column outlet; 2 – detector, integral part of the tube: a – Teflon tube, b – detection wire, c – hot gun glue; 3, 4 – reference and auxiliary electrode; 5 – potentiostat and amperometer; 6 – electrolyte solution (mobile phase); 7 – waste.*

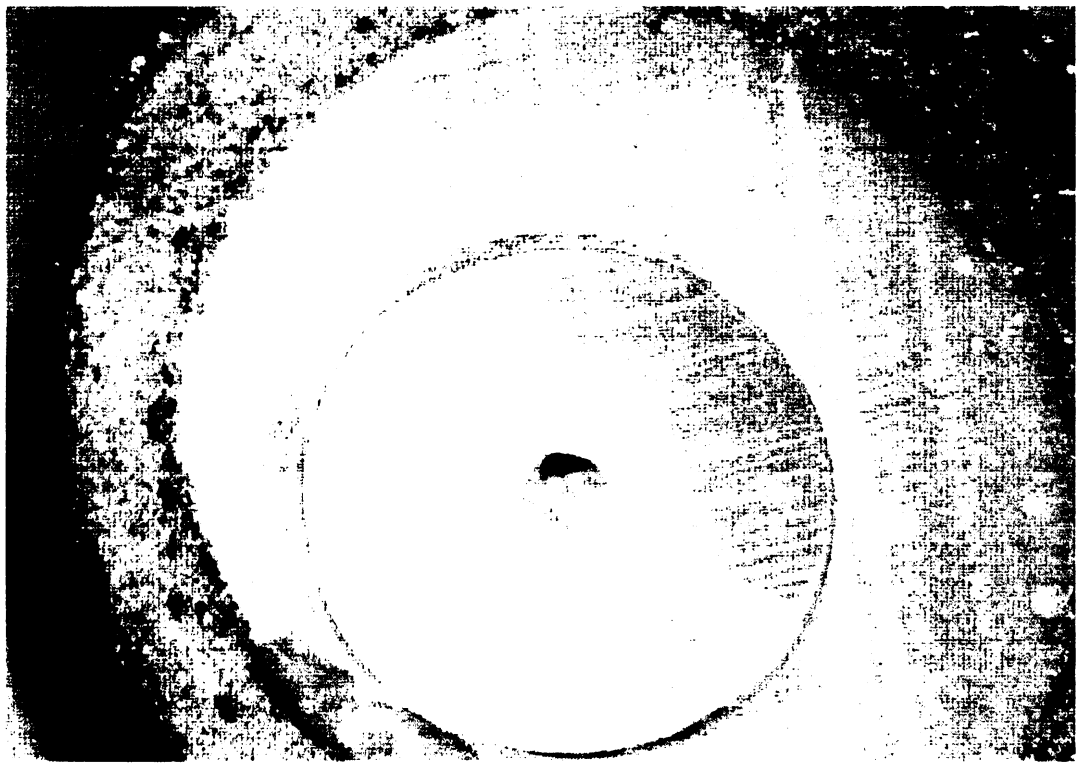

Figure 7.2 *Photo of the integral part of the Teflon tube with microcylindrical electrode (copper wire depicted).*

7.2.2 Apparatus and reagents

The conventional HPLC system LaChrom (Hitachi, Merck, Germany) consisted of the high pressure pump L-7100, D-7000 Interface, L-7400 spectrophotometric detector and L-7200 autosampler controlled by HPLC System Manager (HSM) version 4.0 software. A three electrode arrangement with ADLC2 potentiostat (Laboratorní přístroje, Prague, Czech Republic) was used throughout.

The LiChrospher 100 RP-18, 125x4 mm, 5 μm (Merck, Germany) column was used throughout. Mobile phases were always degassed by passage of helium. The pH values were measured with pH meter 4330 (Jenway, Great Britain) with combined glass electrode. The pH meter was calibrated with standard pH buffers (Sevac, Prague, Czech Republic). De-ionized water was produced by Milli-Qplus system (Millipore, USA). If not stated otherwise, the chemicals were obtained from Lachema Brno, Czech Republic, and were of analytical grade purity. The limit of determination was determined as the concentration that gives the signal equal to three times the noise level. All measurements were carried out at laboratory temperature.

The stock solutions ($c = 1 \cdot 10^{-3}$ mol L^{-1}) of 1-aminonaphthalene (1-AN), 2-aminonaphthalene (2-AN), 1-hydroxynaphthalene (1-OHN), and 2-hydroxynaphthalene (2-OHN) were prepared in acetonitrile (Merck; gradient grade purity) and kept in dark at laboratory temperature. Solutions of lower concentrations were prepared by dilution of stock solutions with mobile phase. For separation of these compounds, 0.01 mol L^{-1} phosphate buffer pH 2.3 - acetonitrile (Merck; gradient grade purity) mixture (60:40, v/v) was used as mobile phase. The phosphate buffer was prepared from disodium hydrogen phosphate, the buffer pH was adjusted by addition of concentrated phosphoric acid. 20 μL of the sample were injected, the flow rate was set at $F_m = 0.5$ mL min^{-1}. For testing of Pt-μCD in HPLC, a mixture of aqueous solution of 0.01 mol L^{-1} imidazole and 0.1 mol L^{-1} KCl at pH 7.5 with acetonitrile (1:1, v/v) was used as mobile phase. 5 μL of $1 \cdot 10^{-4}$ mol L^{-1} 1-AN were injected, the flow rate was set at 0.5 mL s^{-1} and the detection potential used was +0.9 V.

7.3 Results and discussion

7.3.1 Detector parameters

The detector parameters were determined using 1-AN ($c = 5 \cdot 10^{-6}$ mol L^{-1}) in mobile phase containing imidazole - acetonitrile mixture, according to ref. [4]. The retention time of 1-AN in the separation system used was 6.9 min. The effect on the peak width, asymmetry, height and area was evaluated from ten consecutive injections of 1-AN. The results are summarized in Table 7.1 together with corresponding values for Pt-TD [4]. While the values for peak width and plate number, peak height and area repeatability are comparable, there is a substantial difference in current densities. The current density is about five times lower for Pt-μCD than for Pt-TD, as effect of different electrode arrangement. In comparison to Pt-μCD, where the time of contact of the analyte with the working electrode is given basically by the width of the analyte zone, in the case of the tubular arrangement the analyte zone passes along the platinum walls for longer time. As result, the current density is higher for Pt-TD, but the peaks are more tailing. It is obvious from peak asymmetry values in Table 7.1 and is clearly demonstrated in Fig. 7.3 depicting the separation of the mixture of 1-AN, 2-AN, 1-OHN and 2-OHN in phosphate buffer mobile phase. The tailing peaks obtained with Pt-TD for $c = 1 \cdot 10^{-6}$ mol L^{-1} are about the same height as the peaks obtained for Pt-μCD ($c = 1 \cdot 10^{-5}$ mol L^{-1}). The noise calculated from ten measurements in one-minute intervals was 105 ± 14 pA for Pt-TD and 25 ± 3 pA for Pt-μCD, which reflects the difference in their area. The resulting signal/noise ratio favours the tubular detector.

Table 7.1 *Comparison of an amperometric detector with platinum microcylindrical and tubular electrode. Peak parameters for 1-AN (injection 5 μL, c = $5 \cdot 10^{-6}$ mol L^{-1}), mobile phase KCl (0.1 mol L^{-1}), imidazole ($1 \cdot 10^{-2}$ mol L^{-1}), pH 7.5 - acetonitrile (1:1, v/v) at the flow rate 0.5 mL min^{-1}, E_{det} = + 0.9 V.*

Parameter	Pt-microcylindrical detector	Pt-tubular detector [4]
Peak width, $w_{1/2}$ [min]	0.236 ± 0.003	0.247 ± 0.002
Plate number N	4785 ± 108	4720 ± 80
Peak asymmetry	1.23 ± 0.2	1.57 ± 0.3
RSD [a] - peak height [%]	0.44	0.45
RSD [a] - peak area [%]	0.85	0.94
Electrode area [mm^2]	0.08	0.6
Current density [nA mm^{-2}]	18.3	93.3
Noise [pA]	25 ± 3	105 ± 14
Signal/noise ratio	58.5	533

[a] relative standard deviation

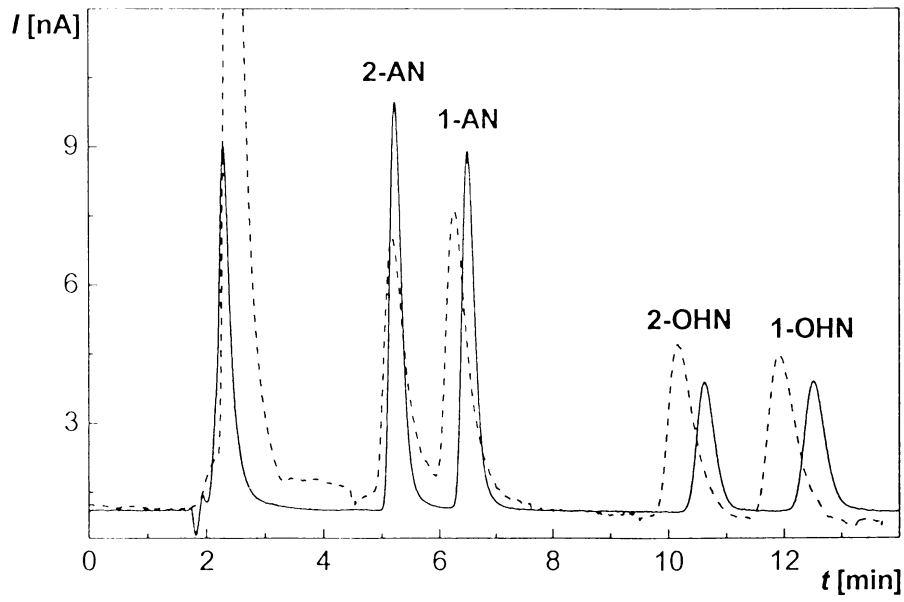

Figure 7.3 *Separation of a mixture of 1-aminonaphthalene, 2-aminonaphthalene, 1-hydroxynaphthalene and 2-hydroxynaphthalene in acetonitrile - 0.01 mol L^{-1} phosphate buffer, pH 2.3 (40:60, v/v) mobile phase, flow rate 0.5 mL min^{-1}. Detection at Pt-μCD (—), concentration c = $1 \cdot 10^{-5}$ mol L^{-1} of each analyte; detection at Pt-TD (---), concentration c = $1 \cdot 10^{-6}$ mol L^{-1} of each analyte.*

7.3.2 Detection of amino and hydroxy naphthalenes using platinum microcylindrical detector

The detector was further employed for detection of 1-AN, 2-AN, 1-OHN, 2-OHN in phosphate buffer (pH 2.3) - acetonitrile (60:40, v/v) mobile phase after their chromatographic separation. The total analysis time using isocratic elution was 14 minutes. First, the detection potential was optimized to detect the analytes of interest with the highest sensitivity. The dependence of peak height and area on the potential applied on the working electrode was investigated in the range of +0.3 to +1.5 V. Corresponding hydrodynamic voltammograms of all compounds are depicted in Fig. 7.4. It is apparent that the oxidation of aminonaphthalenes begins at somewhat lower detection potentials (+0.7 V) than the oxidation of hydroxynaphthalenes (+0.8 V). The derivatives substituted in position one of the aromatic skeleton are oxidizable at slightly lower potentials than these substituted in position two. These results are in concordance with findings at other types of platinum and glassy carbon electrodes [8]. The signal-to-noise ratios reach their maxima at potentials about +1.3 to +1.4 V, nevertheless, the detection potential for further applications was set at +1.2 V due to substantial baseline drift at higher potential values.

The calibration dependences were measured in the concentration range of $1 \cdot 10^{-7}$ mol L^{-1} to $1 \cdot 10^{-4}$ mol L^{-1}, they are linear to the concentration of $6 \cdot 10^{-5}$ mol L^{-1} for each analyte. At higher concentrations the detector response decreases in the series of repeated injections, probably due to formation of polymer films as products of oxidation at platinum electrode, which is a known feature for many aminoaromatics [9,10]. However, at lower concentrations the repeatability is satisfactory, as confirmed in previous chapter. The detection figures of merit are summarized in Table 7.2 with the evaluation from both the peak heights and peak areas; attained correlation coefficients are higher for the latter case. Achieved limits of detection for Pt-μCD are higher than those for the Pt-TD, which are $2 \cdot 10^{-8}$ mol L^{-1}, $2 \cdot 10^{-8}$ mol L^{-1}, $5 \cdot 10^{-8}$ mol L^{-1} and $5 \cdot 10^{-8}$ mol L^{-1} for 1-AN, 2-AN, 1-OHN and 2-OHN, respectively [8]. The achieved LODs prove the applicability of Pt-μCD in trace analysis of electroactive oxidizable substances.

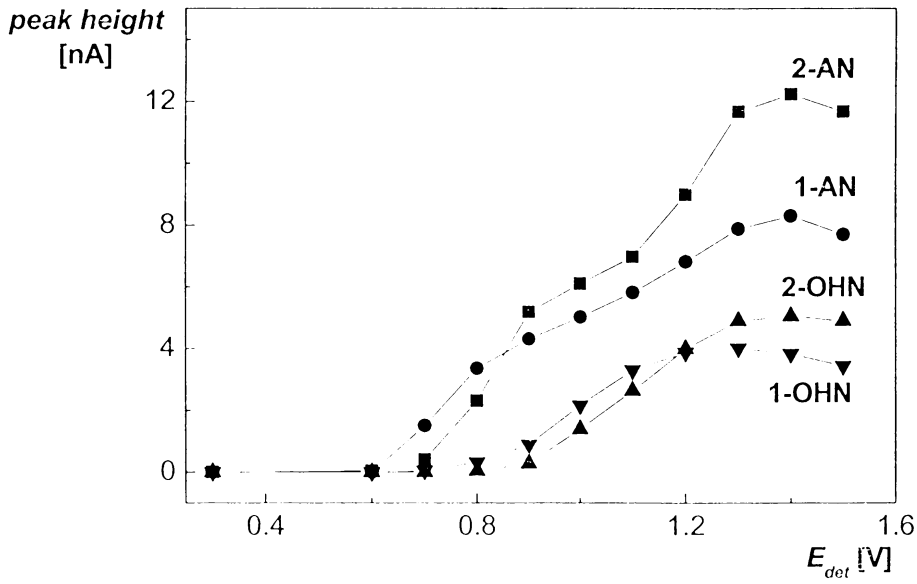

Figure 7.4 *Hydrodynamic voltammograms for a mixture of 1-aminonaphthalene, 2-aminonaphthalene, 1-hydroxynaphthalene and 2-hydroxynaphthalene ($c = 1 \cdot 10^{-5}$ mol L^{-1} of each) in acetonitrile - 0.01 mol L^{-1} phosphate buffer, pH 2.3 (40:60, v/v) mobile phase, flow rate 0.5 mL min^{-1}.*

Table 7.2 *Detection figures of merit for HPLC - Pt-μCD determination of amino and hydroxy derivatives of naphthalene, injection 20 μL, E_{det} = +1.2 V, mobile phase 0.01 mol L^{-1} phosphate buffer pH 2.3 - acetonitrile (60:40, v/v), flow rate 0.5 mL min^{-1}.*

(A) Evaluation from peak heights.

Analyte	Capacity factor	Linear dynamic range [mol L^{-1}]	Slope [mA mol^{-1} L]	Intercept [nA]	Correl. Coef.	LOD [mol L^{-1}]
2-AN	2.02	$1 \cdot 10^{-7}$ - $6 \cdot 10^{-5}$	0.962	0.22	0.9987	$8 \cdot 10^{-8}$
1-AN	2.75	$1 \cdot 10^{-7}$ - $6 \cdot 10^{-5}$	0.671	0.61	0.9987	$1 \cdot 10^{-7}$
2-OHN	10.62	$2 \cdot 10^{-7}$ - $6 \cdot 10^{-5}$	0.295	0.16	0.9986	$3 \cdot 10^{-7}$
1-OHN	12.52	$2 \cdot 10^{-7}$ - $6 \cdot 10^{-5}$	0.271	0.24	0.9974	$3 \cdot 10^{-7}$

(B) Evaluation from peak areas.

Analyte	Linear dynamic range [mol L^{-1}]	Slope [mA s mol^{-1} L]	Intercept [nA s]	Correl. Coef.
2-AN	$1 \cdot 10^{-7}$ - $6 \cdot 10^{-5}$	15.48	0.56	0.9995
1-AN	$1 \cdot 10^{-7}$ - $6 \cdot 10^{-5}$	1.184	1.03	0.9983
2-OHN	$2 \cdot 10^{-7}$ - $6 \cdot 10^{-5}$	7.189	-0.17	0.9995
1-OHN	$2 \cdot 10^{-7}$ - $6 \cdot 10^{-5}$	7.561	1.12	0.9984

7.4 Conclusions

This chapter was devoted to the characterization of a simple, laboratory-made amperometric detector based on a microwire working electrode for application in HPLC. The Pt-μCD was employed for the detection of selected hydroxy and aminoderivatives of PAHs. It was shown, that in comparison with the previously described tubular detector with analogically positioned working, reference and auxiliary electrode, it has the advantage of lower peak tailing, which would be covetable for analysis of more complicated mixtures. The reproducibility of the detector response is satisfactory. The lower sensitivity of the Pt-μCD in comparison to Pt-TD does not have to be its limiting factor, because for analysis of environmental and biological materials an extraction step facilitating simultaneous preconcentration is usually necessary.

The simple construction of the detector enables variation of the working electrode material, simply by changing of the metal detection wire. A copper microcylindrical detector has been already used for the detection of some amino acids [11]. Interesting possibility is electrode mercurization for the analysis of polarographicaly active substances, including nitroderivatives of PAHs. Moreover, the detector design opens wide possibilities for search on compatible HPLC, flow injection analysis, and capillary electrophoresis systems coupled with amperometric detection.

7.5 References

1. Tóth K., Štulík K., Kutner W., Fehér Z., Lindner E.: *Pure Appl. Chem.* 76, 1119-1138 (2004).
2. Štulík K., Pacáková V., in: *Electrochemical Measurements in Flowing Liquids*, chapter 3. Ellis Horwood, Chichester England 1987.
3. Trojanowicz M., Szewczynska M., Weislo M.: *Electroanalysis* 15, 347-365 (2003).
4. Cvačka J., Opekar F., Barek J., Zima J.: *Electroanalysis* 12, 39-43 (2000).
5. Hříbal Z.: *Diploma Thesis.* Charles University, Faculty of Science, Prague 2001.
6. Smutná K.: *Diploma Thesis.* Charles University, Faculty of Science, Prague 2001.
7. Zima J., Vaingatova S., Barek J., Brichac J.: *Chem. Anal.* 48, 805-816 (2003).
8. Mocko V.: *PhD Thesis.* Charles University, Faculty of Science, Prague 2004.
9. Sharma L. R., Manchanda A. K., Singh G., Verma R. S.: *Electrochim. Acta* 27, 223-233 (1982).
10. Cases F., Huerta F., Garcés P., Morallón E., Vázquez J. L.: *J. Electroanal. Chem.* 501, 186-192 (2001).
11. Pecková K., Mocko V., Opekar F., Swain G. M., Barek J.: *Chem. Listy* 100, 124-132 (2006).

8

Conclusions

The presented Thesis describes development of new electroanalytical methods for the determination of toxic derivatives of naphthalene. This compound and its nitro, amino, and hydroxy derivatives are drawing attention as highly hazardous substances. This trend is on raise in last years, because it was proved in 2000 that naphthalene is a possible human carcinogen, despite this fact it is still used in chemical industry as intermediate for the production of a wide spectrum of products. Naphthalene and other PAHs are emitted to the environment as a result of incomplete combustion of organic materials, during industrial processes, and other human activities and may undergo further photochemical atmospheric reactions when a number of other more polar products are formed. Between them, NPAHs represent a considerable health risk to humans due to their genotoxicity and/or carcinogenicity. Mononitronaphthalenes are the most prevalent nitro derivatives of PAHs in polluted urban air. Amino and hydroxy derivatives of PAHs are other extensively studied compounds. They are mainly of anthropogenic origin because of their widespread use as intermediates in chemical industry. Moreover, OHPAHs are metabolites of PAHs and thus are used as biomarkers of exposure.

Taking these facts into account, large scale monitoring of environmental pollutants has become more and more important together with the studies of their biological impact on humans and other organisms. This requires development of independent, sensitive and selective detection techniques.

This Thesis represents a contribution to the search on new analytical methods applicable on environmental and biological samples. The current state-of-art concerning the formation, occurrence, and biological activity of PAHs and their nitro, amino, and hydroxy derivatives was summarized in Chapter 2. Further experimental work was focused on assessment of new approaches in the detection of the studied compounds. Attention was paid mainly to nitronaphthalenes, namely 1-nitronaphthalene and 2-nitronaphthalene and the possibilities of their determination using electroanalytical methods.

It has been shown in Chapter 3 that mercury electrodes in combination with modern polarographic and voltammetric techniques are suitable sensors for the determination of submicromolar and nanomolar concentrations of 1- and 2-nitronaphthalene. New electrochemical methods were developed applying DC tast polarography and DPP at DME in 0.01 mol L^{-1} NaOH - methanol (1:1, pH^f 12.2 (1-NN)) and BR buffer - methanol (1:1, pH^f 8.7 (2-NN)), achieved determination limits are $1 \cdot 10^{-6}$ mol L^{-1} and $2 \cdot 10^{-6}$ mol L^{-1} for DCTP and $1 \cdot 10^{-7}$ mol L^{-1} and $2 \cdot 10^{-7}$ mol L^{-1} for DPP for 1-NN and 2-NN, respectively. For DPV at HMDE, determination limits were $3 \cdot 10^{-8}$ mol L^{-1} (1-NN) and $1 \cdot 10^{-8}$ mol L^{-1} (2-NN) in mixed

0.01 mol L^{-1} NaOH - methanol (9:1, pH^f 12.2) media. The most sensitive method is AdSV, using optimized conditions, the limit of determination reached in 0.001 mol L^{-1} LiOH, pH 10.6, by this method is $2 \cdot 10^{-9}$ mol L^{-1} for both studied analytes. The reduction mechanism studied by cyclic voltammetry in acidic, neutral and alkaline media corresponds to the well known mechanism of nitro group containing aromatics at mercury electrodes with the main signal corresponding to the four-electron reduction of the nitro to the hydroxylamino group followed by two electron reduction of the hydroxylamine to amine in acidic media.

In Chapter 4, the electrochemical reduction processes of 1-NN and 2-NN were studied on recently developed amalgam electrode material, which is a promising nontoxic material fully compatible with the concept of green analytical chemistry. The reduction mechanism in acidic and neutral media of studied analytes corresponds to mercury electrodes with the main signal corresponding to the four-electron reduction of the nitro to the hydroxylamino group. In alkaline media this reduction occurs in two separated steps with the first one being a one electron reduction of the nitro group to the nitro anion radical – a mechanism recognized earlier at silver and other solid electrodes. Another difference in comparison to HMDE is that it is not possible to accumulate studied compounds on the electrode surface to enhance the sensitivity, as confirmed by ELVS. The meniscus modified silver solid amalgam electrode proved satisfactory for the determination of submicromolar concentrations of studied analytes, using DPV the LODs were $3 \cdot 10^{-7}$ and $5 \cdot 10^{-7}$ mol L^{-1} for 1-NN and 2-NN, respectively, in 0.01 mol L^{-1} NaOH - methanol (9:1, pH^f 12.2) media.

Careful and sensitive monitoring of the presence NPAHs as the pollutants in the environment is a matter of great interest due to their toxicity even in very low concentrations. For 1-nitronaphthalene and 2-nitronaphthalene the need on sensitive methods for determination in water is given by their relatively high water solubility. Hence, the electroanalytical methods suitable for the determination of 1-NN and 2-NN in model drinking and water samples were developed in Chapter 5. The direct determination of studied analytes by DPV at HMDE is possible after addition of 0.1 mol L^{-1} NaOH to the water samples, LODs as low as ~ $3 \cdot 10^{-8}$ mol L^{-1} were achieved for drinking and river water samples, respectively. For further decrease of LODs preliminary separation and preconcentration of studied analytes is necessary. Liquid-liquid extraction is applicable only on drinking water samples of 2-NN, 1-NN pass over partially into gaseous phase during the evaporation step. On the other hand, DP voltammetric determination after solid phase extraction using LiChrolut RP-Select B columns for analyte preconcentration is a reliable method for the determination of both analytes, characterized by high recoveries and reproducibility. For drinking water samples,

recoveries higher than 95 % for 1-NN and 71.4 % for 2-NN were obtained with maximum relative standard deviation of 5.8 %. Subnanomolar LODs ($2 \cdot 10^{-10}$ mol L^{-1} (1-NN) and $3 \cdot 10^{-10}$ mol L^{-1} (2-NN)) were achieved for SPE from 1000mL of drinking water samples, for river water samples, the preconcentration could be realized from maximum 100 mL of the sample and determination limits $2 \cdot 10^{-9}$ mol L^{-1} (1-NN) and $3 \cdot 10^{-9}$ mol L^{-1} were achieved.

DPV at HMDE and UV-VIS spectrophotometry were further applied in Chapter 6 for the monitoring of UV photolytical degradation of selected NPAHs as laboratory waste contaminants. Methanolic solutions were irradiated in a laboratory made reactor. Lower efficiencies (80 % 1-NN, 71 % 2-NN) were obtained for UV spectrophotometry due to the increasing absorbance of the degradation products in the range of 400-200 nm. However, after addition of hydrogen peroxide the decomposition proceeded with efficiency higher than ~ 95 %. More suitable for the monitoring is the DPV at HMDE, no peak of 1-NN and 2-NN is observable after 120 min and 150 min of irradiation in air saturated solutions. The standard addition method revealed more than 99.8 % efficiency of the photolysis of both analytes. However, many destruction products are formed as demonstrated by GC-MS. In general, the UV irradiation of oxygen containing solutions proceeds faster than in absence of it, the naphthalene nucleus is destroyed and more polar compounds containing benzene ring are formed. By electrochemical methods, a compound containing probably diol moiety was identified. The irradiation under nitrogen leads mainly to changes in the substitution of the naphthalene nucleus. However, the toxicity of the resulting solutions should be subject to further mutagenicity experiments.

Last part of the Thesis was devoted to the characterization of a simple, laboratory-made amperometric detector based on a microwire working electrode for application in HPLC. The Pt-μCD was employed for the detection of a mixture of 1-aminonaphthalene, 2-aminonaphthalene, 1-hydroxynaphthalene, and 2-hydroxynaphthalene. It was shown, that in comparison to the previously described tubular detector with analogically positioned working, reference and auxiliary electrode, the Pt-μCD has the advantage of lower peak tailing, which would be covetable for analysis of more complicated mixtures. The reproducibility of the detector response is satisfactory even for aminonaphthalenes that are known to form polymerizing films as products of oxidation at platinum or carbon electrodes leading to electrode fouling. The lower sensitivity of the Pt-μCD does not have to be its limiting factor, because for analysis of environmental and biological materials an extraction step facilitating simultaneous preconcentration is usually necessary.

Finally, it can be concluded that:

- Modern polarographic and voltammetric methods at mercury electrodes developed for determination of trace amounts of 1-NN and 2-NN and other NPAHs offer a sensitive, cheap, independent, and reliable alternative to more frequently used chromatographic methods.
- Solid phase extraction can be successfully used for the preliminary separation and preconcentration of 1-NN and 2-NN from water samples with over 71 % extraction efficiency, liquid-liquid extraction and other procedures requiring an evaporation step are not recommendable as nitronaphthalenes, especially 1-nitronaphthalene pass over easily into the gaseous phase.
- m-AgSAE in combination with modern voltammetric techniques is a suitable sensor for the determination of submicromolar concentrations of 1-NN and 2-NN. It provides high stability and reproducibility, although the achieved LODs are about one order of magnitude higher compared to DPV at HMDE. However, amalgam electrodes can replace mercury electrodes in cases where higher robustness and easy operation is required or unsubstantial fear of "toxic" mercury disables its use as electrode material.
- UV-light initiated photochemical reactions lead to quantitative degradation of 1-NN and 2-NN in methanol, DPV at HMDE is more suitable for monitoring of their photolysis than UV-VIS spectrophotometry. Based on GC-MS and voltammetric analysis of irradiated solutions, the degradation is more effective in solutions containing oxygen when the aromatic naphthalene skeleton is broken and mainly lower molecular compounds are formed.
- Amperometry employed at positive detection potentials is sensitive technique for easily oxidizable hydroxy and amino derivatives of naphthalene. The amperometric platinum detector based on a wire microelectrode is suitable for the sensitive and selective detection of mentioned analytes after their chromatographic separation.

Appendix A

List of publications

1. Pecková K., Barek J., Zima J.: *Chem. Listy* 95, 709-712 (2001):
   Polarographic and Voltammetric Determination of Trace Amounts of 1-Nitronaphthalene.

2. Pecková K., Barek J., Moreira J. C., Zima J.: *Anal. Bioanal. Chem.* 381, 520-525 (2005):
   Polarographic and Voltammetric Determination of Trace Amounts of 2-Nitronaphthalene.

3. Pecková K., Mocko V., Opekar F., Swain G. M., Barek J.: *Chem. Listy* 100, 124-132 (2006):
   Miniaturized Amperometric Detectors for HPLC and Capillary Zone Electrophoresis.

4. Park J., Quaiserová-Mocko V., Pecková K., Galligan J. J., Fink G. D., Swain G. M.:
   Diamond Relat. Mat. 15, 761-772 (2006):
   Fabrication, Characterization, and Application of a Diamond Microelectrode for Electrochemical Measurement of Norepinephrine Release from the Sympathetic Nervous System.

5. Barek J., Fischer J., Peckova K., Navratil T., Yosypchuk B.: *Sensors* 6, 445-452 (2006):
   Silver Solid Amalgam Electrodes as Sensors for Chemical Carcinogens.

6. Pecková K., Barek J., Navrátil T., Yosypchuk B., Zima J.: *Anal. Lett.*, accepted:
   Voltammetric Determination of Nitrated Naphthalenes at a Silver Solid Amalgam Electrode.

List of oral presentations and posters

1. Barek J., Fantová N., Pecková K., Quaiserová V., Štěpán R., Zima J.: *Sborník příspěvků – XX. Moderní elektroanalytické metody*, Jetřichovice, 30.5. - 1.6. 2000, p. 2. Česká společnost chemická, Praha 2000:
Elektrochemické stanovení nitrovaných polycyklických aromatických uhlovodíků a jejich metabolitů.

2. Quaiserová V., Pecková K., Zima J., Barek J.: *Sborník příspěvků – XXI. Moderní elektroanalytické metody*, Nedvědice u Nového Města na Moravě, 24. - 26. 4. 2001, p. 20. Česká společnost chemická, Praha 2001:
Elektrochemické stanovení stopových množství genotoxických derivátů naftalenu.

3. Peckova K., Barek J., Drevinek M., Navratil T., Novotny L., Yosypchuk B., Vaingatova S., Zima J.: *Book of Abstracts – US-CZ Workshop on Electrochemical Sensors Prague 2001*, 19 - 22.6. 2001, p. 32. Czech Chemical Society, Prague 2001:
Determination of Nitrated Polycyclic Aromatic Hydrocarbons Using a Solid Amalgam Electrode.

4. Pecková K., Barek J., Zima J.: *Zborník príspevkov – 53. Zjazd chemických spoločností*, Banská Bystrica, 3. - 6.9. 2001, p. 274. FPV Univerzita Mateja Bela, Banská Bystrica 2001:
Voltammetric Determination of Trace Amounts of 1-Nitronaphthalene.

5. Pecková K., Barek J., Zima J.: *Book of Abstracts – Prague - Dresden Electrochemical Seminar*, Jetřichovice, 5.-7.12. 2001:
Polarographic and Voltammetric Determination of Nanomolar Concentrations of 1- and 2- Nitronaphthalene.

6. Pecková K., Fischer J., Zima J., Barek J.: *Sborník příspěvků – XXII. Moderní elektroanalytické metody*, Cikháj, 21. - 23. 5. 2002, p. 4-7. Česká společnost chemická, Praha 2002:
Využití nových elektrodových materiálů pro voltametrické stanovení ekotoxických organických nitrosloučenin.

7. Barek J., Cizek K., Kumaran S., Peckova K., Zima J.: *Book of Abstracts – Euroanalysis 12*, Dortmund, Germany, 8. - 13. 9. 2002, p. 284. Federation of European Chemical Societies, Dortmund 2002:
Polarographic and Voltammetric Determination of Trace Amounts of Genotoxic Nitrated Polycyclic Aromatic Hydrocarbons.

8. Barek J., Shanmugam K., Peckova K., Zima J.: *Conference Proceedings – 3rd International Conference: Instrumental Methods of Analysis: Modern Trends and Applications*, Thessaloniki, Greece, 23. – 27. 9. 2003, str. 170-173. Aristotle University of Thessaloniki, Thessaloniki 2003:
Determination of Trace Amounts of Chemical Carcinogens Using Electrochemical Methods.

9. Pecková K., Opekar F., Zima J., Barek J.: *Sborník přednášek – XXIII. Moderní elektroanalytické metody*, Jetřichovice, 20. - 22. 5. 2003, p. 55-57. Česká společnost chemická, Praha 2003:
Ampérometrický detektor s mikrocylindrickou platinovou elektrodou pro HPLC.

10. Pecková K., Barek J., Zima J.: *Sborník příspěvků – 55. Zjazd chemických spoločností*, Košice, 8. - 12.9. 2003, p. 859-860. Chem. Listy 97 (8), 2003:
Polarografické a voltametrické stanovení stopových množství 1- a 2-nitronaftalenu.

11. Pecková K., Barek J., Zima J.: *Sborník příspěvků, 45. – Zjazd PTCh i SITPCh*, Lublin, Poland, 15. - 18. 9. 2003, p. 1236:
Polarographic and Voltammetric Determination of Genotoxic Naphthalene Derivatives.

12. Pecková K., Opekar F., Zima J., Barek J.: *Sborník příspěvků – XXIV. Moderní elektroanalytické metody*, Jetřichovice, 3. - 6.5. 2004, p. 64-67. Česká společnost chemická, Praha 2004:
Ampérometrický detektor s mikrocylindrickou měděnou elektrodou pro stanovení aminokyselin.

13. Pecková K., Opekar F., Zima J., Barek J.: *Book of Abstracts – 6th Joint Seminar of Young Scientists*, Prague, 24.5. 2004, p. 19:
Amperometric detector with microcylindrical electrode for HPLC.

14. Pecková K., Barek J., Zima J.: *Sborník příspěvků – 56. Sjezd chemických společností*, Ostrava, 6. - 9.9. 2004, p. 613. Chem. Listy 98 (8), 2003:
Monitorování účinnosti fotochemické destrukce nitrovaných derivátů naftalenu.

15. Pecková K., Moreira J. C., Yosypchuk B., Navrátil T., Zima J., Barek J.: *Sborník přednášek – XXV. Moderní elektrochemické metody*, Jetřichovice, 24. - 26.5. 2005, p. 147-152. Česká společnost chemická, Praha 2005:
Využití amalgamových elektrod v elektrochemické analýze azidothymidinu v lékové formě.

16. Pecková K., Mocko V., Barek J., Zima J., Swain G. M.: *Sborník přednášek – XXV. Moderní elektrochemické metody*, Jetřichovice, 24. - 26.5. 2005, p. 153-158. Česká společnost chemická, Praha 2005:
Využití kapilární elektroforézy s elektrochemickou detekcí s borem dopovanou diamantovou mikroelektrodou v analýze katecholaminů a jejich metabolitů v krevní plazmě.

17. Pecková K., Rumlerová A., Barek J., Zima J.: *Sborník příspěvků – 57. Zjazd chemických spoločností*, Tatranské Matliare, 4. - 8.9. 2005, p. 144-145. ChemZi 1 (1), 2005:
Studium elektrochemického chování meso-tetrakis(4-sulfophenyl)porfyrinu s využitím polarografických a voltametrických metod na rtuťových elektrodách.